Paul Demmelmayer, BSc

Isolation of lignosulfonates from spent sulfite liquor using supported liquid membrane permeation

MASTER'S THESIS

to achieve the university degree of

Diplom-Ingenieur

Master's degree programme: Chemical and Pharmaceutical Engineering

submitted to

Graz University of Technology

Supervisor

Ass.Prof. Dipl.-Ing. Dr.techn. Marlene Kienberger

Institute of Chemical Engineering and Environmental Technology

Graz, December 2018

AFFIDAVIT

I declare that I have authored this thesis independently, that I have not used other than the declared sources/resources, and that I have explicitly indicated all material which has been quoted either literally or by content from the sources used. The text document uploaded to TUGRAZonline is identical to the present master‘s thesis.

Date

Signature

Acknowledgment

First, I would like to thank my supervisor Marlene Kienberger for her support and advice during my work and the opportunity to perform my experiments at the Institute of Chemical Engineering and Environmental Technology, Graz University of Technology with all the available equipment. In addition, I would like to thank all members of the biorefinery engineering group and the CPE Task force, Silvia, Ingrid, Larissa, Marion, Larissa, Sophie, Thomas, Pepi, Gernot, Alexander, Alex, Seppi, Sascha and Andi, for their assistance and advice during my thesis and studies. I really enjoyed our group meetings, discussions, and cake and coffee breaks. A special thanks to Silvia for proof reading my thesis. Thanks also to Julio for helping me to perform the equilibrium measurements.

I also would like to thank all members of the Institute of Chemical Engineering and Environmental Technology for their assistance and the company Sappi Gratkorn for the financial support and the opportunity to work on such an interesting topic.

Finally, a huge thanks to my family for supporting and encouraging me during my studies.

Abstract

Spent sulfite liquor is a process stream from the pulp and paper industry containing carbohydrates, inorganic cooking chemicals and lignosulfonates. Interest in isolation of lignosulfonates arose because of their various applications, e.g. as dispersant, as flocculant, or in lead-acid storage batteries. In this work, the selective extraction of lignosulfonates using supported liquid membrane permeation with different amines as extractant is investigated.

Phase equilibria measurements revealed that lignosulfonate extraction using amines diluted in 1-octanol works best under acidic conditions, whereas the back-extraction has to be performed under alkaline conditions. Further, the extraction efficiency of amines for lignosulfonates from model solutions and spent liquor decreases in the order quaternary > primary > secondary > tertiary amines. The efficiency of the back-extraction performed with 0.3 M NaOH is between 94.0 and 99.9 % for primary, secondary and tertiary amines, and 11.0 % for the quaternary amine Aliquat336. Crud formation in model solutions increases with increasing substitution of the nitrogen atom, whereas in spent liquor the opposite trend is observed.

Supported liquid membrane experiments carried out in batch mode in the U-tube setup with a membrane area of 2.27 cm^2 showed that trioctylamine and dioctylamine are the most promising amines in terms of overall efficiency and crud formation. By increasing the effective membrane area to 25 cm^2 in a small-scale reactor, stable operation was achieved for 172 hours with PE support layers. The gained knowledge was applied to continuous lignosulfonate extraction from spent liquor with a lignosulfonate concentration of 80-100 $g \cdot l^{-1}$ using supported liquid membrane permeation. After 6 hours, a lignosulfonate concentration of 2 $g \cdot l^{-1}$ was measured in the stripping phase in a flat sheet membrane reactor with an exchange area of 123 cm^2.

The experiments conducted in the present thesis show that the isolation of lignosulfonates from model solutions and spent liquor using supported liquid membrane technology is possible, and with the right choice of membrane phase, crud formation is prevented.

Zusammenfassung

Die Ablauge aus dem Sulfit-Prozess der Papier- und Zellstoffindustrie enthält neben den Kochchemikalien auch Kohlenhydrate und Lignosulfonate. Das wachsende Interesse an der Isolierung von Lignosulfonaten ist deren vielseitigen Einsatzmöglichkeiten zuzuschreiben, wie zum Beispiel als Dispergiermittel, als Flockungsmittel oder in Bleiakkumulatoren. In dieser Arbeit wird die Flüssigmembranpermeation mit gestützten Membranen auf ihre Eignung zur selektiven Abtrennung von Lignosulfonaten untersucht werden, wobei verschiedene Amine als Extraktionsmittel zum Einsatz kommen.

Aus den Phasengleichgewichtsmessungen geht hervor, dass die Extraktion von Lignosulfonaten mit einem Amin:1-Octanol-Gemisch als organische Phase in saurem Milieu eine höhere Effizienz aufweist, als in alkalischem Milieu. Die Rückextraktion hingegen hat bei hohem pH-Wert zu erfolgen. Hinsichtlich der Substitution des Stickstoffatoms sinkt die Effizienz in der Reihenfolge quaternäre > primäre > sekundäre > tertiäre Amine, sowohl für Modelllösungen, als auch für die Ablauge. Die Effizienz der Rückextraktion liegt für primäre, sekundäre und tertiäre Amine zwischen 94.0 % und 99.9 %, sowie bei 11.0 % für das quaternäre Amin Aliquat336. Die Emulsionsbildung steigt bei der Verwendung von Modelllösungen mit steigender Substitution am Stickstoffatom an, für den realen Prozessstrom ist das umgekehrte Verhalten beobachtbar.

Im nächsten Schritt zeigten die beiden Amine Dioctylamin und Trioctylamin in der Flüssigmembranpermeation (FMP) mit gestützten Membranen im U-Rohr mit einer Membranfläche von 2.27 cm^2 die geringste Emulsionsbildung bei gleichzeitig hoher Gesamteffizienz. Im small-scale Membranreaktor, welcher eine PE Membran mit einer Austauschfläche von 25 cm^2 hat, konnte ein stabiler Betrieb über 172 Stunden im Batch-Modus realisiert werden. Abschließend wurde die kontinuierliche Extraktion von Lignosulfonaten aus der Ablauge mit einer Lignosulfonat-Konzentration von 80-100 $g \cdot l^{-1}$ in einem FMP-Reaktor mit einer Austauschfläche von 123 cm^2 durchgeführt. Hier konnte nach 6 Stunden stabilen Betriebs eine Lignosulfonat-Konzentration von 2 $g \cdot l^{-1}$ in der Strip-Phase gemessen werden.

Die Ergebnisse zeigen, dass Flüssigmembranpermeation mit gestützten Membranen die Isolierung von Lignosulfonaten ermöglichen und die richtige Wahl der Membranphase Emulsionsbildung verhindert.

Content

1. Motivation

Global warming, environmental disasters, and depletion of fossil fuels are clear indices for overworking our planet. Immediate actions are mandatory in order to preserve the chance to balance the sensible ecosystem. This means a shift of paradigm is necessary to ensure the future of nature and humanity. One important point to address is the switch from fossil-based, non-renewables to bio-based, renewable resources. A process that can be regarded as renewable is the pulp and paper process. Here woody biomass, which mainly consists of cellulose, hemicelluloses, lignin, and extractives, is used to produce pulp and paper [1,2]. However, there is huge potential for improving the exploitation of certain process streams in order to produce additional value added products. The spent liquor in the sulfite process, which is the residual liquid stream after the separation of cellulose, is an example of such a process stream. It primarily contains carbohydrates, inorganic cooking chemicals and lignosulfonates. [2,3]

Lignosulfonates are formed by sulfonation of lignin during delignification of wood. Lignin is a randomly branched polyphenol and consists of the three hydroxycinnamyl alcohols, or monolignols, coniferyl, sinapyl, and *p*-coumaryl alcohol (Figure 1.1) linked by various ether and C-C bonds, e.g. β-O-4, β-β, β-5, or α-O-4 bonds. [1,4,5] When incorporated into the lignin structure the different units are called guaiacyl (G), syringyl (S), and p-hydroxyphenyl (H) units. [6] The distribution of the different units depends on the wood species, e.g. softwoods contain a higher amount of G units, whereas hardwood lignins are mainly made of G and S units [7].

The exact structure of lignin molecules solubilized in the course of pulp production varies strongly and depends on the feed material, the cooking process and the process conditions. Figure 1.2 shows the structure of native poplar lignin proposed by Stewart et al. [8].

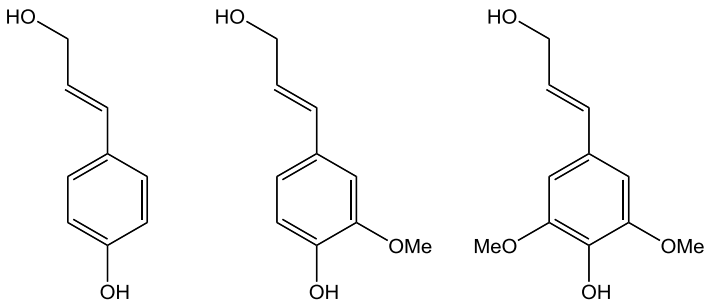

Figure 1.1: Chemical structure of the three monolignols: p-coumaryl, coniferyl and sinapyl alcohol. Adapted from [9].

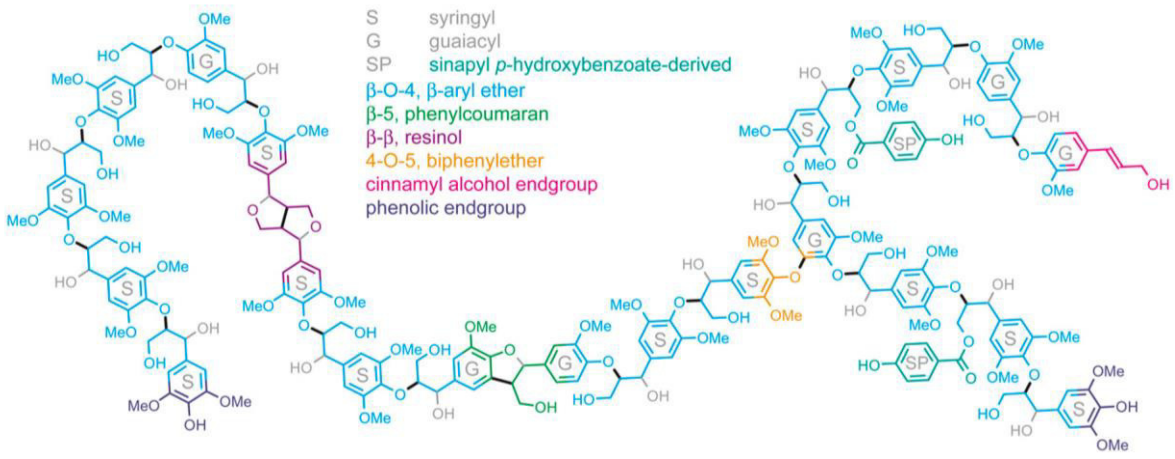

Figure 1.2: Proposed structure of a lignin molecule showing the different monolignols including different bonds [6,8].

The functions of lignin in the plant tissue are the decrease of the permeation flow of water across the cell walls, the enhancement of the rigidity of the cell walls, and, together with hemicelluloses, it serves as binder between the cells. Furthermore, lignin prevents the penetration of destructive enzymes into the cell walls. [7]

As already stated, lignin in the spent sulfite liquor exists in form of lignosulfonates which contain about 6 wt% sulfur in form of sulfonate groups [10–12]. Figure 1.3 shows the structure of a lignosulfonate molecule including the different bonds between the monolignols and the sulfonate groups (SO_3M) where M represents the counter ion, e.g. sodium (Na^+) or magnesium (Mg^{2+}) [13]. Due to the anionic charge of the sulfonate groups, lignosulfonates are, in contrast to native lignin, water-soluble over the entire pH range. [5]

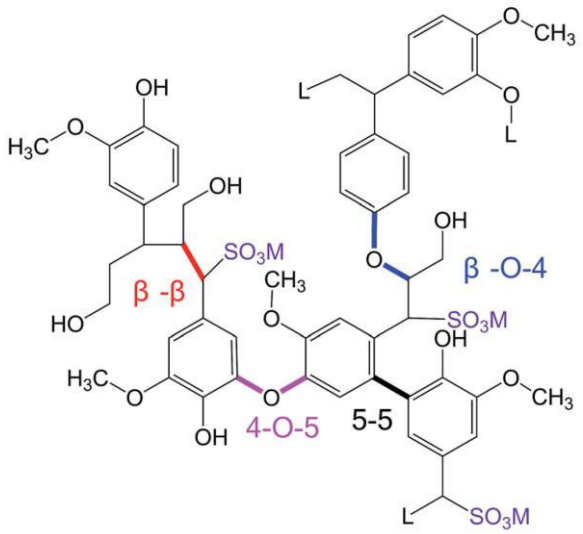

Figure 1.3: Proposed structure of a lignosulfonate molecule including the different bonds between the monolignols and the sulfonate groups (SO_3M), where M represents the counter ion [13].

Interest in isolation of lignosulfonates arose due to the various possible applications, e.g. as dispersant, concrete additive, flocculant, dust suppressant, or in lead-acid storage batteries [1,14,15]. As is the case for native lignin, lignosulfonates too exhibit high variations in terms of product quality, meaning that polydispersity, molecular weight, and degree of sulfonation show strong fluctuations [14]. Nevertheless, many products require a constant lignosulfonate quality and therefore, efficient und selective separation processes are required. State of the art methods, e.g. the Howard process, ultrafiltration or spray-drying of spent liquor, lack of selectivity and high product quality.

A possible technology for the selective isolation of lignosulfonates is solvent extraction where the targeted component is transferred from an aqueous feed phase into an organic solvent phase. One disadvantage of this technology is, especially when dealing with bio-based process streams, the formation of crud, which prohibits the phase separation. The spatial separation of the two phases by a porous support layer offers the possibility to prevent the formation of such a stable emulsion [16]. However, two process steps, namely the extraction and e.g. the back-extraction, are needed as well as considerable amounts of solvent. Supported liquid membrane permeation combines the two process steps in one single step and is able to strongly reduce the required amount of solvent. When choosing the right combination of solvent phase, specifically carrier, solvent, and modifier, emulsion formation and membrane fouling can be prevented. This was already shown in previous studies at the Institute of Chemical Engineering and Environmental Technology at Graz University of Technology for the isolation of carboxylic acids [17,18]. Previous research has shown that lignosulfonates can be extracted using different amines [15,19,20]. Goal of the present thesis is to combine these two approaches for the selective extraction of lignosulfonates using supported liquid membrane permeation.

2. Research questions

Having the main task, namely the selective isolation of lignosulfonates from spent sulfite liquor using supported liquid membrane permeation, in mind, the present thesis seeks to address the following research questions.

In a first step the extraction of lignosulfonates using amines as carrier agent shall be investigated in a two-phase contact without a support layer for spatial phase separation. By varying the amine, the influence of the substitution of the nitrogen atom and the chain length of the alkyl chains of the amine on the extraction efficiency are determined. In addition, the influence of the pH value is crucial for the separation process and shall be investigated. With the obtained data the distribution ratio of lignosulfonate between the aqueous and solvent phase, and the extraction efficiency are calculated.

Secondly, the principle is applied to three-phase contact experiments in supported liquid membrane configurations. As for the two-phase contact, the influence of the chosen amine on the lignosulfonates transport is investigated. In addition, the dependency of extraction efficiency on the used support layer material and the prevention of crud formation shall be examined.

Applying the gained knowledge of the first two research questions, the final task of this study is to verify whether a continuously operated supported liquid membrane process for the isolation of lignosulfonates is possible respectively feasible.

3. Theoretical background

3.1. Sulfite process

In the pulp and paper process, cellulose is liberated from the wood matrix to produce pulp, which can be further processed to paper. In general, it is distinguished between mechanical pulping where the fibers are released by grinding and pressing of wood, and chemical pulping where the separation of cellulose from the wood matrix is achieved by chemical degradation of lignin. Also a combination of the two methods is applied. Chemical pulping possesses the advantages of higher fiber length and quality, compared to mechanical pulping which contains a large portion of fines. The disadvantage of chemical pulping is that the chemical reactions are not selective and also degrade parts of hemicellulose and cellulose, leading to a lower fiber yield of 45-55 % [21,22], compared to about 90 % [22] in case of mechanical pulping. The two main processes applied in the chemical pulping industry are the Kraft and the sulfite process, whereas the Kraft process is the dominant method representing 75 % [23] of the overall pulp production. [21,22] An advantage of the sulfite process is the production of a less colored pulp which is easier to bleach and hence can be used in high quality paper production. Drawbacks compared to the Kraft process are the lower strength of the fibers and the higher sensitivity with regard to the wood species. Softwoods, containing higher amounts of resins and tannin-containing hardwoods can usually not be processed by the sulfite process. [23]

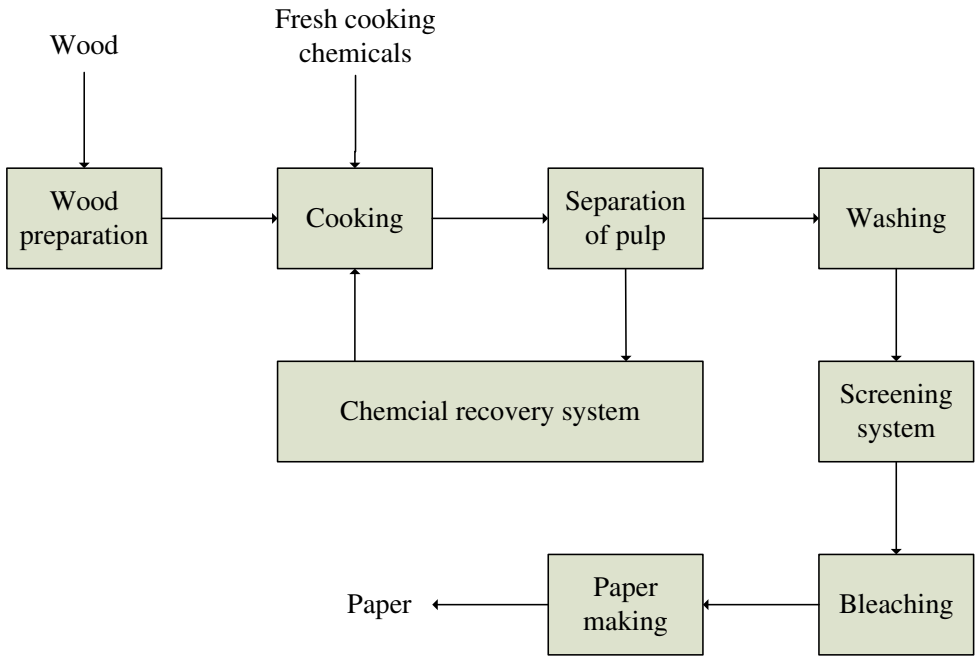

Figure 3.1: General process flow chart of a chemical pulp and paper industry.

Figure 3.1 depicts the general process steps involved in the chemical paper making processes. The first step is the wood preparation including debarking and chipping of the wood logs. The wood chips are then introduced into the pressurized cooking unit, where the delignification takes place. After separation of the cellulose fibers (pulp) the cooking liquor is introduced into the chemical recovery system to regain the cooking chemicals and to produce energy. The pulp is washed and screened to remove foreign matter, dirt, and residual cooking chemicals. The next step in the pulp treatment is bleaching. [23] Here the brownish color resulting from the remaining lignin is removed by oxidation of lignin and subsequent extraction. Common bleaching agents are oxygen, hydrogen peroxide, chlorine, and chlorine dioxide. Finally, the bleached pulp is processed in paper producing machines. [22]

In the sulfite process, the delignification is done by action of bisulfite ions (HSO_3^-) with sodium, calcium, magnesium, or ammonium as counter ion. Due to the sulfonation, lignosulfonates are water soluble and can be separated from cellulose. In general, the sulfite process can be carried out under acidic, neutral or alkaline conditions. [22,24] Since the spent liquor used in the experiments of the present thesis originates from the pulp and paper mill Sappi Gratkorn, Styria, Austria where a magnefite process under acidic conditions is applied, further considerations are based on the acidic sulfite process. In the magnefite process, magnesium is the counter ion and the corresponding pH is in the range of 3-5 [24]. Depending on the actual pH value, also the hydrolysis of ether linkages in carbohydrates and lignin contributes to the delignification of the woody feed material. Furthermore, it is known that the degree of sulfonation of lignin increases with decreasing pH value. Figure 3.2 shows the mechanism of the sulfonation of lignin in the acidic sulfite process, where the bisulfite ion reacts with the phenylpropane unit. The ether group is protonated, followed by the elimination of water and addition of a bisulfite ion. [1,22,24]

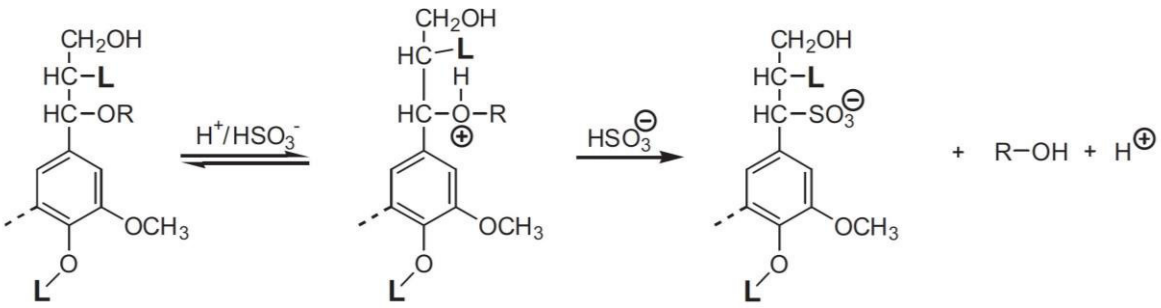

Figure 3.2: Mechanism of the sulfonation of lignin in the acidic sulfite process [22].

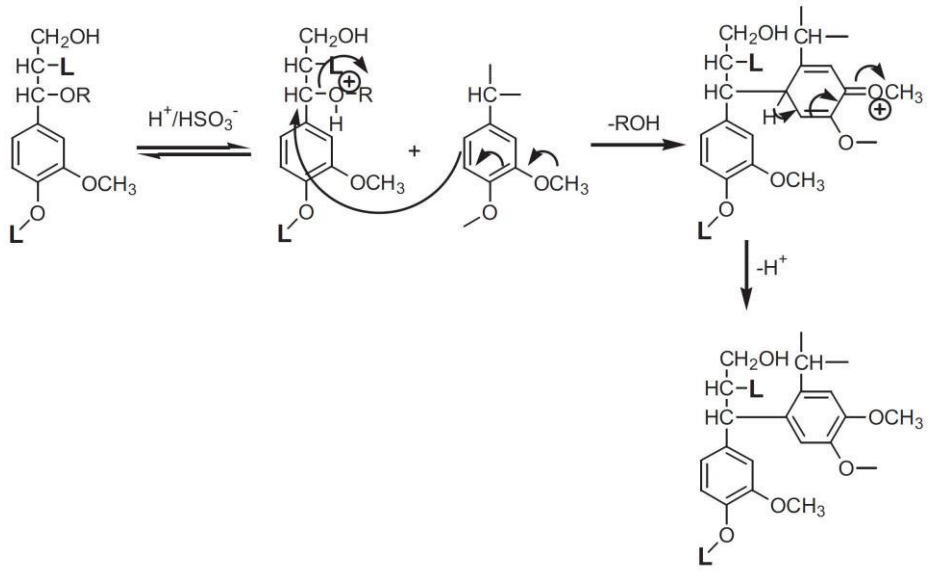

Figure 3.3: Mechanism of the acid catalyzed condensation of lignin during the delignification process [22].

The competing reaction to sulfonation is condensation (Figure 3.3). The free aromatic carbon atom in para position to the methoxyl group facilitates the formation of a carbon-carbon linkage to the benzylic carbon atom of an adjacent phenylpropane unit. The prerequisite is that this phenylpropane unit can form a carbonium ion by proton-elimination of the oxygen group. [1,22,24]

The other major reaction occurring in the acidic sulfite process, is the acid catalyzed hydrolysis of polysaccharides resulting in the production of large amounts of monomeric sugars by the hydrolysis of glucosidic linkages. Some of these sugars can be converted into furfural and hydroxymethylfurfural during sulfite cooking. [22]

3.1.1. Spent Sulfite Liquor

The spent sulfite liquor or spent liquor is the process stream leaving the process after the separation of the cellulose fibers. In case of the acidic magnefite process it contains the cooking chemicals, lignosulfonates, and sugars. [2,3] Table 3.1 displays the general properties of spent sulfite liquor [3].

Table 3.1: General properties of spent sulfite liquor [3].

pH	3-4	
Lignosulfonates	7.9-8.5	[wt%]
Sugars	4.0-5.7	[wt%]
Total solids	16.9-17.1	[wt%]

3.1.2. Separation of lignosulfonates

The fact that lignosulfonates are water-soluble over the entire pH range implies that precipitation by pH change is not possible and makes the separation procedure more challenging, compared to e.g. Kraft lignin. The two most commonly applied methods for lignosulfonate isolation are the so-called Howard process and ultrafiltration. [1,25]

Ultrafiltration is applied since 1981 in Norway in a calcium bisulfite process at Borregaard Industries [26]. With this method it is possible to isolate lignosulfonates from the spent liquor due to the difference in molecular weight. However, the overlap in molecular weight with other components decreases the product quality. Further, membrane fouling and concentration polarization are drawbacks of this method. An alternative is the Howard process, which is also commercially applied. In a first precipitation step calcium sulfite ($CaSO_3$) is precipitated by addition of lime (CaO). After the removal of $CaSO_3$, a second precipitation step is performed using lime to produce calcium lignosulfonate, which precipitates at a pH greater than 12. However, the consumption of chemicals of this method is very high. [1,15,25] Another method for the isolation of lignosulfonates was applied at a pulp and paper mill in Canada in the 1990s which used an ammonia based sulfite process. After an evaporation step the sugars present in the spent liquor were fermented to produce ethanol and the remaining liquor was used to produce liquid or spray-dried lignosulfonates. [26] In addition, there are several isolation methods conducted at lab-scale, such as ion exchange with resins, electrolysis, and amine extraction. [15,25,26] Recently, liquid membrane technology has emerged as separation technique for different substances, e.g. metal ions [15]. In this context, research has shown that supported liquid membrane permeation using amines as extraction agent is a promising technology for the isolation of lignosulfonates from spent liquor. The right choice of the solvent phase and support material enables a selective and fractional separation. [14,15,19,27]

3.2. Solvent extraction in the bio-based environment

In solvent extraction two immiscible liquid phases, most commonly an aqueous and an organic phase, are brought into intense contact. Thus, the component of interest is distributed between the two phases in accordance to its distribution coefficient. Beside operation in batch mode, solvent extraction can be carried out in continuous operation. For simplification of the following process description, the general nomenclature of the different streams or phases is given in Figure 3.4. The two streams entering the extraction unit are the feed phase containing the component of interest, *A*, which should be separated from the liquid phase *C*, and the solvent

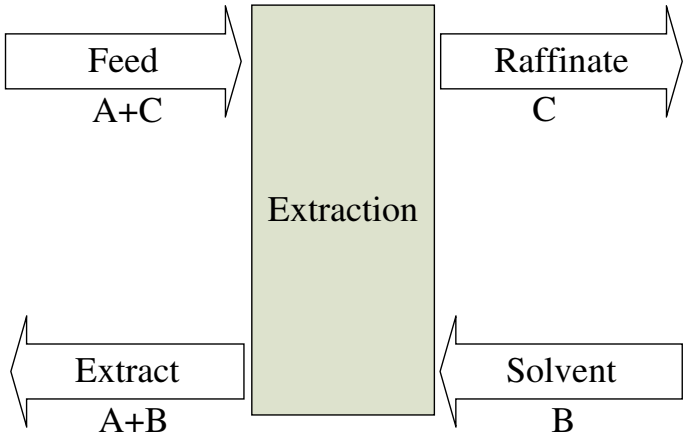

Figure 3.4: Basic principle of solvent extraction with definition of the different streams entering and leaving the process. Adapted from [28].

phase *B* which is used to extract component *A* from the feed phase. The two leaving streams are the extract phase containing the targeted component *A* and solvent *B*, and the raffinate phase containing component *C* from the feed stream. In real processes the raffinate phase still contains a certain amount of *A* since the extraction efficiency usually is below 100 %. [28,29]

After the extraction, a second process step is needed to recover the solute *A* from the loaded solvent phase, e.g. distillation or back-extraction. Figure 3.5 shows a flow chart of a continuously operated solvent extraction process, where the loaded solvent phase is introduced into the back-extraction step to transfer the solute from the solvent phase into the stripping phase. [30,31]

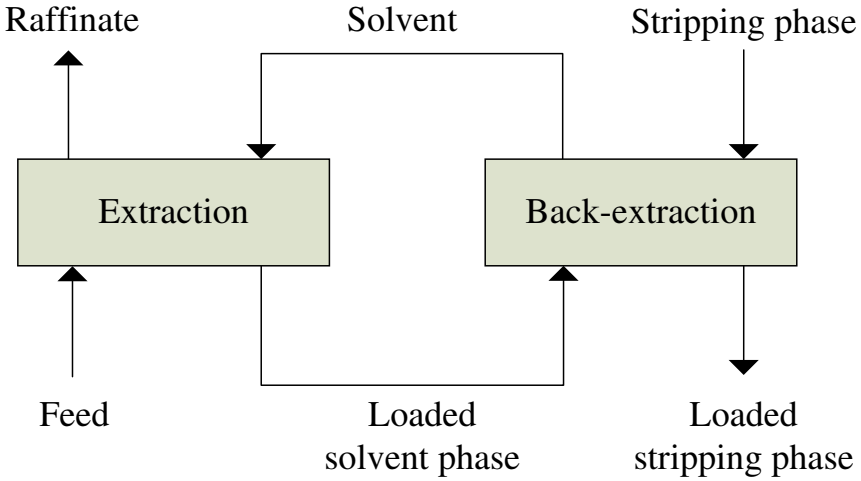

Figure 3.5: Simple representation of a solvent extraction process with solvent regeneration. Adapted from [31].

In comparison to distillation, solvent extraction can be used to separate azeotropes, heat sensitive components, and components with very high, very low or similar boiling points. Even the simultaneous separation of components having different boiling points is possible. [28,32] Such aspects often apply to bio-based materials, making solvent extraction a powerful tool in different fields in the bio-based environment.

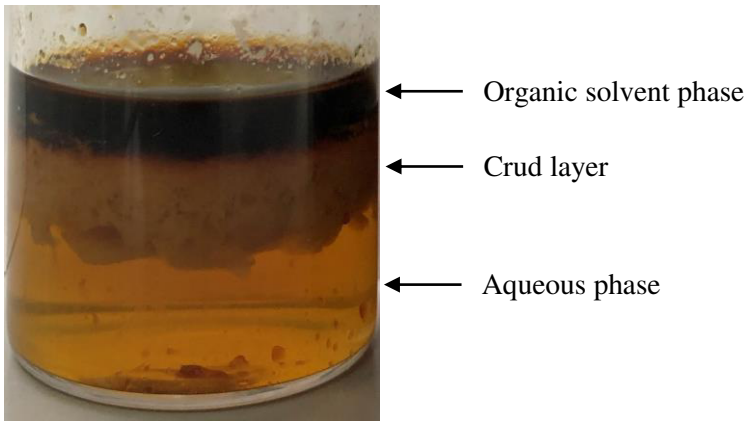

Figure 3.6: Crud formation during the extraction of lignosulfonate from spent liquor. Dark brown layer represents the organic solvent phase and the clear lower phase the aqueous phase. The two phases are separated by a stable crud layer.

A common issue with solvent extraction, especially when dealing with bio-based process streams, is the undesired crud formation (Figure 3.6). Crud is defined as a stable emulsion of the aqueous phase, the solvent phase and fine particles which typically collects at the interface between the two phases [33]. The stability of crud strongly influences the process. It leads to solvent loss, influences the flow characteristics, and inhibits the phase separation. The main influencing factors for crud formation are process conditions, e.g. pH and temperature, and the nature of the feed and solvent phase. Small particles and bacteria in the feed are known for the formation of stable emulsions in the form of crud. Also insufficient ionic strength of the aqueous feed phase and the presence of organic matter, like lignin or humic acid, promote the formation of crud. The composition of the solvent phase is important with regard to both, the efficiency of the extraction process and the emulsion or crud formation. Beside the variation of extractant and solvent, the addition of a modifier can be beneficial in terms of crud prevention. [32,34]

The formation of a third liquid phase is another known phenomenon in solvent extraction. During the extraction a complex is formed between the targeted component and the extractant. At a certain point the solubility of this complex in the solvent is exceeded resulting in the formation of a third phase. [32]

3.2.1. Phase Equilibria

For the design of a solvent extraction process and the choice of the solvent phase the study of phase equilibria, meaning the distribution of the targeted component between the two phases and its dependency on process parameters like pH, pressure and temperature, is required. This is done by phase equilibria measurements, where the two phases are brought into intense contact, e.g. through shaking in separation funnels, and subsequent measurement of the concentration of the targeted component after phase separation. The distribution of the targeted species, which depends on its relative solubility in the two phases, is then described by the distribution coefficient and extraction efficiency. In the following two sections, the extraction of the targeted component from an aqueous phase into an organic solvent phase is assumed. [31,32,34]

In 1898 W. Nernst established the Nernst distribution law based on the thermodynamic equilibrium conditions, which relates the concentration of the solute in the organic phase to its concentration in the aqueous phase [34,35]. The distribution law for the equilibrium reaction

$$A_{aqu} \leftrightarrow A_{org} \tag{3.1}$$

is written

$$K_{D,A} = \frac{concentration\ of\ A\ in\ organic\ phase}{concentration\ of\ A\ in\ aqueous\ phase} = \frac{c_{A,org}}{c_{A,aqu}} \tag{3.2}$$

, where $K_{D,A}$ is the distribution constant or partition coefficient of solute *A*. This equation is basically only valid for pure solvents. However, in reality solvents are always saturated with molecules of the other phase, e.g. water molecules in the organic phase. Furthermore, the solute can be solvated in different forms in the two phases. In practice Eq. (3.2) can be applied under the following two conditions. [34]

- Mutual solubilities of the solvents are very small, < 1 %
- Activity coefficients of the system can be assumed to be constant

In case these conditions are not fulfilled for the considered system, Eq. (3.3) has to be used

$$K^0_{D,A} = \frac{\gamma_{A,org} \cdot c_{A,org}}{\gamma_{A,aqu} \cdot c_{A,aqu}} = \frac{\gamma_{A,org}}{\gamma_{A,aqu}} \cdot K_{D,A} \tag{3.3}$$

, where γ is the activity coefficient of solute *A* in the respective phase. [34,36] The distribution law according to Nernst requires that the species of interest is present in the same chemical form in both phases.

Another quantity describing the phase equilibrium in solvent extraction is the distribution ratio, D_A, defined according to IUPAC: [34,36]

$$D_A = \frac{concentration\ of\ all\ species\ containing\ A\ in\ organic\ phase}{concentration\ of\ all\ species\ containing\ A\ in\ aqueous\ phase} = \frac{c_{AY,t,org}}{c_{AX,t,aqu}} \quad (3.4)$$

In contrast to the distribution law according to Nernst, component *A* can be present in different complexed forms in the considered phases, e.g. as AX in the feed, AY in the organic, and AZ in the stripping phase, in Eq. (3.4). [34]

Since the extraction mechanism of lignosulfonates is assumed to be based on a complex formation between the extractant and the lignosulfonate molecule, the distribution ratio, D_A, is used for the evaluation of the equilibrium data [19,27]. In the present thesis, the distribution ratio for the extraction and back-extraction is calculated according to Eq. (3.5) and (3.6), where all concentrations are measured in equilibrium state.

$$D_{A,extr} = \frac{c_{AY,t,org}}{c_{AX,t,feed}} \quad (3.5)$$

$$D_{A,back-extr} = \frac{c_{AY,t,org}}{c_{AZ,t,strip}} \quad (3.6)$$

For practical purpose it is common to calculate the extraction efficiency, *E*, according to Eq. (3.7). [34]

$$E_{extr} = \frac{D_{A,extr}}{1 + D_{A,extr}} \cdot 100\ \% \quad (3.7)$$

However, when calculating the extraction efficiency for the back-extraction the following inconsistency emerges. On the one hand a high value for $D_{A,extr}$ indicates that a high amount of the targeted species is extracted into the organic phase, resulting in a high extraction efficiency, E_{extr}. An efficient back-extraction on the other hand is characterized by a low value of $D_{A,back\text{-}extr}$ which results in a low extraction efficiency, $E_{back\text{-}extr}$. Hence, the extraction efficiency for the back-extraction and for the overall process is calculated according to Eq. (3.8) and (3.9).

$$E_{back-extr} = \frac{c_{AZ,strip,after\ back-extraction}}{c_{AY,org,after\ extraction}} \cdot 100\ \% \quad (3.8)$$

$$E_{total} = \frac{c_{AZ,strip,after\ back-extraction}}{c_{AX,feed,initial}} \cdot 100\ \% \quad (3.9)$$

The results of equilibrium data are typically represented in form of different diagrams. Commonly, they include the distribution coefficient, *D*, or the extraction efficiency, *E*, as function of the variable Z of the aqueous phase, e.g. pH or concentration of the substance in the organic phase (Figure 3.7). [34] Other possibilities to represent equilibrium data are diagrams containing the concentration of the targeted species in the different phases, e.g. its concentration in the organic phase as function of the concentration in the aqueous phase. [36]

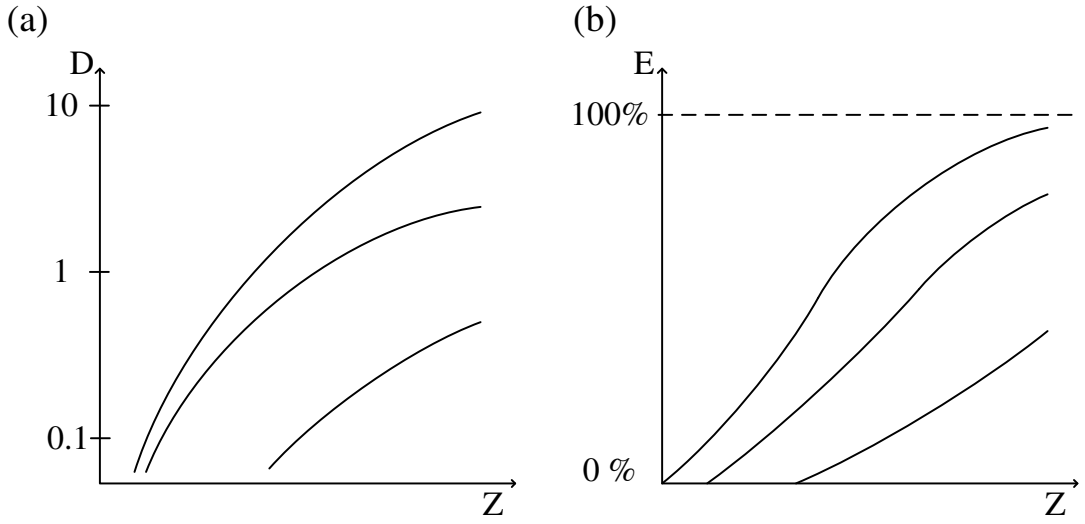

Figure 3.7: Representation of the distribution ratio, *D*, (a) and the extraction efficiency, *E*, (b) for different components as function of the variable Z of the aqueous phase, e.g. pH or concentration [34].

3.2.2. Reactive extraction

In order to increase the selectivity of the extraction process the principle of reactive extraction is introduced. Reactive extraction is the extraction of a component by a chemical reaction with a liquid ion exchanger, also stated carrier. The reactive extraction agents are usually expensive chemicals, and they possess a high viscosity which strongly affects the diffusion coefficient of the formed complex. Therefore, diluents are added which are immiscible with the aqueous phase and decrease the viscosity. In some cases, an additional agent, the modifier, is needed to improve the solubility of the solute-extractant-complex in the organic phase and prohibit third phase formation. [35,37]

The mechanism of reactive extraction depends on the reactive extraction agent, which can be an anion exchange, cation exchange, or solvating agent, and on the targeted species in the feed phase. Following, the different mechanisms of reactive extraction are given, where bars indicate species in the organic phase. [35]

Cation exchange

Eq. (3.10) shows the mechanism of the cation exchange, where the cation (Cat^{n+}) of the extraction agent is exchanged by the cation of the targeted component. This results in a decrease of the pH value in the feed phase because of the release of protons (H^+). Commonly used extraction agents ($\overline{RH}$) are carboxylic acids, sulfonic acids, and phosphoric acids. The back-extraction is done using strong acids, e.g. H_2SO_4 or HNO_3. [35,38]

$$Cat^{m+} + m\,\overline{RH} \leftrightarrow \overline{CatR_m} + m\,H^+ \tag{3.10}$$

Anion exchange

Eq. (3.11) and Eq. (3.12) represent the mechanism for the anion exchange using a tertiary amine as extractant. After activation of the amine according to Eq. (3.11), the anion (An^{m-}) is extracted from the aqueous phase as depicted in Eq. (3.12). [38]

$$H^+ + A^- + \overline{R_3N} \leftrightarrow \overline{R_3NHA} \tag{3.11}$$

$$m\,\overline{R_3NHA} + An^{m-} \leftrightarrow \overline{(R_3NH)_mAn} + m\,A^- \tag{3.12}$$

Extraction agents used for the exchange of anions are primary, secondary or tertiary amines, or R_4-alkyl-substituted ammonium chlorides. The back extraction can be done using a surplus of e.g. hydroxide or chloride ions. [35]

Solvation

Solvation is the extraction of neutral molecules by the formation of a complex with the extraction agent. Solvating extractants are for example tri-butyl phosphate (TBP) or methyl-isobutyl ketone (MIBK). Back-extraction is achieved with pure water and at elevated temperature. [35]

$$ZnCl_2 + n\,\overline{TBP} \leftrightarrow \overline{ZnCl_2(TBP)_n} \tag{3.13}$$

Chelation

In case of chelation, which is preferentially used for extraction of heavy metals and alkaline earth metals, a chelate complex is formed between the chelating agent and the metal ion. Such a chelating agent is for example ethylenediaminetetraacetic acid (EDTA). The back-extraction varies with different chelation agents, e.g. water or nitric acid are used for this purpose. [35,39–42]

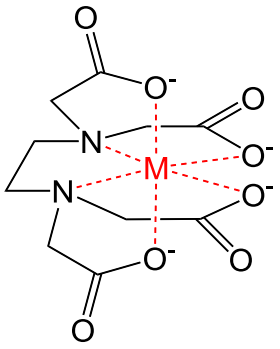

Figure 3.8: Chelate-complex of ethylenediaminetetra acetic acid (EDTA) with a metal ion (M). Adapted from [39].

3.3. Liquid membrane technology

Membrane technology in general implies the separation of a mixture containing different species using a thin semipermeable and porous film, the membrane. Some components of the mixture are able to pass the membrane, whereas others are rejected. However, membrane processes lack selectivity since the separation is mostly based on molecular size, diffusion rate or charge. [43,44] In this context, liquid membrane technology offers the advantage of selective extraction with simultaneous fractionation by selective interaction between the solvent phase, which is stated membrane phase in liquid membrane technologies, and the targeted species in the feed phase. [14,19,27]

Liquid membrane technology was first mentioned in 1960s and resulted in the first pilot plant used for the separation of metals in the 1970s [45]. This technology has gained huge interest in recent years because of its simple construction, energy efficiency, and high selectivity. Beside the selective extraction, the realization of extraction and back-extraction in one process step is another advantage of liquid membrane technology. [27]

In the following section, different configurations of liquid membranes are illustrated.

Bulk liquid membrane (BLM)

Figure 3.9 represents a possible configuration of a BLM setup. The feed and stripping phase are separated by a bulk membrane phase enabling the transport of the targeted species from the feed phase into the stripping phase. All three phases are mixed to enhance mass transfer. [25,46]

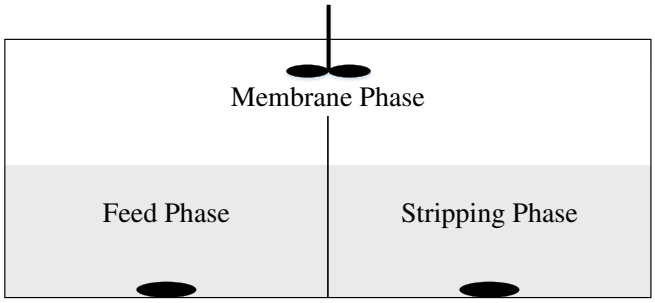

Figure 3.9: Configuration of bulk liquid membranes without porous support layer for phase separation. Adapted from [46].

Figure 3.10 shows another possible setup where the membrane phase is separated from the two aqueous phases by a porous support layer. [47]

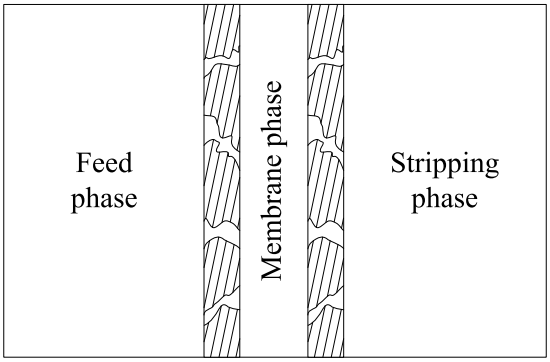

Figure 3.10: Configuration of bulk liquid membranes with porous support layer for phase separation. Adapted from[47].

To increase the interfacial area hollow fiber modules can be used (Figure 3.11). Here, the aqueous feed phase flows within or outside of the fibers and the membrane phase on the other side. The component of interest is transferred from the feed into the membrane phase. For the back-extraction, a second module is needed. [16,48,49]

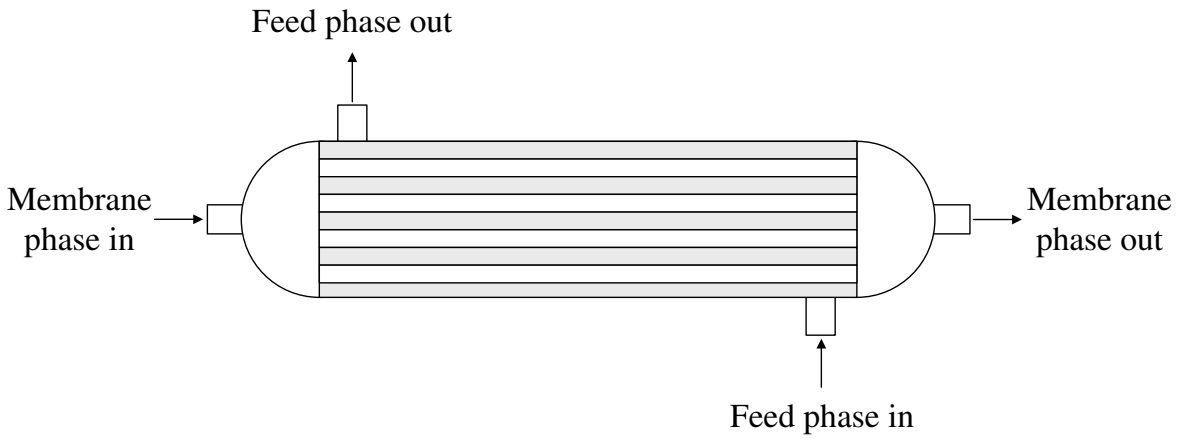

Figure 3.11: Hollow fiber membrane module for continuous solvent extraction. Adapted from [48].

Emulsion liquid membrane (ELM)

In emulsion liquid membrane technology, a stable emulsion between two phases is formed (Figure 3.12). There are two possible combinations of emulsion formation: aqueous-organic-aqueous (A/O/A) and organic-aqueous-organic (O/A/O). In case of the A/O/A type the organic phase is the membrane phase, and in case of the O/A/O configuration the aqueous phase is the membrane phase. The most common methods for emulsion preparation are high speed mixing and homogenizers. After the extraction process high voltage de-emulsification techniques are used for emulsion breakage. Three advantages of ELM are the higher mass transfer area, the intense contact between the involved phases, and the possibility of continuous operation by using standard extraction equipment. [28,47]

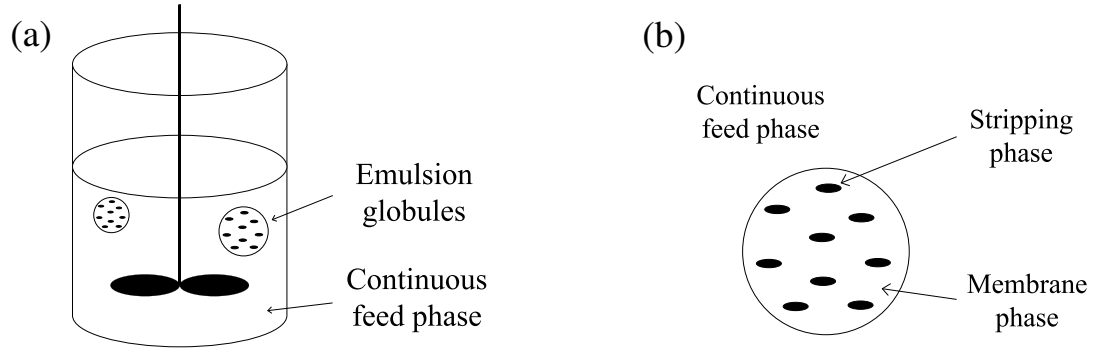

Figure 3.12: Principle of emulsion liquid membrane technology (a) and composition of emulsion globules (b). Adapted from [20].

Supported liquid membrane (SLM)

In supported liquid membrane technology two aqueous phases, namely the feed and the stripping phase, are separated by a thin layer of micro-porous material (Figure 3.13). The pores of this support layer sheet are filled with membrane phase, which is held in the structure by capillary forces. The purpose of the support material is the prevention of membrane phase loss, and it guarantees stable operation. For construction of a SLM module it is important to bear in mind that the mass-transfer resistance increases with increasing thickness of the membrane phase because of the lack of mixing and the low diffusion coefficient within the membrane phase. [43,47]

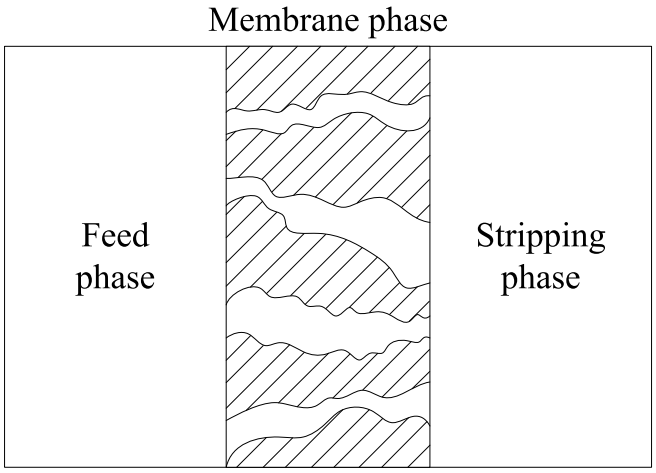

Figure 3.13: Principle of supported liquid membranes. Adapted from [47].

Advantages of supported liquid membranes are: [43,47]

- High selectivity
- Simultaneous extraction and back-extraction in one process step
- Fractionation and isolation in one step possible
- Small amount of membrane phase
- Possibility of high separation factors
- Low separation costs

3.3.1. Driving force in supported liquid membranes

The transport process in supported liquid membranes is a non-equilibrium process with a mass transfer originating from the difference in chemical potential across the membrane. Eq. (3.14) gives the change in chemical potential of component i. [47]

$$\mathrm{d}\mu_i = R \cdot T \cdot \mathrm{d}\ \ln c_i + R \cdot T \cdot \mathrm{d}\ \ln \gamma_i \tag{3.14}$$

In Eq. (3.14), c_i denotes the molar concentration of component i, γ_i its activity coefficient and μ_i its chemical potential.

The concentration gradient in a supported liquid membrane setup depicted in Figure 3.14 results from the different distribution coefficients of the targeted component at the feed-membrane and the membrane-strip interface [50–52].

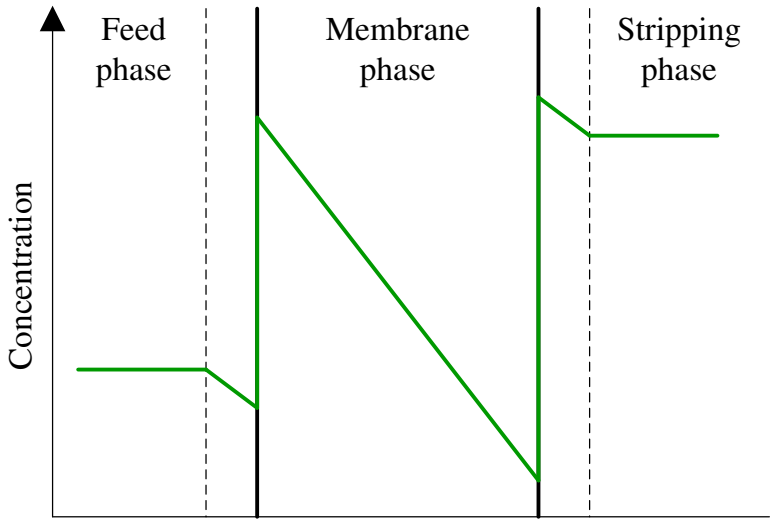

Figure 3.14: Concentration profile in a supported liquid membrane. Adapted from [50–52].

The general steps involved in the transport of the targeted component from the feed to the stripping phase are: [50–52]

- Diffusion across the boundary layer in the aqueous feed phase
- Reaction at the feed-membrane interface
- Diffusion through the membrane phase
- Reaction at the membrane-strip interface
- Diffusion across the boundary layer in the stripping phase

3.3.2. Transport mechanism in supported liquid membranes

The transport of the targeted substance through the supported liquid membrane can occur according to different mechanisms. The following section shall give an overview of the possible transport mechanisms.

Simple permeation

The simplest transport mechanism is the dissolution of the targeted component in the membrane phase and subsequent diffusion to the stripping side (Figure 3.15 a), whereas the targeted component is present in the same form in all three phases. The selectivity and the efficiency of the separation can be enhanced when the permeating component undergoes a chemical reaction on the stripping side (Figure 3.15 b). This prevents the diffusion back into the membrane phase in case an impermeable component is formed, and in consequence a high concentration gradient across the liquid membrane is maintained. [47]

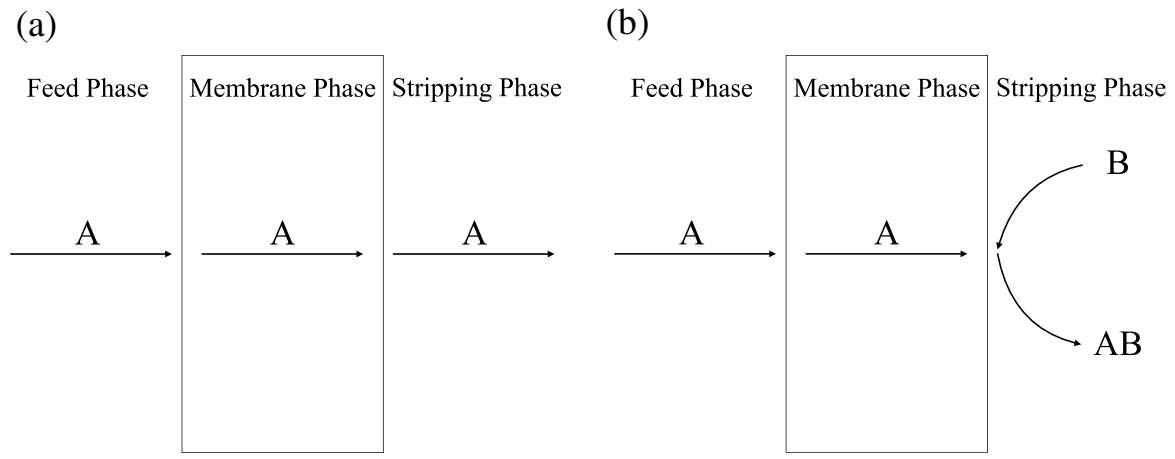

Figure 3.15: Transport mechanism in simple permeation: simple transport (a), simple transport with chemical reaction (b). Adapted from [47].

Carrier-mediated permeation

In case of low solubility of the targeted component in the membrane phase, the selectivity and permeability can be enhanced by adding a carrier or chelating agent to the membrane phase. In a reversible reaction between the species of interest and the carrier or chelating agent, a complex is formed which is transported through the membrane phase. This reaction takes place at the interface between the membrane phase and the feed phase. At the membrane-strip interface the back-extraction takes place. The reaction kinetics and the diffusion of the complex are the two factors which can limit the transport efficiency. [47]

Figure 3.16 a shows the simple carrier-mediated transport mechanism. The complex between the solute and the carrier, which is built at the feed-membrane interface, diffuses through the membrane phase. At the membrane-strip interface the solute is released into the stripping phase by formation of a stronger complex with the stripping agent. Figure 3.16 b displays the carrier-mediated co-transport indicating that an additional species is transported into the same direction as the complex. This mechanism applies in case the carrier exists in uncharged form in the membrane phase and the ionic substance has to be extracted as ion pair. Finally, Figure 3.16 c depicts the carrier-mediated counter-transport, where the additional component is transported into the opposite direction. This mechanism takes place when permanently charged components, e.g. amino acids, are extracted using ionic carriers. [47]

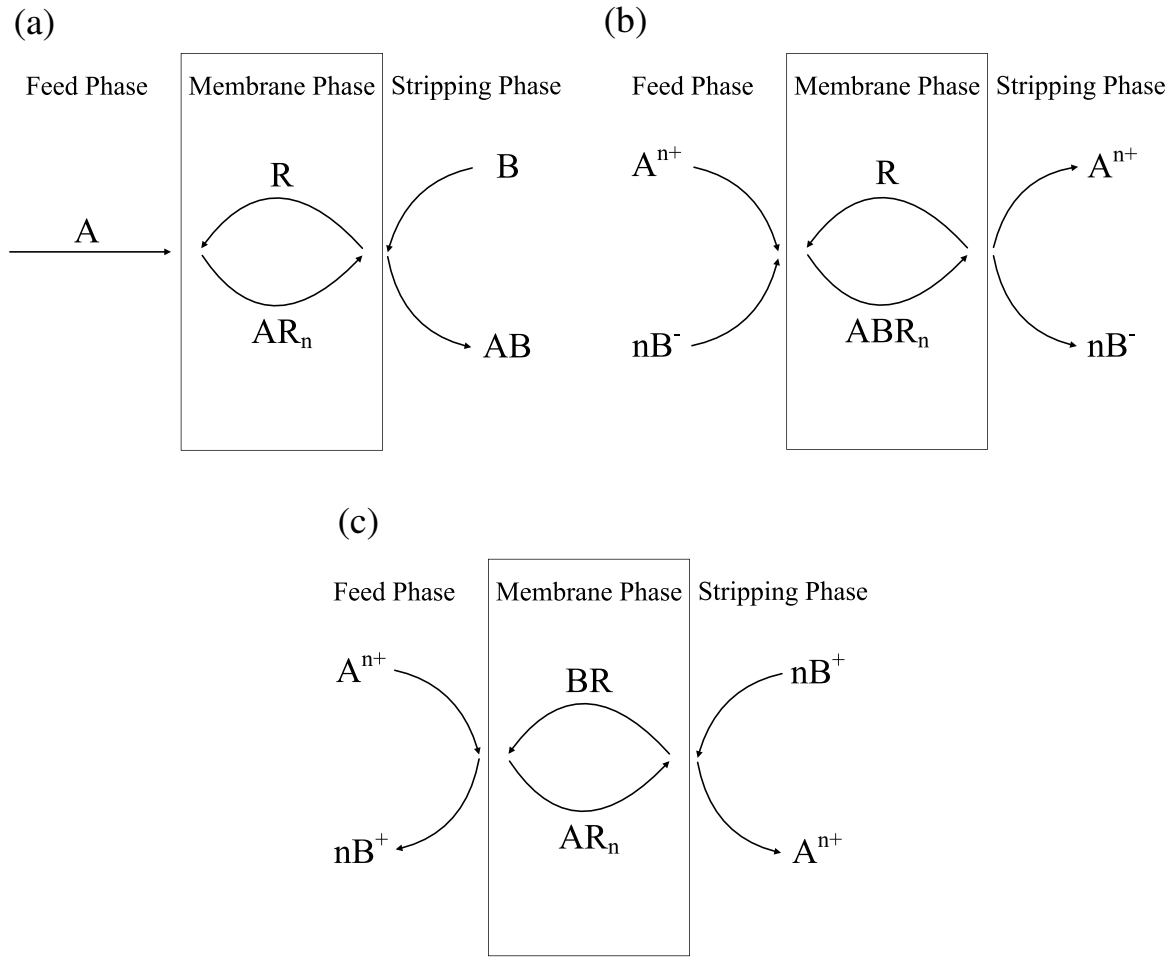

Figure 3.16: Transport mechanism in carrier-mediated permeation: simple carrier mediated transport (a), carrier mediated co-transport (b), and carrier mediated counter- transport (c). Adapted from [47].

3.3.3. Transport mechanism of the isolation of lignosulfonates using supported liquid membrane technology

Kontturi et al. have proposed the reaction mechanism for the extraction of lignosulfonates from aqueous solution using supported liquid membranes with amines as extraction agent, where bars indicate species in the organic membrane phase. In a first step, Eq. (3.15), the ion exchanger (amine hydrochloride) is prepared by the reaction of the amine with hydrochloric acid (HCl). [19,27]

$$\overline{R_3N} + HCl \leftrightarrow \overline{R_3NH^+Cl^-} \tag{3.15}$$

The reaction between the lignosulfonates and the ion exchanger is given in Eq. (3.16). [19,25]

$$\overline{R_3NH^+Cl^-} + LSNa_n \leftrightarrow \overline{R_3NHLSNa_{(n-1)}} + NaCl \tag{3.16}$$

, where $\overline{R_3N}$ is the amine and $LSNa_n$ is sodium lignosulfonate.

In case of the reaction on the stripping side of the liquid membrane it is necessary to distinguish between co-transport, Eq. (3.17), and counter-transport, Eq. (3.18), which in turn depends on the stripping agent used. When sodium hydroxide (NaOH) is used, Eq. (3.17), co-transport mode is observed, and when sodium chloride (NaCl) is used, Eq. (3.18), counter transport takes place. [19,25]

$$\overline{R_3NHLSNa_{(n-1)}} + NaOH \leftrightarrow \overline{R_3N} + LSNa_n + H_2O \tag{3.17}$$

$$\overline{R_3NHLSNa_{(n-1)}} + NaCl \leftrightarrow \overline{R_3NH^+Cl^-} + LSNa_n \tag{3.18}$$

Figure 3.17 a shows the co-transport mode and Figure 3.17 b displays the counter transport mode in lignosulfonate extraction using supported liquid membrane technology. [25]

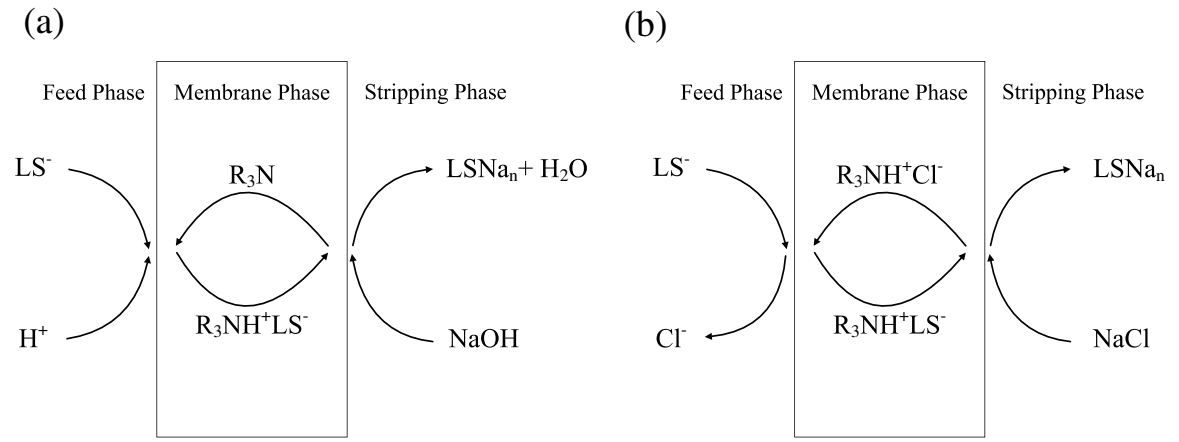

Figure 3.17: Co-transport model (a) and counter-transport model (b) for lignosulfonate extraction using supported liquid membranes. Adapted from [25].

4. Materials and methods

4.1. Used chemicals and materials

Table 4.1 and Table 4.2 show the specifications of the amines and other chemicals used in the experiments of the present thesis. In addition, Table 4.3 lists all utilized devices and materials.

Table 4.1: Specification of the amines used as reactive agent.

Substance	Formula	CAS number	Supplier	Purity
Di-hexylamine	$[CH_3(CH_2)_5]_2NH$	143-16-8	Sigma Aldrich	97 %
Tri-hexylamine	$[CH_3(CH_2)_5]_3N$	102-86-3	Sigma Aldrich	96 %
Octylamine	$CH_3(CH_2)_7NH_2$	111-86-4	Sigma Aldrich	99 %
Di-octylamine	$[CH_3(CH_2)_7]_2NH$	1120-48-5	Sigma Aldrich	97 %
Tri-octylamine	$[CH_3(CH_2)_7]_3N$	1116-76-3	Sigma Aldrich	98 %
Decylamine	$CH_3(CH_2)_9NH_2$	2016-57-1	Sigma Aldrich	95 %
Aliquat336	$[CH_3(CH_2)_7]_3NCH_3Cl$	63393-96-4	Alfa Aesar	-
Dodecylamine	$CH_3(CH_2)_{11}NH_2$	124-22-1	Sigma Aldrich	98 %
Di-dodecylamine	$[CH_3(CH_2)_{11}]_2NH$	3007-31-6	Sigma Aldrich	≥ 97 % (GC)
Tri-dodecylamine	$[CH_3(CH_2)_{11}]_3N$	102-87-4	Sigma Aldrich	≥ 97 % (GC)

Table 4.2: Specifications of utilized chemicals.

Substance	Formula	CAS number	Supplier	Purity	Additional information
Sodium hydroxide	NaOH	1310-73-2	Carl Roth	≥ 32 %	GC
Sulfuric acid	H_2SO_4	7664-93-9	Sigma Aldrich	95-97 %	
1-octanol	$C_8H_{18}O$	111-87-5	Carl Roth	≥ 99 %	GC
Lignosulfonic acid sodium salt	Na-LS	8061-51-6	Sigma Aldrich	-	M_w ~ 52000, M_n ~ 7000
Lignosulfonic acid calcium salt	Ca-LS	8061-52-7	Sigma Aldrich	-	M_w ~ 18000, M_n ~ 2500
pH 4 buffer	-	585-29-5	Hamilton Duracal	-	pH 4.01 ± 0.02 (25 °C)
pH 7 buffer	-	7558-79-4	Carl Roth	-	pH 7.00 ± 0.02 (20 °C)
pH 10 buffer	-	-	Hamilton	-	pH 10.01 ± 0.02 (25 °C)
pH 12 buffer	-	-	Reagecon	-	pH 12.454 ± 0.05 (25 °C)

Table 4.3: List of devices and materials.

Device/material	Manufacturer	Identification	Additional information
Ultrasonic bath	Elma	S300 Elmasonic	Ultrasonic frequency: 37 kHz
Laboratory shaker	Janke & Kunkel GMBH & CO.KG IKA-Labortechnik	HS500	Speed 10 – 300 min^{-1}
Thermostat	Lauda	RE 206	Temperature stability 0.01 °C
Photometer	Shimadzu	UV-1800	
Photometer temperature control and cell positioner	Shimadzu	CPS-240A	
UV-cuvettes		UV-Cuvette makro	12.5x12.5x45 mm, 3 ml
pH meter	WTW	Inolab pH level	
pH electrode	SI Analytics	A 164 1 M DIN ID	Reference system: Silamid®, material: glass, d_o = 12 mm, electrolyte: KCl 3 M, pH 0-14
PE support layer hydrophobic	Porex	XS-96191	Polyethylene (PE), 7-12 µm, hydrophobic, pore volume > 35 %

Device/material	Manufacturer	Identification	Additional information
PE support layer hydrophilic	Porex	XS-8259	Polyethylene (PE), 7-12 µm, hydrophilic, pore volume > 35 %
PTFE seal small scale reactor	Ammerflon®		PTFE-flat gasket band, 3x1.5 mm, 25 meter/role
Peristaltic pump for lab-scale reactor	ISMATEC	Reglo Digital ISM834C	8 pump roles
Hoses for ISM834C	ISMATEC	SC0224T	Tygon, d_i = 3.17 mm, flow rate 0.35-35 ml·min^{-1}
Peristaltic pump for tubular reactor	ISMATEC	ISM1091	Consists of ISM1077 ECOLINE drive and MF0313 Easy-Load pump head, 3 pump roles
Hoses for ISM1091	Cole-Parmer	Masterflex Tygon L/S 17	GZ-06475-17
Superglue	Loctite	Gel Max Power Flex	
Epoxy resin glue	R&G Faserverbundwerkstoffe GmbH	Epoxyharz L and Härter L	

4.1.1. Characterization of the spent sulfite liquor feed

The spent sulfite liquor used in the experiments had acidic pH and lignosulfonates were present with magnesium as counter ion. Table 4.4 gives the main feed characteristics provided by the supplier Sappi.

Table 4.4: Characterization of spent sulfite liquor feed.

Supplier	Sappi	
pH	3.7	
Density	1.059	[kg·l^{-1}]
Dry matter content	12.62	[%]
LS content	97	[g·l^{-1}]
Phenol content	2350	[mg·l^{-1}]
Xylose	0.17 / 0.2	[%] / [g·l^{-1}]
Mannose	2.24 / 3	[%] / [g·l^{-1}]

4.1.2. Preparation of phases

In all extraction experiments three phases were required: the feed, the solvent/membrane, and the stripping phase. The feed phase was either untreated spent sulfite liquor or model solutions containing a certain amount of sodium or calcium lignosulfonic acid salt dissolved in ultrapure water, the resulting concentration is stated $c_{LS,0}$ [g·l^{-1}]. The pH adjustment of the model solutions was done with concentrated or 1 M sulfuric acid.

The solvent/membrane phases were prepared by dissolving the required amount of amine, considering its purity, in the respective amount of 1-octanol, which was regarded as pure ($\geq$ 99 %). In addition, one solvent/membrane phase was prepared by shaking equal volumes of 0.05 M TOA solution in 1-octanol and 1 M HCl for 5 minutes. To remove excess HCl, the solvent/membrane phase was washed twice with ultrapure water. This solvent/membrane phase is defined as TOAH.

As stripping solution 0.3 M NaOH solution was used prepared with a 37 % NaOH and ultrapure water.

4.2. Analysis

The concentration of lignosulfonate can be measured using UV-Vis spectroscopy. Lignosulfonates show two strong absorption bands at 210 nm and 280 nm because of the present chromophoric groups and aromatic ring structures. The peak at 280 nm results from the presence of guaiacyl (G) units. More G units and also a higher quantity of conjugated structures result in a redshift of this peak. Further, the wavelength of both bands changes with changing conditions of the pulping process. [4,53] Figure 4.1 and Figure 4.2 show the UV-Vis spectra of sodium lignosulfonates (Na-LS), calcium lignosulfonates (Ca-LS) and spent liquor in ultrapure water and 0.3 M NaOH, respectively.

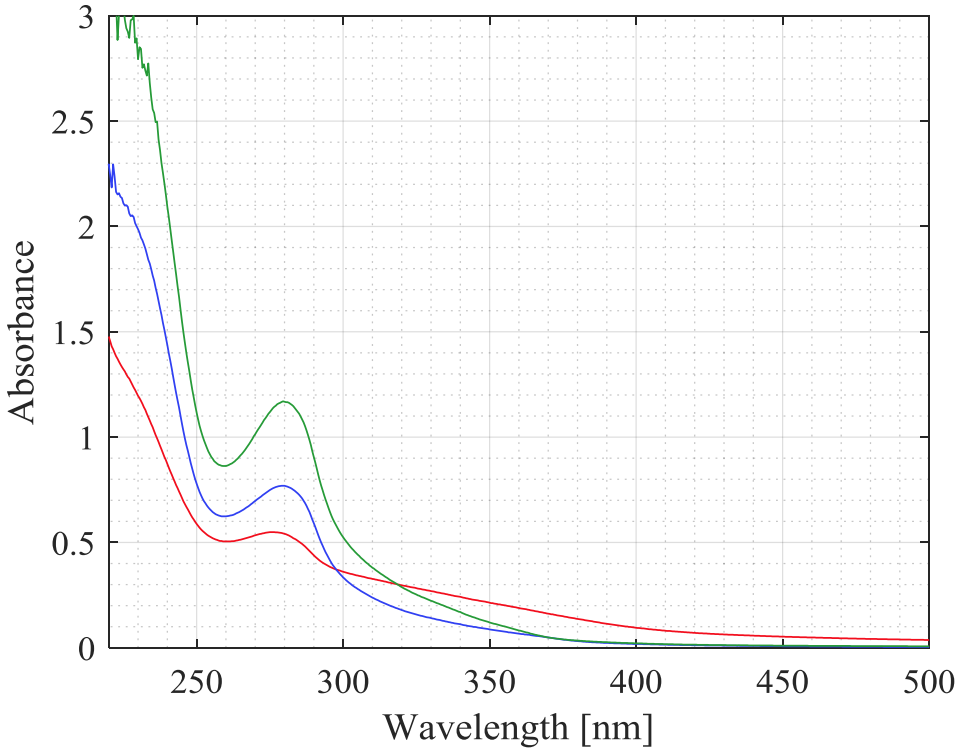

Figure 4.1: UV-Vis spectra of Na-LS (red), Ca-LS (blue) and spent liquor (green). Samples were diluted with ultrapure water, and measured at T = 25 °C and ambient pressure.

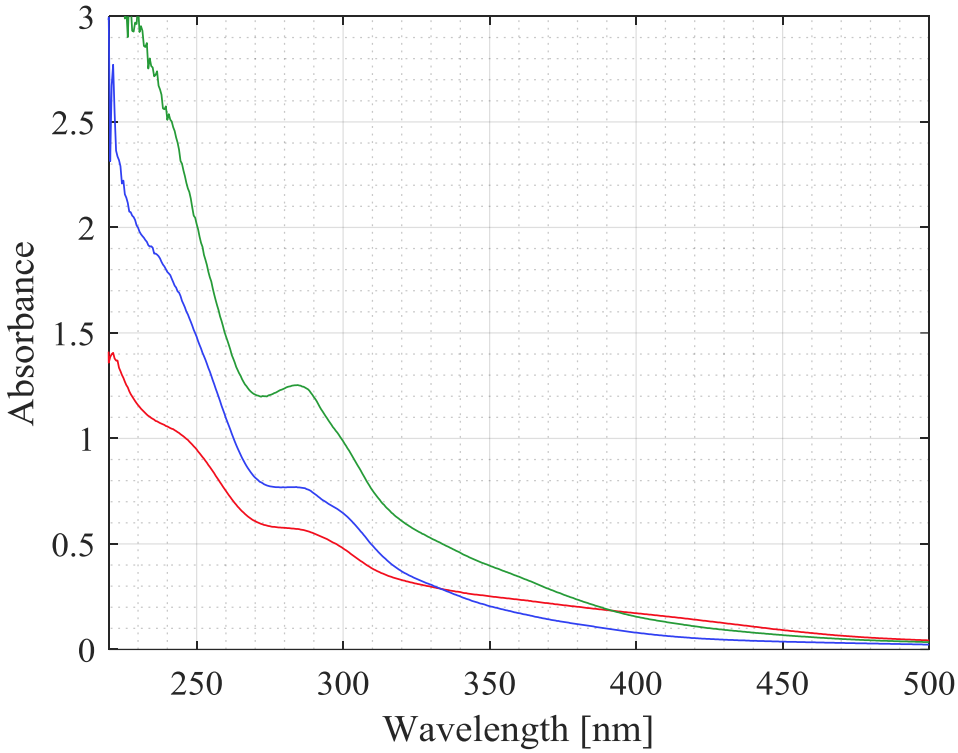

Figure 4.2: UV-Vis spectra of Na-LS (red), Ca-LS (blue) and spent liquor (green). Samples were diluted with 0.3 M NaOH, and measured at T = 25 °C and ambient pressure.

For determination of the lignosulfonate concentration in the aqueous phase calibration curves for Na-LS and Ca-LS were recorded. High lignosulfonate concentrations occurring in the feed phases required a dilution of up to 1:1000, whereas lignosulfonate concentrations in the stripping phase were low and no dilution at all was required. In addition, the pH value had to be constant for all measurements. This led to the decision that all samples were measured in 0.3 M NaOH, which was also used as stripping phase in the extraction experiments, although a slight redshift is observed for spent liquor in 0.3 M NaOH.

The mathematical basis for the concentration measurement using UV-Vis spectroscopy is the Bouguer-Lambert-Beer law given in Eq. (4.1).

$$\log\left(\frac{I_0}{I}\right) \equiv A = \varepsilon \cdot c \cdot d \tag{4.1}$$

, where I_0 represents the intensity of the monochromatic light entering the sample, I the intensity of the light after passing the sample, A the absorbance, ε [$l \cdot g^{-1} \cdot cm^{-1}$] the extinction coefficient, c [$g \cdot l^{-1}$] the concentration of the light-absorbing species, and d [cm] the path length of the light within the sample. [54] By transformation of Eq. (4.1), an expression for the concentration is obtained, Eq. (4.2). [54]

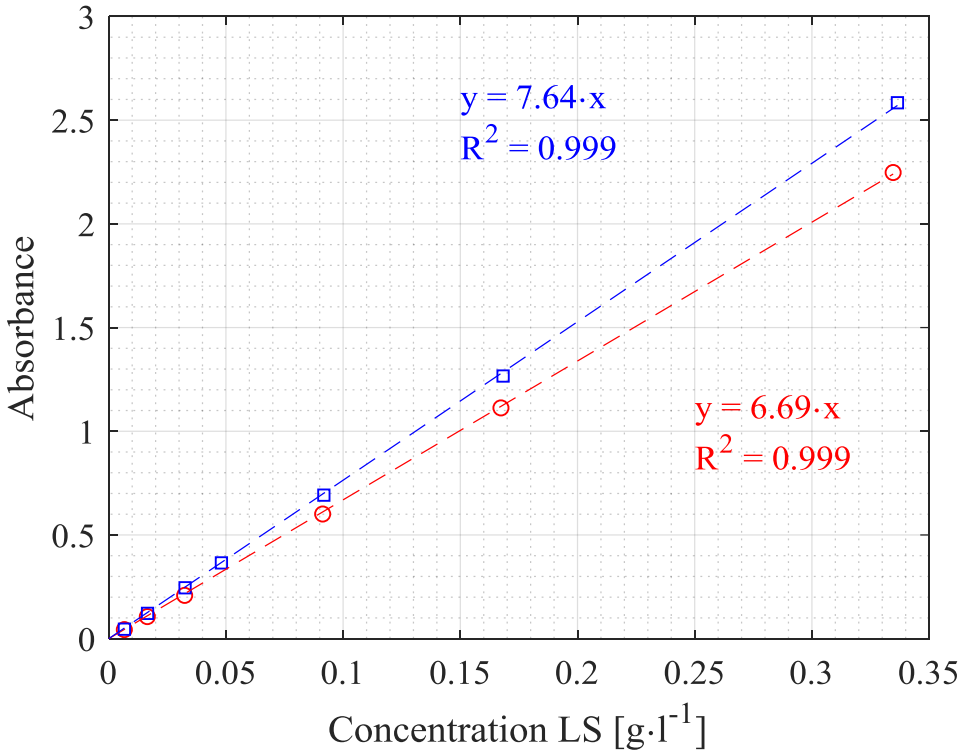

Figure 4.3: Calibration curve of Na-LS (○ red) and Ca-LS (□ blue) for concentration measurement in 0.3 M NaOH using UV-Vis spectroscopy (T = 25 °C, ambient pressure).

$$c = \frac{A}{\varepsilon \cdot d} \tag{4.2}$$

Since ε depends on the species analyzed, a calibration curve for Na-LS and Ca-LS was recorded by preparing solutions with known concentrations of lignosulfonates and measuring the absorbance. Figure 4.3 depicts the calibration curves for Na-LS and Ca-LS.

For a constant path length d the slope in the diagram showing the concentration on the x-axis and the absorbance on the y-axis is equal to ε. The lignosulfonates in the spent liquor are present as magnesium lignosulfonates. Here the extinction coefficient according to literature was applied [19]. Table 4.5 summarizes the three different extinction coefficients used for calculating the lignosulfonate concentrations in the experiments conducted in the present thesis.

Table 4.5: UV-Vis extinction coefficients, ε, for Na-LS, Ca-LS and LS present in spent liquor at 280 nm [19].

ε_{Na-LS}	6.69	[l·g^{-1}·cm^{-1}]
ε_{Ca-LS}	7.64	[l·g^{-1}·cm^{-1}]
$\varepsilon_{LS\ spent\ liquor}$	13.2	[l·g^{-1}·cm^{-1}]

As already mentioned above, the UV-absorption of lignosulfonate molecules varies with different process conditions which leads to fluctuations in the concentration measurement [4,53]. To verify the standard deviation for the lignosulfonate concentration and pH measurement, a Ca-LS solution and spent liquor were placed in an air-tight container at 25 °C and ambient pressure, and regular measurements were conducted over 579 hours. Both solutions had a starting concentration of 100 $g \cdot l^{-1}$. Table 4.6 shows the corresponding results.

Table 4.6: LS concentration ($c_{LS,mean}$) and pH of Ca-LS and spent liquor in an air-tight container at 25 °C and ambient pressure over 579 hours to verify the standard deviation (σ) of UV absorption measurements.

	$c_{LS,mean}$ [$g \cdot l^{-1}$]	σ_{conc} [$g \cdot l^{-1}$]	$c_{LS,min}$ [$g \cdot l^{-1}$]	$c_{LS,max}$ [$g \cdot l^{-1}$]	pH	σ_{pH}	pH_{min}	pH_{max}
Ca-LS	100.1	3.48	93.6	105.9	3.69	0.03	3.66	3.75
Spent liquor	97.2	3.50	90.5	106.0	3.62	0.03	3.58	3.67

For the concentration, 10 measurements with triple determination were conducted over 579 hours resulting in 30 measurement points in total. The standard deviation for the Ca-LS model solutions is 3.48 $g \cdot l^{-1}$ and for the spent liquor 3.50 $g \cdot l^{-1}$. However, the difference between the minimum and maximum concentrations is 12.3 $g \cdot l^{-1}$ respectively 15.5 $g \cdot l^{-1}$, and therefore, results for the lignosulfonate concentration obtained by UV-Vis spectroscopy comprises a certain error which in this case is higher than twice the standard deviation.

Other than the concentration, the pH value shows higher accuracy for both solutions, the corresponding standard deviation is 0.03 for the Ca-LS solution and the spent liquor.

4.3. Setups used for the extraction of lignosulfonates

The isolation of lignosulfonates was conducted using the experimental setups illustrated in the following section. The experimental procedure is outlined in section 4.4.

4.3.1. Separation funnels for equilibrium measurements

In the first step, phase equilibria of lignosulfonates between the aqueous and the solvent phase were investigated. This was done in 6 double-walled separation funnels (Figure 4.4 a) with a volume of 100 ml each. For temperature control, a thermostat was connected to the funnels. To ensure the same intense phase contact for all experiments, the funnels were mounted on an automatic laboratory shaker (Figure 4.4 b).

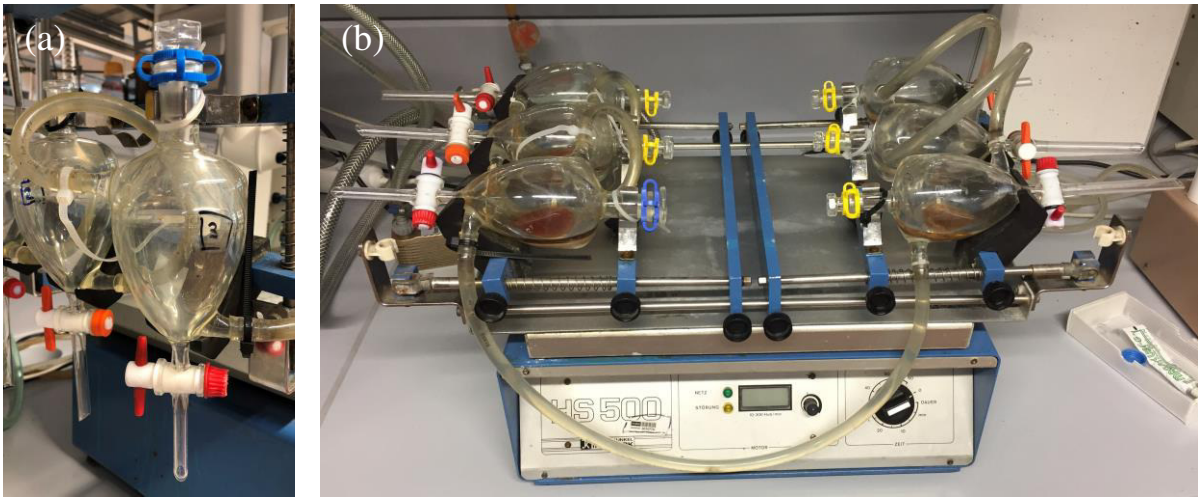

Figure 4.4: Experimental setup for equilibrium measurements. Six double-walled separation funnels (a) mounted on a laboratory shaker (b).

4.3.2. U-tube setup

Figure 4.5 depicts the configuration of the U-tube setup used in the first three-phase extraction experiment.

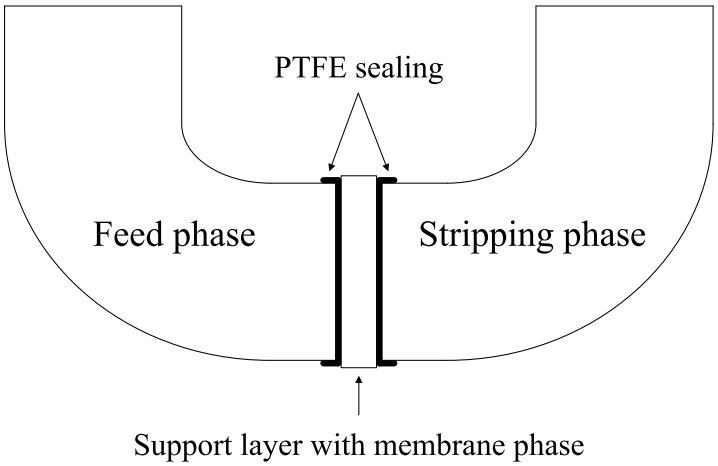

Figure 4.5: Principle construction of the U-tube setup used for three-phase extraction experiments.

In Figure 4.6 a, the different parts building up the U-tube are displayed. The two tubes (6) were held together using flanges (3) with three screws (4). To prevent breakage of the glass tubes, a protection material (5) was used between the tubes and the flanges. The support layer, PE 7-12 µm hydrophobic, (2) was placed between the two glass parts, each covered with a PTFE seal (1) to prohibit leakage. The screws were hand-tight tightened without destroying the support layer. In order to prevent loss of solution due to evaporation, both ends of the U-tube were covered with parafilm.

The tubes had an inner diameter of 1.7 cm which results in an effective membrane area of 2.27 cm^2. With the volume of the aqueous phases of 15 ml each, the exchange area to feed volume ratio results in 0.15 $cm^2 \cdot cm^{-3}$.

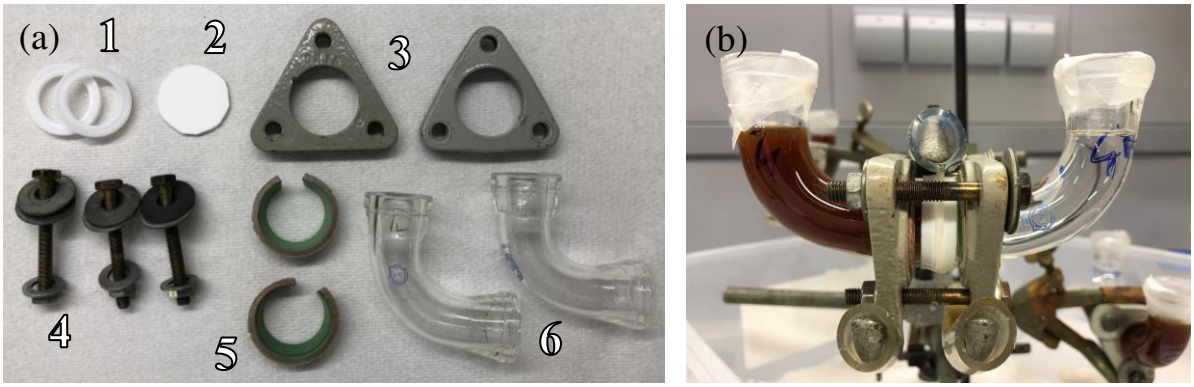

Figure 4.6: Different components of the U-tube setup (a): PTFE seal (1), PE support layer 7-12 µm hydrophobic (2), clamps (3), screws (4), protection material (5), and glass tubes (6). Mounted U-tube setup (b).

4.3.3. Small-scale membrane reactor

To increase the exchange area to feed volume ratio, the small-scale membrane reactor configuration was used. Figure 4.7 depicts the setup which was made of PVC and consisted of three main components: two compartment modules (1,3) and one membrane module (2). The three parts were held together with 5 threaded rods.

The membrane module (Figure 4.8) had an effective membrane area of 25 cm^2 and possessed one inlet and one outlet for re-impregnation of the support layer. Hydrophobic and hydrophilic

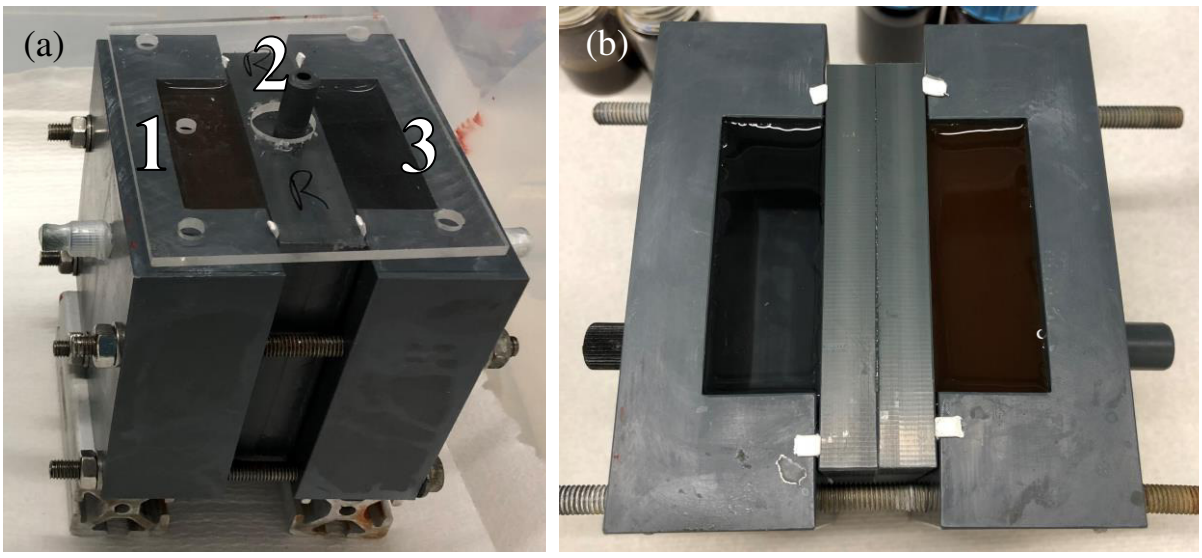

Figure 4.7: Setup of the small-scale laboratory membrane reactor (a) consisting of two compartment modules (1,3) and one membrane module (2). Top view of the membrane cell (b).

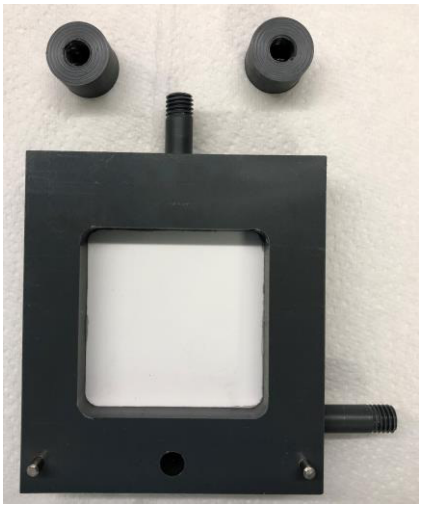

Figure 4.8: Membrane module of the small-scale membrane reactor with in- and outlet for re-impregnation of the support layer, and two PVC screws to seal the in- and outlet.

PE support layers were glued into the membrane module using an epoxy resin glue or superglue. To prevent membrane phase loss when the membrane phase was not continuously pumped through the membrane module, some modules were equipped with a thread on the inlet and outlet tubes to enable sealing with corresponding screws made of PVC (Figure 4.8). The volume of each compartment module was 99.5 ml. For continuous operation, the compartment modules were equipped with inlets and outlets. The exchange area to feed volume ratio of this membrane reactor is 0.25 $cm^2 \cdot cm^{-3}$.

To set up the small-scale reactor, 3 x 1.5 mm self-bonding PTFE seal (Ammerflon®) was attached to the two compartment modules, the membrane module was placed in between and the 5 screws were tightened until the seal was compressed as shown in Figure 4.7 b. In order to ensure high leakproofness, the surfaces were thoroughly cleaned with acetone in advance.

4.3.4. Lab-scale membrane reactor

Up to this point all setups were operated in batch mode. To conduct the lignosulfonate extraction in continuous operation mode, the lab-scale membrane reactor setup was used. Figure 4.9 a shows its configuration consisting of the feed (2) and stripping solution (3), the membrane module (4) which can be re-impregnated with membrane phase (5), and a peristaltic pump (1). The hoses connecting the membrane module with the two storage containers were HPLC hoses with corresponding screws wrapped with Teflon strap. The membrane module was mounted in vertical position and operated in co-current mode from bottom to top.

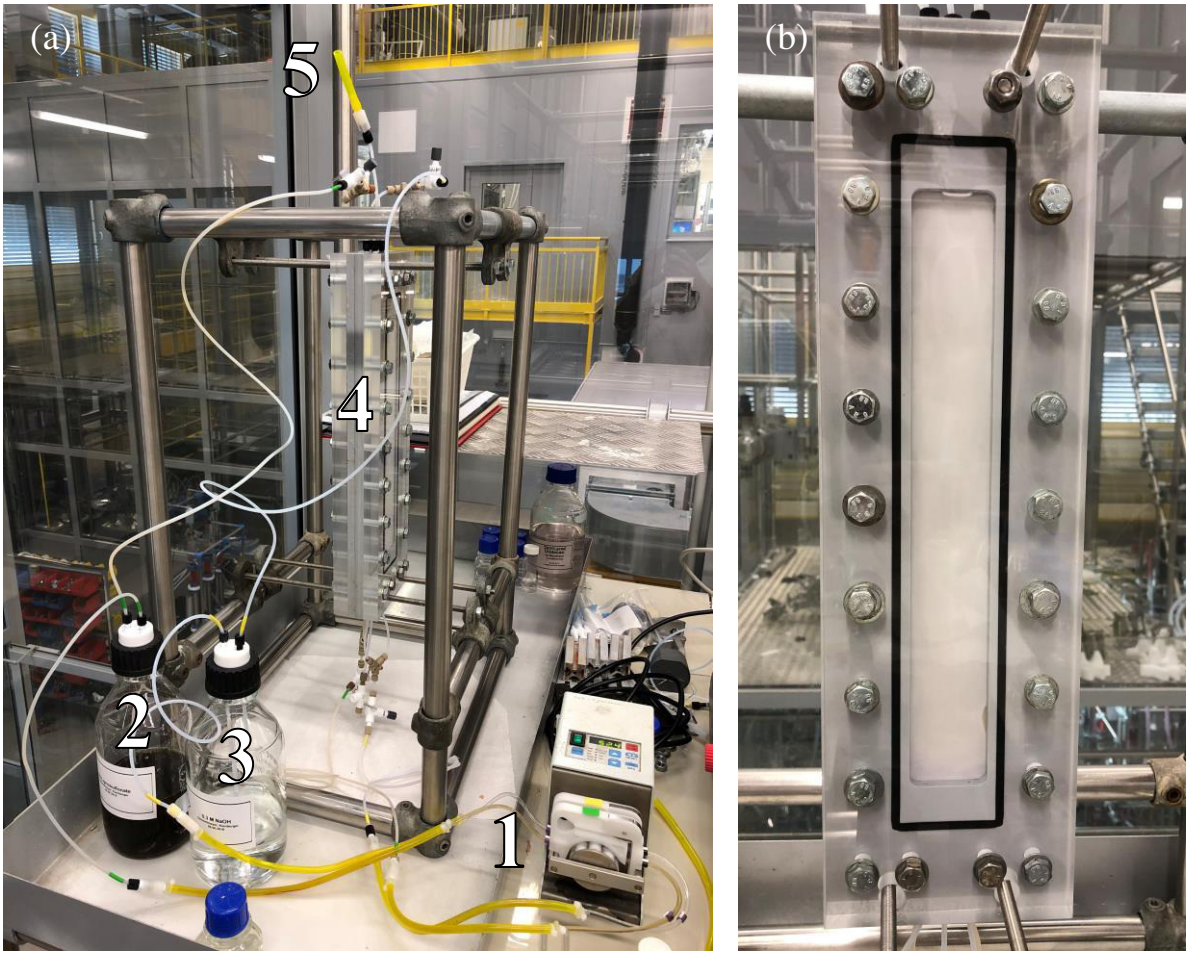

Figure 4.9: (a) Setup of the lab-scale membrane reactor: peristaltic pump (1), feed solution (2), stripping solution (3), membrane module (4), hose for re-impregnation of membrane phase (5). (b) Membrane module of the lab-scale membrane reactor.

Figure 4.9 b displays the membrane module which consisted of two Plexiglas® plates (thickness 20 mm) and the PVC frame holding the flat sheet support layer. The seal used between the Plexiglas® plates and the PVC module was made of viton (FKM-75, d_o = 3.5 mm) to ensure resistance against the used chemicals. The three parts were held together by 22 screws which had to be tightened carefully to prevent breakage of the Plexiglas® plates. Figure 4.10 shows the dimensions of the lab-scale membrane module. The effective membrane area of the module was 123 cm^2 and each compartment held 123 ml of aqueous phase. This results in an exchange area to feed volume ratio of 1.0 $cm^2 \cdot cm^{-3}$ in this reactor.

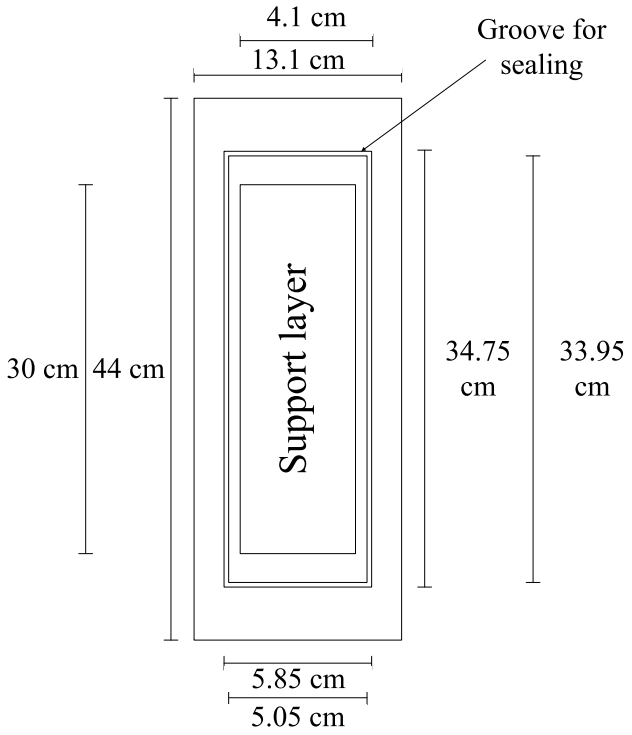

Figure 4.10: Dimensions of the membrane module in the lab-scale membrane reactor setup.

4.3.5. Tubular membrane reactor

The tubular membrane reactor was an item on loan from the company Memo3, Möhnlin Switzerland. This setup can only be operated in two-phase contact – a second module is necessary for the back-extraction – but it offers a significantly higher exchange area to feed volume ratio, compared to the lab-scale membrane reactor. Figure 4.11 shows the dimensions of the different parts of the tubular membrane reactor module.

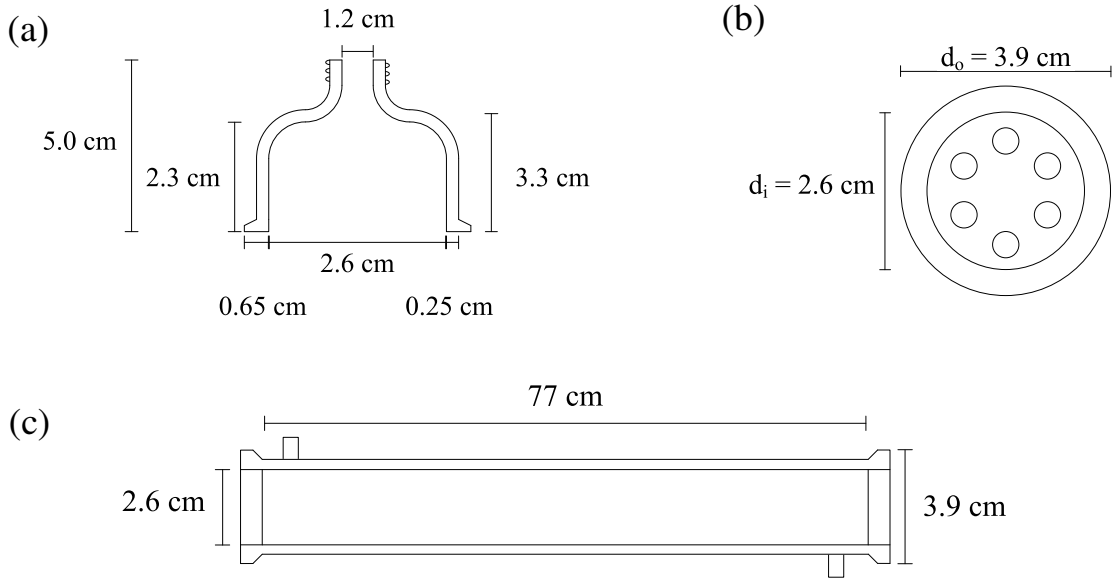

Figure 4.11: Dimensions of the different components of the tubular membrane reactor.

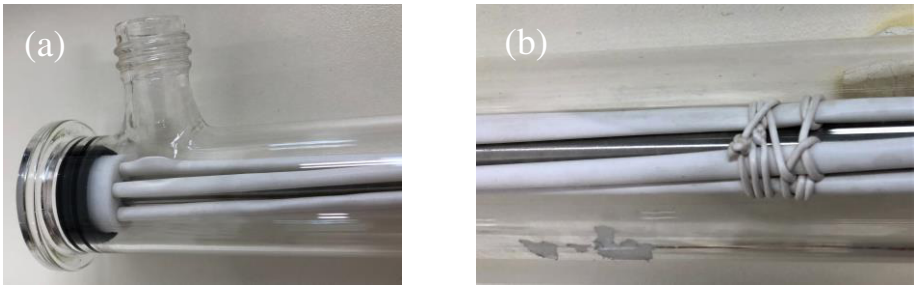

Figure 4.12: Installation of the PTFE hoses in the tubular membrane reactor (Memo3).

One module consisted of six PTFE hoses (d_o = 3 mm, d_i = 2.7 mm, pore size < 0.1 µm, porosity 50-70 %) in a glass tube. The hoses were fixed on a stainless-steel rod in the center of the module (Figure 4.12).

In operation, one phase was carried within the hoses and the other one outside, enabling the transfer of the targeted species through the support layer.

Both ends of the module were equipped with a glass cap (1) mounted with a link chain (3) and an O-ring (2) (Figure 4.13 a). It was mandatory to carefully tighten the screw at the link chain to prevent glass breakage. The PTFE hoses (d_o = 0.8 cm) connecting the module with the storage flasks were mounted using BOLA GL18 connections with PTFE seals. To prevent breakthrough, the outer aqueous phase was impinged with an overpressure of 80-100 mbar, which was adjusted with a BOLA valve and a pressure indicator (Figure 4.13 d).

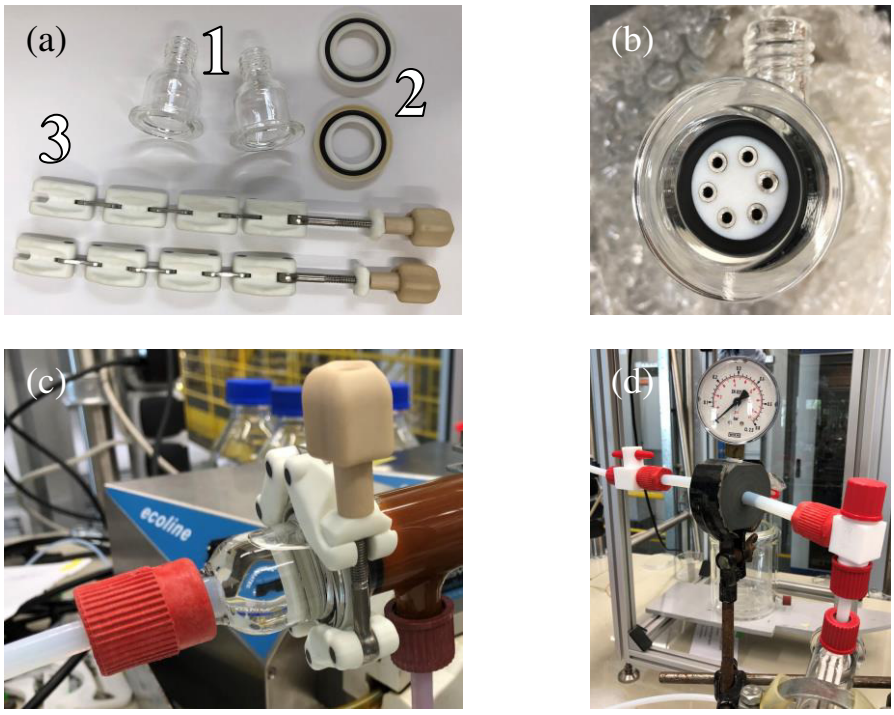

Figure 4.13: (a) Components of the tubular membrane reactor: Glass cap (1), O-ring seal (2) and link chain (3). (b) Fixture of the PTFE hoses. (c) Mounted glass cap on the module. d) Pressure control of the feed phase to prevent breakthrough.

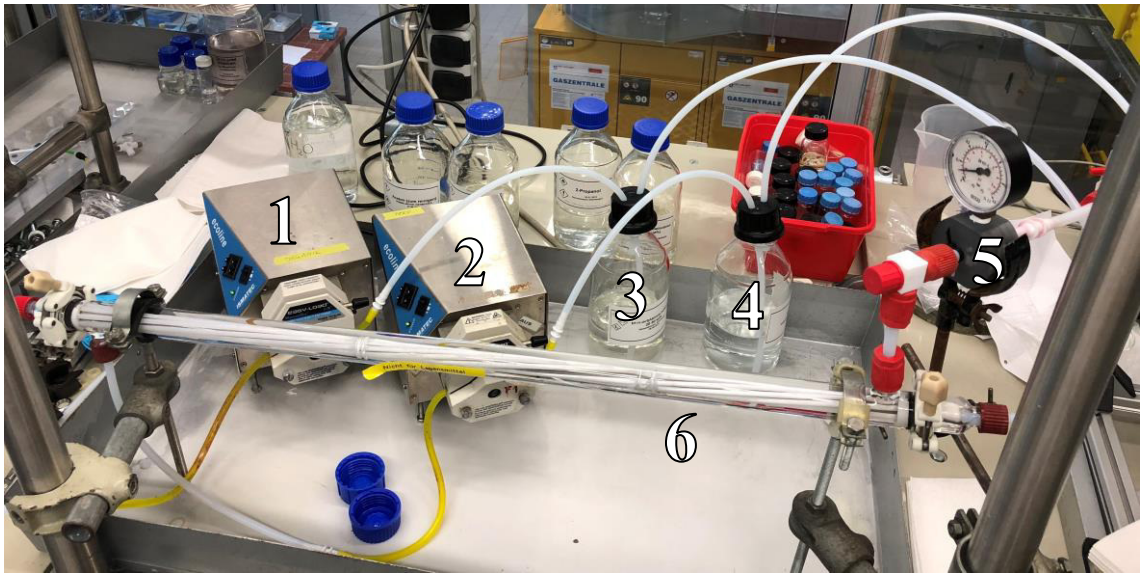

Figure 4.14: Complete setup of the tubular membrane reactor: Pump for membrane phase (1), pump for feed phase (2), membrane phase (3), feed solution (4), pressure control for aqueous phase (5), and tubular membrane module (6)

According to the specifications of the PTFE hoses the total surface area was 435 cm^2. Further, the volume of aqueous feed phase was 371 ml leading to an exchange area to feed volume ratio of 1.17 $cm^2 \cdot cm^{-3}$. Figure 4.14 shows the complete setup of the tubular membrane reactor.

4.4. Experimental procedure

4.4.1. Equilibrium measurements

For determination of the phase equilibria for extraction and back-extraction, 10 ml of feed and 10 ml of solvent phase were mixed together. The phases were measured in measuring cylinders on a precision scale to increase the accuracy of the experiments. After adjusting the temperature of the thermostat to 25 °C, the two solutions were thoroughly mixed for 30 minutes in the tempered separation funnels on the laboratory shaker (speed: 160 strokes per minute; ambient pressure). Thereafter, the funnels were brought into an upright position and phase separation was achieved by leaving the funnels to settle for 21 hours (temperature: 25 °C; ambient pressure). Finally, the two phases were separated and the lignosulfonate concentration and the pH value were measured in the aqueous phase.

The same procedure was performed for the back-extraction, with the difference that the volumes changed to 8 ml of loaded solvent phase from the extraction step and 8 ml of stripping phase. The reason for the difference in volumes was the crud formation in the extraction step. Thereby, some solvent phase was trapped in the crud and less solvent phase was available for the back-extraction step.

Figure 4.15 represents the flow chart of the whole experimental procedure for the equilibrium measurement. Lignosulfonate concentrations in the aqueous phases, $c_{LS,F,0}$, $c_{LS,F,1}$ and $c_{LS,S,3}$, were determined using UV-Vis spectroscopy at 280 nm with the extinction coefficients given in Table 4.5. The concentration in the solvent phase after extraction, $c_{LS,O,1}$, was determined by subtraction of the concentration in the feed phase after extraction, $c_{LS,F,1}$, from the initial feed concentration, $c_{LS,F,0}$. For the back-extraction step, $c_{LS,O,3}$ was calculated by subtraction of the concentration in the stripping phase after back-extraction, $c_{LS,S,3}$, from the concentration in the solvent phase after the extraction, $c_{LS,O,1}$. The initial lignosulfonate concentration in the organic, $c_{LS,O,0}$, and stripping phase, $c_{LS,S,0}$, is zero.

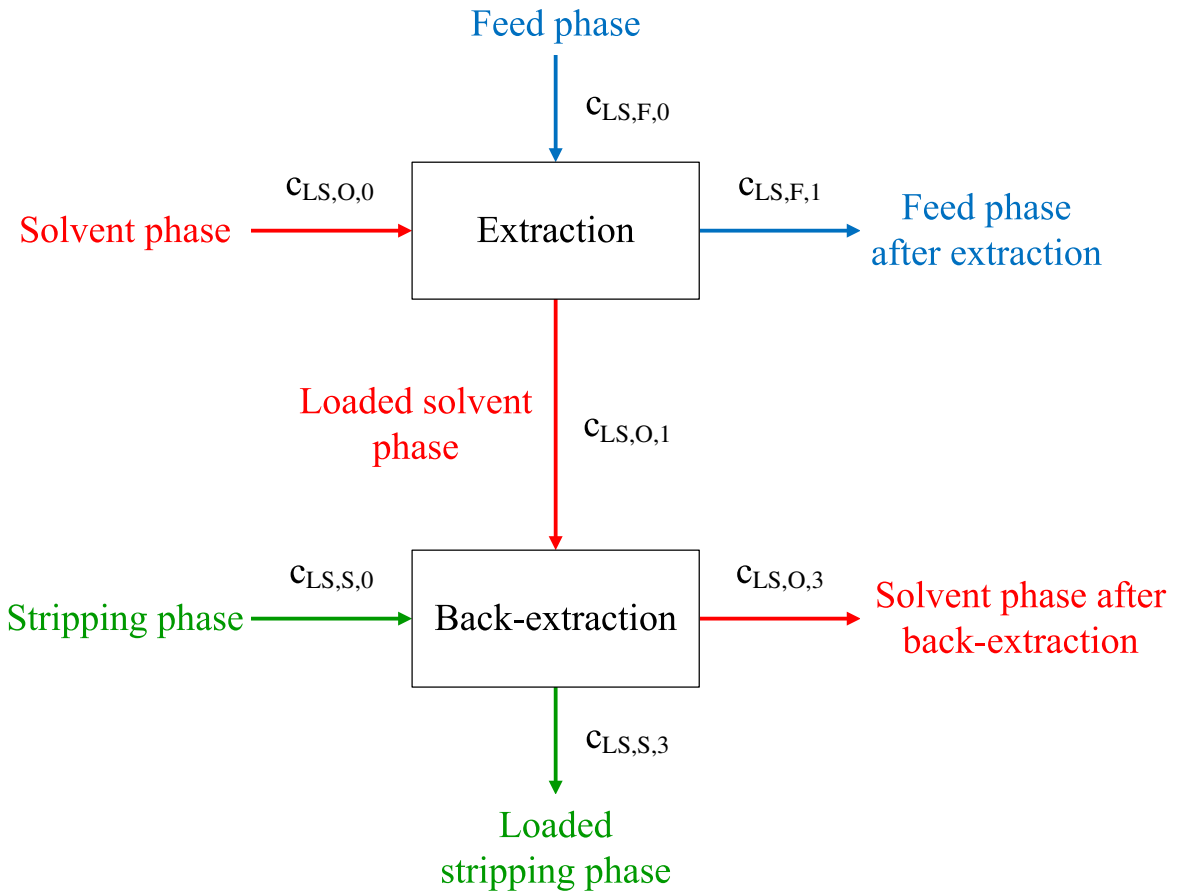

Figure 4.15: Flow chart of the equilibrium measurements in the separation funnels with the notation for the lignosulfonate concentration in the different phases.

4.4.2. Three phase contact in U-tube and small-scale membrane reactor

The first setup used for three phase experiments was the U-tube. At the beginning, the support layer had to be impregnated with the membrane phase. To ensure complete saturation of the pores, the support layer was immersed in membrane phase and placed in an ultrasonic bath for 30 min (Figure 4.16).

Thereafter, the U-tube was assembled as described in section 4.3.2, and 15 ml of the feed and the stripping phase were simultaneously filled into the two compartments. After 48 hours, the aqueous phases were poured into two small beakers and each solution was thoroughly mixed in order to guarantee constant, homogeneous conditions for evaluation of all experiments.

In case of the small-scale reactor, the support layer was impregnated by pouring the membrane phase onto the membrane module. As soon as the membrane phase left the support layer on the other side, it was assumed that the pores were saturated. After cleaning the frame of the membrane module with acetone, the setup was assembled as depicted in section 4.3.3. The two compartments were simultaneously filled with feed and stripping phase, and covered with parafilm to prevent evaporation. Measurements were performed in intervals over the incubation time.

For both setups, support layer cleaning to remove the solvent phase was done in a beaker filled with isopropanol placed in the ultrasonic bath. Residual lignosulfonates were removed with water.

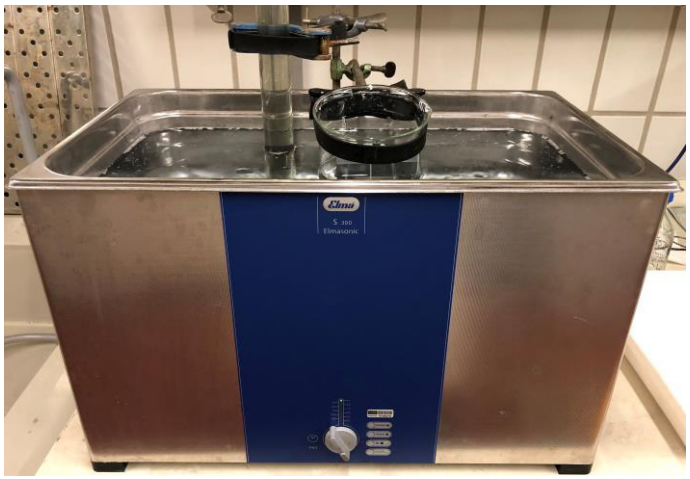

Figure 4.16: Ultrasonic bath with a beaker for complete impregnation of the support layer with membrane phase for the U-tube experiments.

4.4.3. Three phase experiments in continuous operation mode

The procedure for the lab-scale reactor was the same as for the small-scale reactor. After impregnation of the support layer with membrane phase, the setup was assembled as shown in section 4.3.4. The two storage flasks were connected to the membrane reactor as illustrated in Figure 4.17 and the peristaltic pump setting was adjusted to 50 which equals a flow rate of 0.58 $l \cdot min^{-1}$. In the experiments conducted in this thesis, the feed and stripping solutions were recycled back into the storage flask.

After simultaneous filling of the two compartments with aqueous solution, analysis of the feed and stripping phase was done in regular time intervals. In order to prevent breakthrough, the liquid membrane was continuously re-impregnated from the top. After the experiment, the support layer was cleaned with isopropanol and water.

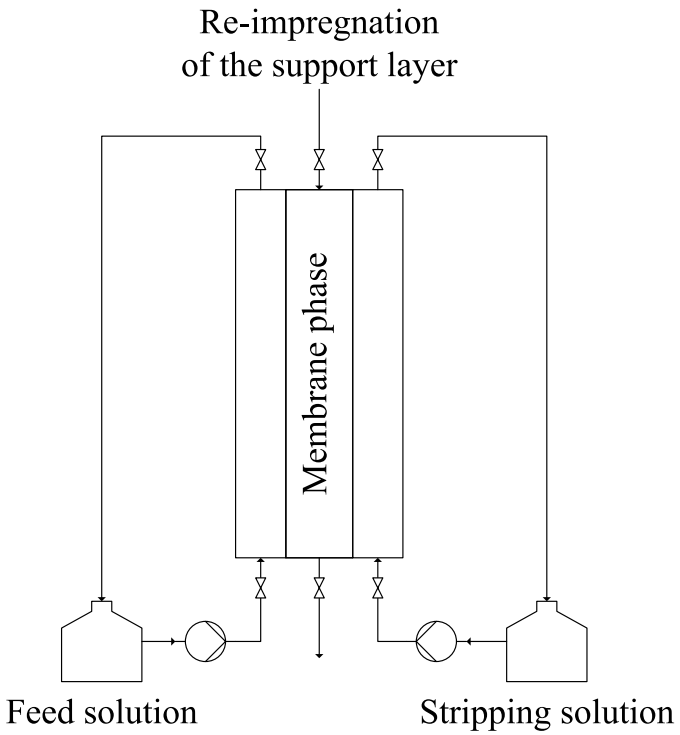

Figure 4.17: Flow chart of the lab-scale membrane reactor.

The final setup was the tubular membrane reactor. The first step after mounting the glass tube as shown in Figure 4.14 was to connect all hoses in the right manner as outlined in Figure 4.18.

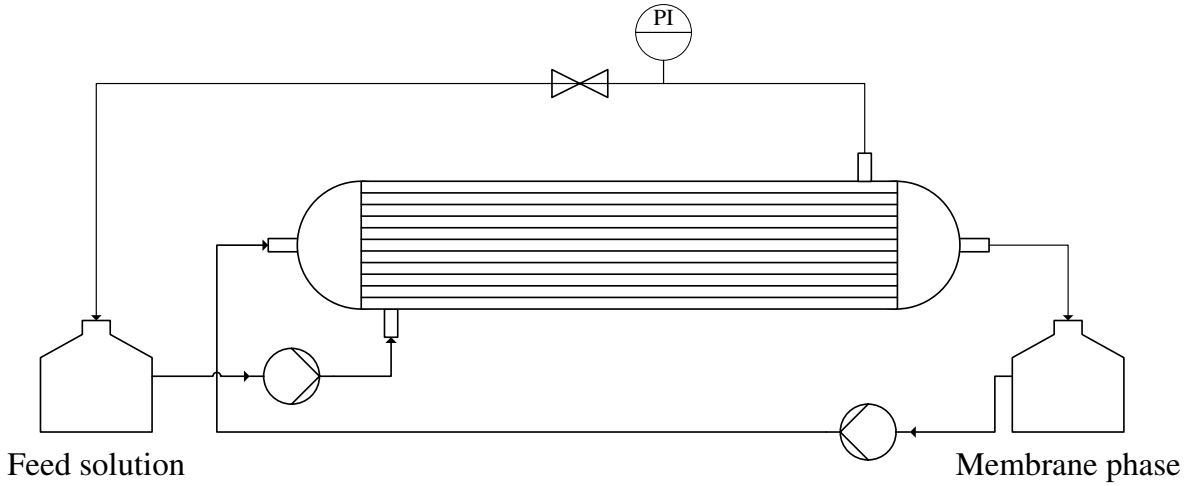

Figure 4.18: Flow chart of the tubular membrane reactor.

At first, the feed phase was continuously pumped through the jacket tube with an overpressure of 80-100 mbar and a flowrate of 2.5 $l \cdot min^{-1}$ without connecting the hoses of the membrane phase. In case no feed phase passed through the hydrophobic PTFE support layer hoses after half an hour, the membrane phase was introduced into the PTFE hoses with a flowrate of 0.73 $l \cdot min^{-1}$. During continuous operation, sampling of the feed phase was done in regular time intervals.

After the experiment, the module was rinsed with water to remove remaining lignosulfonates. Subsequently, the module was thoroughly cleaned with acetone until the PTFE hoses appeared translucent when soaked with acetone. In order to dry the module, it was flushed with pure nitrogen.

5. Results and discussion

5.1. Experimental matrix

Table 5.1 represents the experimental matrix summarizing all experiments conducted (x) in the present thesis.

Table 5.1: Experimental matrix for the reactive lignosulfonate extraction with different amines using different equipment. Equil…phase equilibrium measurement; small…small-scale membrane reactor; Lab…lab-scale membrane reactor; tubular…tubular membrane reactor; x…experiment conducted; -…experiment not performed.

Characteristics amine			Extraction equipment				
Substitution	C atoms	Name	Equil	U-tube	Small	Lab	Tubular
Primary	8	Octylamine (OA)	x	x	-	-	-
	10	Decylamine (DEA)	x	x	-	-	-
	12	Dodecylamine (DA)	x	x	-	-	-
Secondary	6	Dihexylamine (DHA)	x	x	-	-	-
	8	Dioctylamine (DOA)	x	x	-	-	-
	12	Didodecylamine (DDA)	-*	x	-	-	-
Tertiary	6	Trihexylamine (THA)	x	x	-	-	-
	8	Trioctylamine (TOA)	x	x	x	x	x
	8	Trioctylamine-HCl (TOAH)	-	x	-	-	-
	12	Tridodecylamine (TDA)	x	x	-	-	-
Quaternary	8-10	Aliquat336 (ALIQ)	x	x	-	-	-

* DDA solidified under the experimental conditions.

5.2. Phase equilibria

Prior to the comparison of the extraction efficiency for the different amines, the influence of the species of lignosulfonate in the feed and the initial feed pH value on the extraction process were determined using TOA as extractant. TOA showed to be suitable for the extraction of lignosulfonates from aqueous solution in several experiments described in the literature [15,20,25,55].

Table 5.2 shows the equilibrium concentrations for the lignosulfonate extraction with TOA:1-octanol (20:80 wt%) as solvent phase from model Na-LS solutions, with a starting concentrations, $c_{LS,0}$, between 0.1 and 100 $g \cdot l^{-1}$ and a starting pH, pH_{Feed}, of either 3.6-3.9 or 8.9-9.1. Comparing the concentrations in the feed, $c_{LS,F,1}$, and solvent phase, $c_{LS,O,1}$, after the

extraction step, it can be concluded that a higher amount of lignosulfonate is extracted into the solvent phase at lower pH values. Although the pH value for the back-extraction is the same for all experiments since 0.3 M NaOH is always used as stripping phase, a higher efficiency is observed for the acidic feed.

Table 5.2: Equilibrium concentrations (c_{LS}) for lignosulfonate extraction from Na-LS model solutions with different starting pH values using TOA:1-octanol (20:80 wt%) as extractant; alkaline: $pH_{feed,0}$ = 8.9-9.1; acidic: $pH_{feed,0}$ = 3.6-3.9; T = 25 °C; ambient pressure.
Indices: LS,0…initial feed concentration based on the weighted mass of LS. 1…extraction; 3…back-extraction; F…feed phase; O…solvent phase; S…stripping phase.

	Alkaline					Acidic				
$c_{LS,0}$ [g·l^{-1}]	$c_{LS,F,0}$ [g·l^{-1}]	$c_{LS,F,1}$ [g·l^{-1}]	$c_{LS,O,1}$ [g·l^{-1}]	$c_{LS,S,3}$ [g·l^{-1}]	$c_{LS,O,3}$ [g·l^{-1}]	$c_{LS,F,0}$ [g·l^{-1}]	$c_{LS,F,1}$ [g·l^{-1}]	$c_{LS,O,1}$ [g·l^{-1}]	$c_{LS,S,3}$ [g·l^{-1}]	$c_{LS,O,3}$ [g·l^{-1}]
0.1	0.08	0.05	0.03	0.03	0.00	0.10	0.05	0.05	0.05	0.00
1	0.95	0.82	0.13	0.08	0.05	0.91	0.34	0.57	0.50	0.07
15	15.3	14.4	0.85	0.29	0.55	12.7	7.24	5.51	5.48	0.03
30	27.5	27.3	0.19	0.53	N.A.*	26.5	15.6	10.9	10.3	0.61
50	47.2	45.1	2.11	1.03	1.08	43.2	25.5	17.7	17.7	0.02
100	93.0	87.9	5.07	1.53	3.54	91.6	53.0	38.6	32.9	5.74

* Not applicable because of an error in the UV-Vis measurement.

On the one hand, the higher lignosulfonate extraction under acidic conditions results in higher distribution ratios for the extraction step, $D_{A,extr}$, as shown in Table 5.3. On the other hand, a lower value is obtained for the back-extraction step, $D_{A,back\text{-}extr}$, for the acidic feed because of the definition of the distribution ratio given in Eq. (3.6). The extraction efficiency for the extraction step, E_{extr}, the back-extraction step, $E_{back\text{-}extr}$, and the total process, E_{tot}, is higher for the acidic feed. No results are shown for $D_{A,back\text{-}extr}$ and $E_{back\text{-}extr}$ for the experiment with $c_{LS,0}$ = 30 g·l^{-1} and alkaline conditions because of a measurement error in the UV-Vis measurement.

The outcome of this series of experiments fits well with the results obtained by Chakrabarty et al. [25]. They justified the higher extraction efficiency under acidic conditions with the protonation of TOA at the feed-membrane interface according to Eq. (3.15). The higher amount of protonated TOA molecules in the solvent phase increases the extraction efficiency of lignosulfonates according to Eq. (3.16). The incomplete protonation of TOA at high pH values causes low extraction efficiency for the alkaline feed.

Table 5.3: Distribution ratio (D_A) and extraction efficiency (E) for the extraction (extr), the back-extraction (back-extr) and the overall process (tot) for the lignosulfonate extraction from Na-LS model solutions with different starting pH values using TOA:1-octanol (20:80 wt%) as extractant; alkaline: $pH_{feed,0}$ = 8.9-9.1; acidic: $pH_{feed,0}$ = 3.6-3.9; T = 25 °C; ambient pressure; LS,0…initial feed concentration based on weighted mass of LS.

	Alkaline					Acidic				
$c_{LS,0}$ [g·l^{-1}]	$D_{A,extr}$	$D_{A,back-extr}$	E_{extr} [%]	$E_{back-extr}$ [%]	E_{tot} [%]	$D_{A,extr}$	$D_{A,back-extr}$	E_{extr} [%]	$E_{back-extr}$ [%]	E_{tot} [%]
0.1	0.62	0.14	38.3	87.9	33.7	1.12	0.00	52.9	100.0	55.6
1	0.16	0.59	13.6	62.9	8.6	1.67	0.14	62.5	88.1	55.1
15	0.06	1.89	5.5	34.7	1.9	0.76	0.00	43.2	100.0	43.0
30	0.01	N.A.*	0.7	N.A.*	1.9	0.70	0.06	41.0	94.4	38.7
50	0.05	1.05	4.5	48.9	2.2	0.70	0.00	41.0	99.9	41.0
100	0.06	2.31	5.5	30.2	1.6	0.73	0.17	42.1	85.1	35.9

* Not applicable because of an error in the UV-Vis measurement.

Beside the extraction efficiency, crud formation is a crucial factor for solvent extraction processes. The classification for crud formation is done based on the solutions shown in Figure 5.1. In Figure 5.1 a, no crud layer is detected, whereas Figure 5.1 b clearly shows a light-brownish layer of stable crud.

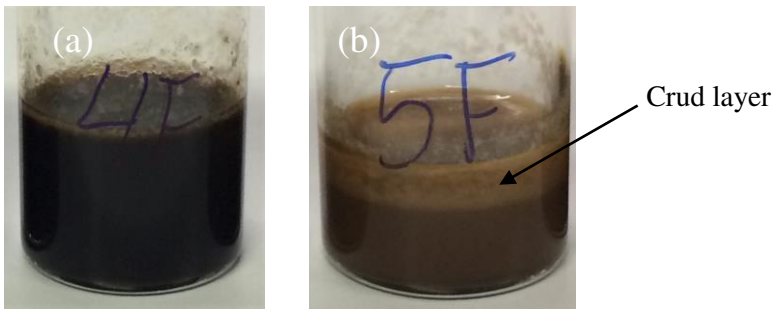

Figure 5.1: Visual evaluation of crud formation for lignosulfonate extraction from Na-LS model solutions with different starting pH values using TOA:1-octanol (20:80 wt%) as extractant; T = 25 °C; ambient pressure. The solution in vial (a) shows no crud layer under alkaline conditions ($pH_{feed,0}$ = 8.9-9.1), whereas in vial (b) high crud formation is observed for acidic conditions ($pH_{feed,0}$ = 3.6-3.9).

Table 5.4 summarizes the results for the visual evaluation of crud formation for the lignosulfonate extraction from alkaline and acidic Na-LS feed solution. No crud layer is observed for the extraction from alkaline feed solutions and the back-extraction of all experiments. This is in accordance with Kontturi and Sundholm [19] who stated that crud easily dissolves under alkaline conditions. For the extraction from acidic feed the crud formation increases with increasing lignosulfonate concentration in the feed solution.

Table 5.4: Visual evaluation of crud formation for lignosulfonate extraction from Na-LS model solutions with different starting pH values using TOA:1-octanol (20:80 wt%) as extractant; alkaline: $pH_{feed,0}$ = 8.9-9.1; acidic: $pH_{feed,0}$ = 3.6-3.9; T = 25 °C; ambient pressure; LS,0…initial feed concentration based on weighted mass of LS.

	Alkaline		Acidic	
$c_{LS,0}$ [g·l^{-1}]	Extraction	Back-extraction	Extraction	Back-extraction
0.1	NO	NO	NO	NO
1	NO	NO	LOW	NO
15	NO	NO	MEDIUM	NO
30	NO	NO	MEDIUM	NO
50	NO	NO	MEDIUM	NO
100	NO	NO	HIGH	NO

Since the extraction efficiency is higher under acidic conditions and the spent sulfite liquor used in this thesis has a pH of 3.6-3.7, further experiments are conducted at this pH range. In addition, the starting concentration of 100 g·l^{-1} is chosen since the lignosulfonate concentration in the spent liquor is in the range of 80-100 g·l^{-1} (Table 4.4).

To investigate the influence of the counter ion of lignosulfonates in the feed on the extraction process, lignosulfonate extraction with three different amines from solutions containing Na-LS and Ca-LS, respectively, were compared. The results for the distribution ratio, D_A, and the extraction efficiency, E, are shown in Table 5.5. Higher values of $D_{A,extr}$ and E_{extr} imply higher extraction efficiency for Na-LS solutions, whereas lower values of $D_{A,back\text{-}extr}$ and a higher $E_{back\text{-}extr}$ denote better performance of the back-extraction step for Ca-LS solutions. The overall extraction efficiency, E_{tot}, is found to be similar for the two lignosulfonates. Equilibrium concentrations are given in the appendix in Table 12.4.

Table 5.5: Comparison of the distribution ratio (D_A) and extraction efficiency (E) for the lignosulfonate extraction from Na-LS and Ca-LS model solutions using three different amines; $c_{LS,0}$ = 100 g·l^{-1}; $pH_{feed,0}$ = 3.75; T = 25 °C; ambient pressure; amine:1-octanol 20:80 wt%; extr…extraction; back-extr…back-extraction; tot…overall process.

LS	Amine	$D_{A,extr}$	$D_{A,back\text{-}extr}$	E_{extr} [%]	$E_{back\text{-}extr}$ [%]	E_{tot} [%]
Na-LS	OA	1.93	0.26	65.9	79.5	52.4
	DOA	1.18	0.26	54.1	79.1	42.8
	TOA	0.76	0.20	43.3	83.5	36.1
Ca-LS	OA	1.63	0.04	61.9	95.9	59.4
	DOA	0.84	0.02	45.5	97.7	44.5
	TOA	0.34	0.00	25.5	99.9	25.5

Comparing the crud formation for the experiments with Na-LS and Ca-LS solutions, crud is observed for both solutions, however, Ca-LS exhibits lower tendency to form a stable crud layer.

As lower crud formation is observed with Ca-LS solutions and spent liquor from the magnefite process contains lignosulfonates with magnesium, another divalent ion, as counter ion, further experiments are conducted using Ca-LS solutions with a concentration of 100 $g \cdot l^{-1}$ and a pH between 3.6-3.8.

Figure 5.2 represents the equilibrium concentrations for the lignosulfonate extraction from Ca-LS model solutions using different amines. In accordance with the findings of Kontturi and Sundholm [19], the lignosulfonate concentration in the solvent phase after the extraction step (light blue) decreases with increasing substitution of the nitrogen atom for primary, secondary and tertiary amines, which implies a decrease in the distribution ratio, $D_{A,extr}$, and extraction efficiency, E_{extr} (Table 5.6).

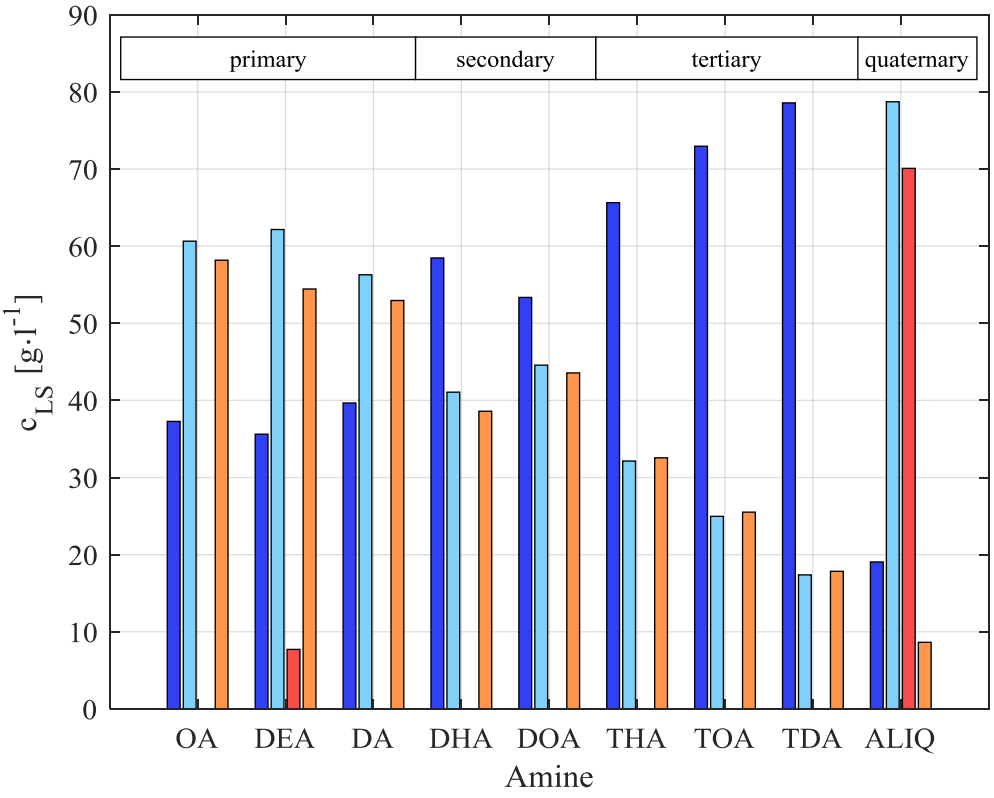

Figure 5.2: Equilibrium concentrations (c_{LS}) for lignosulfonate extraction from Ca-LS model solutions using different amines; $c_{LS,0}$ = 100 $g \cdot l^{-1}$; $pH_{feed,0}$ = 3.75; T = 25 °C; ambient pressure; amine:1-octanol 20:80 wt%. Blue: extraction (dark blue = feed phase; light blue = solvent phase), red/orange: back-extraction (red = solvent phase; orange = stripping phase), all data are given in equilibrium.

Frolov et al. explained this observation by the formation of intramolecular hydrogen bonds of unsubstituted amines which increase the extraction capacity [19,56,57]. The quaternary amine ALIQ does not fit into this trend since it shows a higher lignosulfonate concentration in the solvent phase than the primary amines. The back-extraction works best for tertiary amines, but $E_{back\text{-}extr}$ lies in the range of 94.0 and 99.9 % for all amines except for ALIQ which exhibits a back-extraction efficiency of 11.0 %. To enhance the efficiency of the back-extraction for ALIQ, a different stripping phase consisting of either ultrapure water or 0.1 M H_2SO_4 was applied.

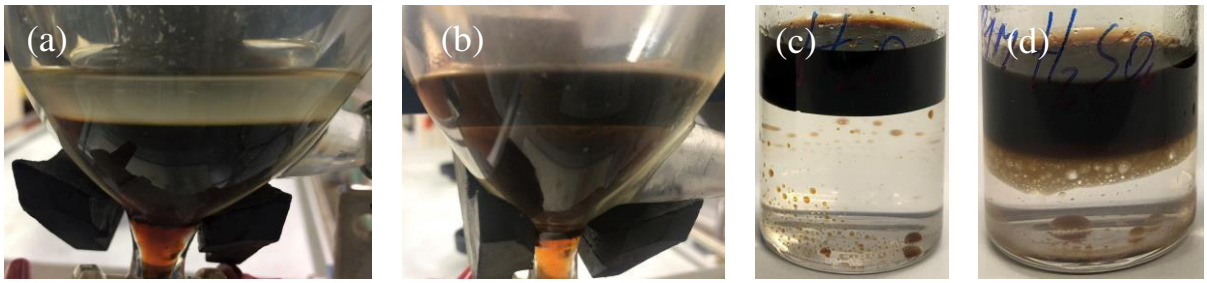

Figure 5.3: Back-extraction for TDA using 0.3 M NaOH (a) and for ALIQ using 0.3 M NaOH (b), ultrapure water (c) and 0.1 M H_2SO_4 (d) as stripping solution (T = 25 °C; ambient pressure). The aqueous stripping phase is the lower phase.

In Figure 5.3 a, the clear solvent phase (upper phase) indicates the complete back-extraction of lignosulfonates from TDA using 0.3 M NaOH as stripping phase. Figure 5.3 b shows the back-extraction for ALIQ using 0.3 M NaOH, where the dark brown solvent phase refers to the low $E_{back\text{-}extr}$ of ALIQ stated above. Figure 5.3 c and Figure 5.3 d show that the change in pH value of the stripping solution has no effect on the back-extraction and no lignosulfonates are transferred to the stripping phase indicated by the clear aqueous phase.

No clear dependence of the extraction efficiency on the chain length of the alkyl chains is observed for primary and secondary amines. However, for tertiary amines the extraction efficiency decreases with increasing alkyl chain length. Shanker et al. stated that the extraction efficiency of ruthenium(III) with long chain amines decreases with increasing chain length [58]. In contrast, Hong et al. reported an increasing efficiency for acid recovery with tertiary amines with increasing chain length [59,60].

Therefore, it can be concluded that the influence of the chain length on the extraction efficiency depends on the targeted species and shows a trend only for tertiary amines in case of lignosulfonate extraction.

All equilibrium concentrations are given in the appendix in Table 12.5.

Table 5.6: Distribution ratio (D_A), extraction efficiency (E), equilibrium pH and crud formation for the lignosulfonate extraction from Ca-LS model solutions using different amines; $c_{LS,0}$ = 100 g·l^{-1}; $pH_{feed,0}$ = 3.75; T = 25 °C; ambient pressure; amine:1-octanol 20:80 wt%; extr…extraction; back-extr…back-extraction; tot…overall process.

Amine	$D_{A,extr}$	$D_{A,back\text{-}extr}$	E_{extr} [%]	$E_{back\text{-}extr}$ [%]	E_{tot} [%]	pH_{feed}	pH_{strip}	Crud extraction	Crud back-extraction
OA	1.63	0.00	61.9	95.9	59.4	9.78	12.67	low	no
DEA	1.75	0.14	63.6	87.6	55.7	9.66	12.68	no	no
DA	1.42	0.00	58.7	94.1	55.2	9.69	12.74	medium	no
DHA	0.70	0.00	41.3	94.0	38.8	8.43	13.22	low	no
DOA	0.84	0.00	45.5	97.7	44.5	8.08	12.66	medium	no
THA	0.49	0.00	32.9	99.9	32.8	6.35	12.72	medium	no
TOA	0.34	0.00	25.5	99.8	25.4	6.05	12.69	high	no
TDA	0.22	0.00	18.1	99.9	18.1	5.96	12.78	medium	no
ALIQ	4.13	8.12	80.5	11.0	8.8	3.78	12.61	medium	no

The equilibrium pH value of the feed phase in the extraction step, pH_{feed}, given in Table 5.6 increases with increasing extraction efficiency for primary, secondary and tertiary amines. This corresponds to the scheme given in Figure 3.17 a where the hydrogen ion (H^+) is needed for the protonation of the amine. With increasing degree of extraction, the H^+-concentration decreases which results in an increase of the pH value. Again, ALIQ shows another behavior since it exhibits the lowest pH value of all amines although showing the highest value for E_{extr}. The equilibrium pH value for the back-extraction is always between 12.61 and 13.22.

Crud formation is only observed for the extraction step and increases with increasing substitution of the nitrogen atom, clearly demonstrated in case of OA, DOA and TOA. This implies that higher branching of the amine increases the probability of crud formation. The visual evaluation of crud formation in Table 5.6 is done based on the solutions depicted in Figure 5.4, where Figure 5.4 a shows no and Figure 5.4 b shows high crud formation. The crud layer in Figure 5.4 b is the heavier phase because aqueous phase and matter is entrapped.

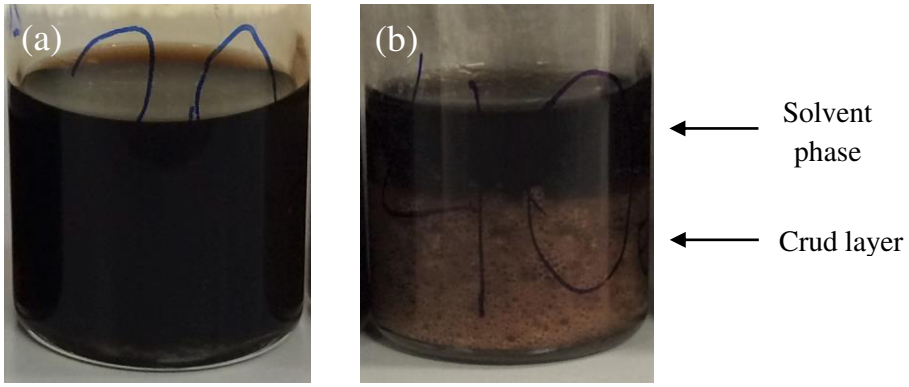

Figure 5.4: Visual evaluation of crud formation for lignosulfonate extraction from Ca-LS model solutions using different amines; $c_{LS,0}$ = 100 g·l^{-1}; $pH_{feed,0}$ = 3.75; T = 25 °C; ambient pressure; amine:1-octanol 20:80 wt%. The solution in (a) shows the solvent phases from two-phase experiments with DEA and Ca-LS solution without crud formation, whereas in (b) high crud formation is observed for TOA.

Since the final goal is to apply reactive lignosulfonate extraction to the real process stream, the same experiments were carried out with spent liquor.

Figure 5.5 illustrates the equilibrium concentrations for the extraction of lignosulfonate from spent liquor using different amines. In Table 5.7, the distribution ratio and the extraction efficiency are represented. $D_{A,extr}$, $D_{A,back\text{-}extr}$, E_{extr}, $E_{back\text{-}extr}$, and E_{tot} show the same trends regarding substitution of the nitrogen atom and chain length of the alkyl chain as in the experiments with Ca-LS model solutions (Figure 5.2 and Table 5.6). $E_{back\text{-}extr}$ is lower, compared to the experiments conducted with Ca-LS model solutions because of higher crud formation of spent liquor. The equilibrium pH values of the extraction step again increase with increasing E_{extr}. The pH values for primary amines were not measured since no aqueous phase was present due to high crud formation. Equilibrium pH for the back-extraction is with 12.51 to 13.22 in the same range as for the Ca-LS model solutions.

In contrast to the experiments with Ca-LS solution, the crud formation tendency in spent liquor shows the opposite trend. Primary amines exhibit higher crud formation than secondary and tertiary amines (Table 5.7 and Figure 5.6). This difference can be explained by the presence of other constituents in the spent liquor, e.g. sugars and hemicelluloses, which might show a different behavior in terms of crud formation.

Values for Equilibrium concentrations are given in the appendix in Table 12.6.

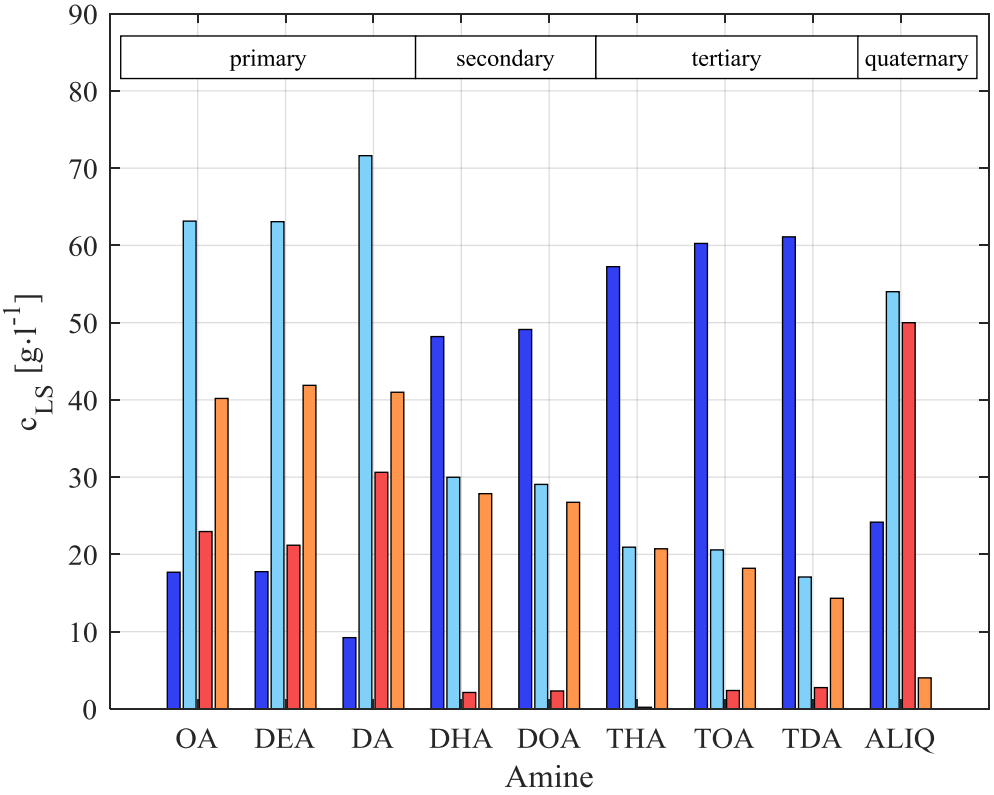

Figure 5.5: Equilibrium concentrations (c_{LS}) for lignosulfonate extraction from spent sulfite liquor using different amines; $c_{LS,0}$ = 80 g·l^{-1}; $pH_{feed,0}$ = 3.60; T = 25 °C; ambient pressure; amine:1-octanol 20:80 wt%. Blue: extraction (dark blue = feed; light blue = organic), red/orange: back-extraction (red = organic; orange = stripping phase), all data given in equilibrium.

Table 5.7: Distribution ratio (D_A), extraction efficiency (E), equilibrium pH and crud formation for lignosulfonate extraction from spent sulfite liquor using different amines; $c_{LS,0}$ = 80 g·l^{-1}; $pH_{feed,0}$ = 3.60; T = 25 °C; ambient pressure; amine:1-octanol 20:80 wt%; extr…extraction; back-extr…back-extraction; tot…overall process.

Amine	$D_{A,extr}$	$D_{A,back-extr}$	E_{extr} [%]	$E_{back-xtr}$ [%]	E_{tot} [%]	pH_{feed}	pH_{strip}	Crud extraction	Crud back-extraction
OA	3.57	0.57	78.1	63.6	49.7	-	12.87	high	low
DEA	3.55	0.51	78.0	66.4	51.8	-	12.95	high	no
DA	7.77	0.75	88.6	57.2	50.7	-	12.79	high	no
DHA	0.62	0.08	38.4	92.9	35.6	8.09	12.68	low	no
DOA	0.59	0.09	37.2	92.0	34.2	7.91	12.66	low	no
THA	0.37	0.01	26.8	99.0	26.5	6.00	12.64	low	no
TOA	0.34	0.13	25.5	88.4	22.5	5.75	13.22	medium	no
TDA	0.28	0.19	21.8	83.9	18.3	5.57	12.70	low	no
ALIQ	2.23	12.46	69.1	7.4	5.1	3.62	12.51	low	low

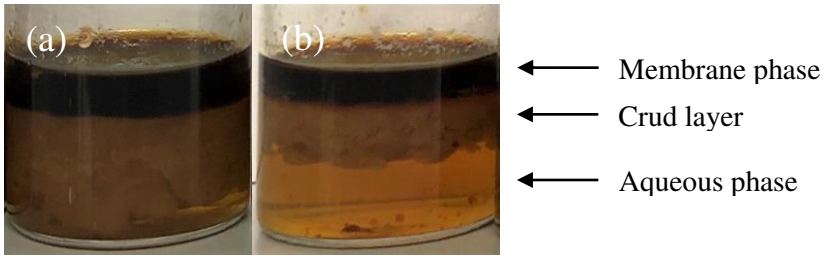

Figure 5.6: Visual evaluation of crud formation for lignosulfonate extraction from spent sulfite liquor using different amines; $c_{LS,0}$ = 80 g·l^{-1}; $pH_{feed,0}$ = 3.60; T = 25 °C; ambient pressure; amine: 1-octanol 20:80 wt%. High crud formation is observed for OA (a) and medium crud formation for TOA (b).

As a conclusion of the two-phase experiments for the lignosulfonate extraction from spent liquor using different amines, DOA is chosen as the best option since it exhibits low crud formation tendency and a higher E_{tot} than tertiary and quaternary amines. The reasons for neglecting primary amines are that they possess a relatively high water solubility, which is a disadvantage for the application in supported liquid membranes, and they show a high crud formation with spent liquor.

In the next experiments, the dependence of the amine concentration in the membrane phase on the overall extraction efficiency was determined and phase equilibria at various pH values were investigated. This was done using Ca-LS model solutions and DOA:1-octanol.

Figure 5.7 represents the overall extraction efficiency, E_{tot}, for the lignosulfonate extraction from Ca-LS model solutions for different DOA concentrations in the membrane phase.

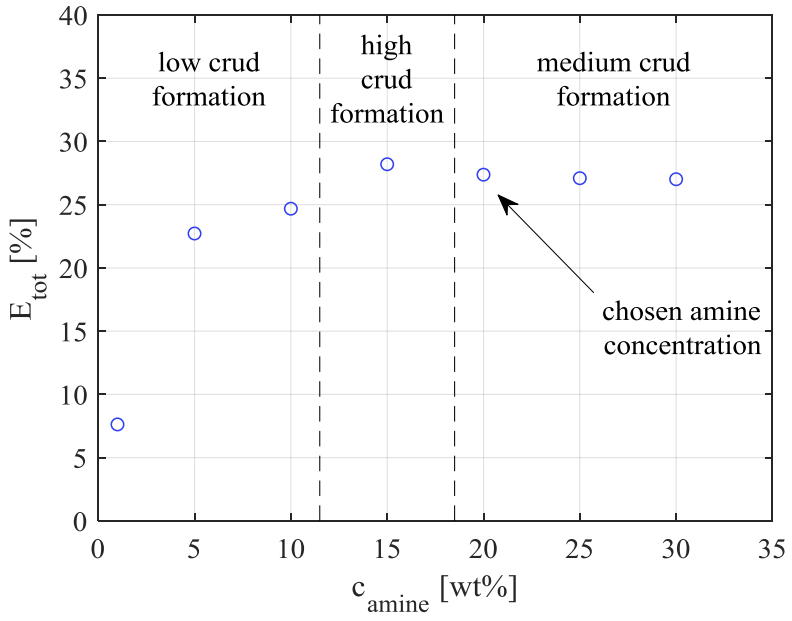

Figure 5.7: Overall extraction efficiency, E_{tot}, using DOA:1-octanol for lignosulfonate extraction from Ca-LS model solutions for different amine concentrations (c_{amine}) in the solvent phase; $c_{LS,0}$ = 100 g·l^{-1}; $pH_{feed,0}$ = 3.71; T = 25 °C; ambient pressure.

E_{tot} increases with increasing amine concentration up to 15 wt%, higher concentrations result in a decrease of E_{tot}. The highest crud formation is observed for an amine concentration of 15 wt%. Lower concentrations show low, whereas higher concentrations exhibit medium crud formation. All equilibrium concentrations are given in the appendix in Table 12.7.

Due to the performance in terms of extraction efficiency and crud formation, a weight ratio of 20:80 wt% between DOA and 1-octanol is chosen for further experiments.

In Figure 5.8, the equilibrium concentration of lignosulfonate in the solvent phase in dependence on its equilibrium concentration in the aqueous feed phase is displayed at different equilibrium pH values. All equilibrium concentrations are given in the appendix in Table 12.8.

The equilibrium measurements verify the data from Table 5.2 and Table 5.3, the equilibrium concentration of lignosulfonate in the solvent phase, $c_{LS,org}$, increases with decreasing equilibrium pH value. In contrast, the equilibrium concentration in the aqueous phase, $c_{LS,aqu}$, increases with increasing equilibrium pH. This implies that low pH values in the feed solution

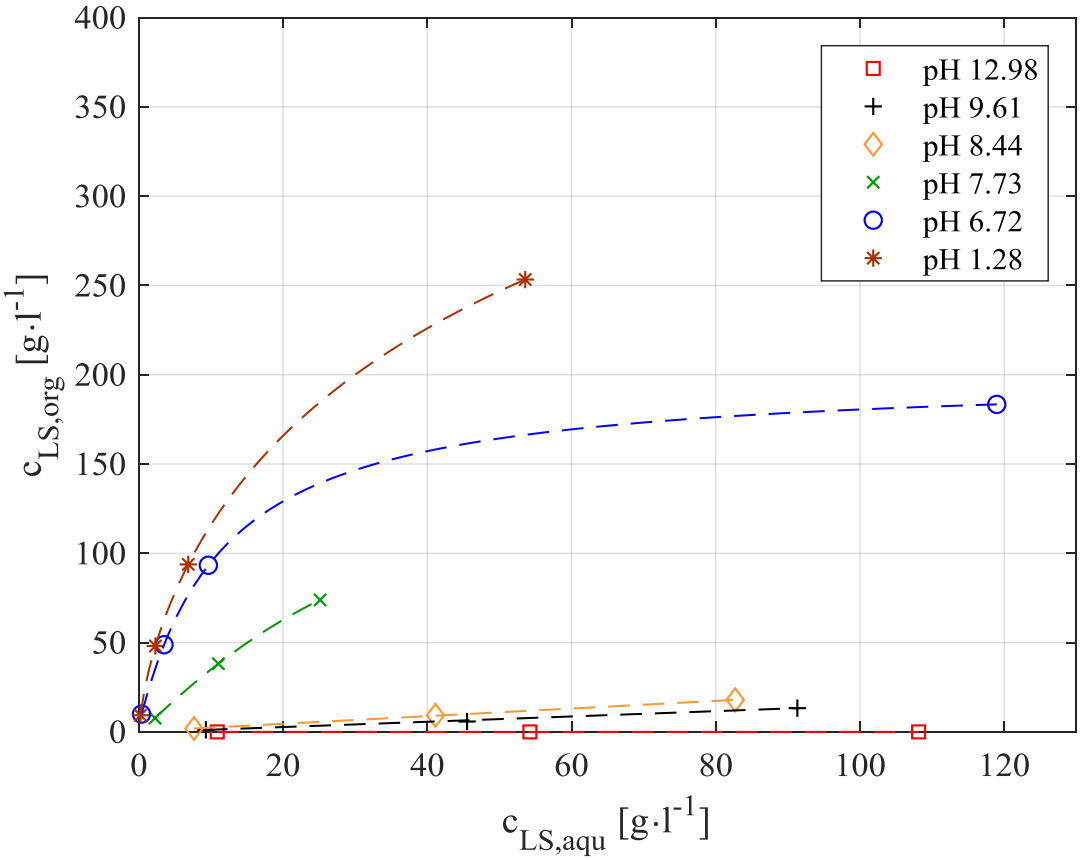

Figure 5.8: Equilibrium concentrations for lignosulfonate extraction from Ca-LS model solutions in two-phase contact using DOA:1-octanol (20:80 wt%) at different equilibrium pH values; T = 25 °C; ambient pressure.

are beneficial for the extraction step, and high pH values are necessary for the back-extraction to transfer most lignosulfonates from the organic to the aqueous stripping solution.

Figure 5.9 shows another illustration of the equilibrium data for the extraction of lignosulfonates using DOA:1-octanol (20:80 wt%) by representing the dependence of the distribution ratio for the extraction, $D_{A,extr}$, on the equilibrium pH value in the aqueous feed phase, pH_{feed}, for different starting concentrations. The high values of $D_{A,extr}$ for low equilibrium pH values again indicate that a low pH value has to be maintained in the extraction step, while the back-extraction requires a constantly high pH value, indicated by the low distribution ratio. In terms of crud formation, no differences to the experiments discussed before are observed (appendix Table 12.9). All equilibrium concentrations are given in the appendix in Table 12.8.

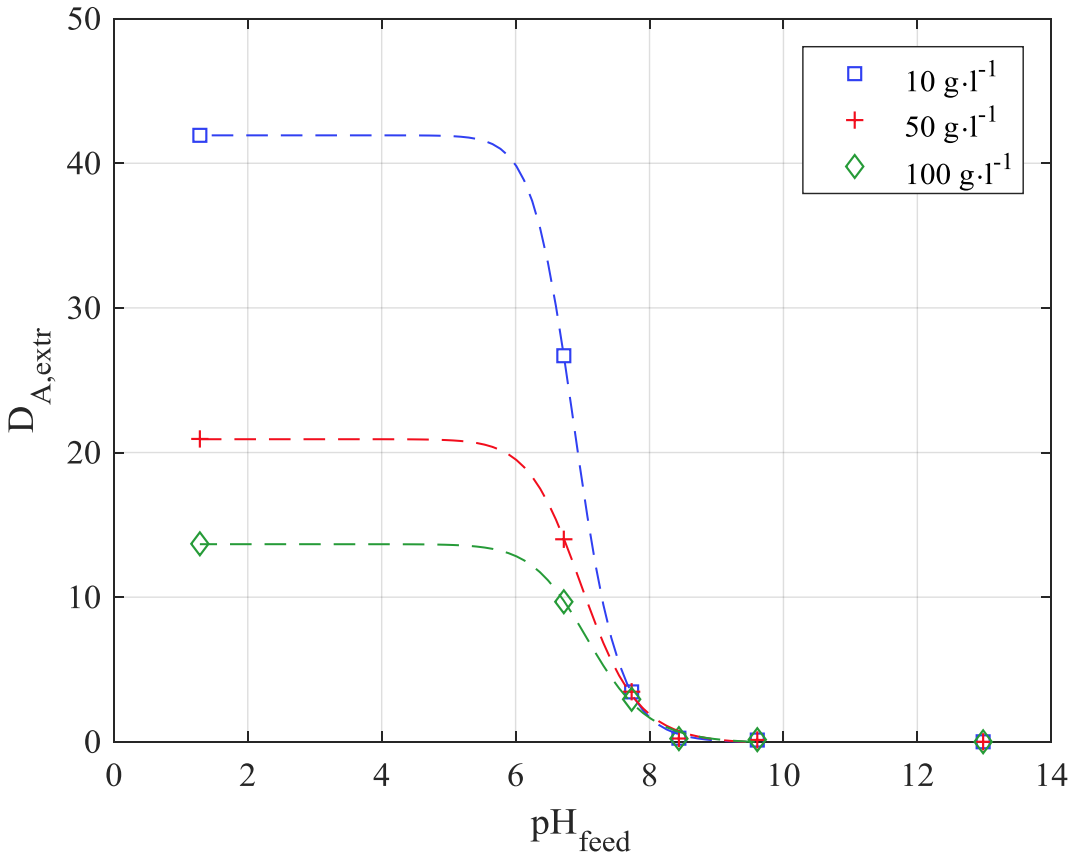

Figure 5.9: Dependence of the distribution ratio on the equilibrium pH for the lignosulfonate extraction from Ca-LS model solutions with different starting concentrations using DOA:1-octanol (20:80 wt%); T = 25 °C; ambient pressure.

5.3. U-tubes

With the knowledge gained in the two-phase experiments, the lignosulfonate extraction from spent liquor is transferred into the three-phase contact. In the first step, different amines are tested in the U-tube setup to verify whether the trend of the extraction efficiency is the same as for the two-phase experiments. Figure 5.10 represents the lignosulfonate concentration in the stripping phase, $c_{LS,strip}$, after an incubation time of 48 hours.

The lignosulfonate concentration in the stripping phase shows the same trend as for the two-phase experiments with spent liquor (orange bars in Figure 5.5). Overall, it decreases with increasing substitution of the nitrogen atom. All data are given in the appendix in Table 12.10.

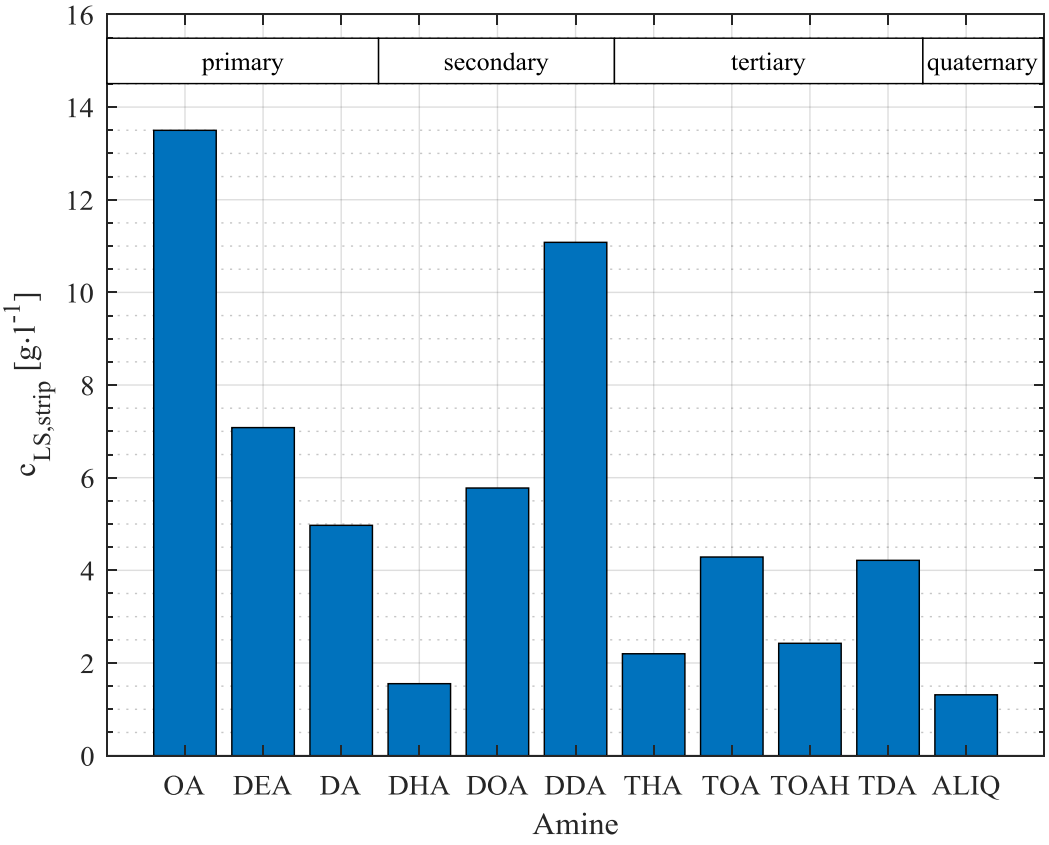

Figure 5.10: Lignosulfonate extraction from spent sulfite liquor using supported liquid membrane permeation (U-tube) and different amines; $c_{LS,0}$ = 80 g·l^{-1}; $pH_{feed,0}$ = 3.60; T = 25 °C; ambient pressure; amine:1-octanol 20:80 wt%; $A_{membrane}$ = 2.27 cm^2; time = 48 hours; support layer: PE 7-12 µm hydrophobic; $c_{LS,strip}$…LS concentration in the stripping phase.

Table 5.8: Visual evaluation of crud formation for lignosulfonate extraction from spent sulfite liquor using supported liquid membrane permeation (U-tube) and different amines; $c_{LS,0}$ = 80 g·l^{-1}; $pH_{feed,0}$ = 3.60; T = 25 °C; ambient pressure; amine:1-octanol 20:80 wt%; $A_{membrane}$ = 2.27 cm^2; time = 48 hours; support layer: PE 7-12 µm hydrophobic.

Amine	Crud formation
OA, DEA, DA, DDA, ALIQ	yes
DOA, DHA, TOA, TDA, TOAH, THA	no

In supported liquid membrane processes the term crud formation refers to the formation of a gel layer on the support layer surface. In addition, crud formation can occur within the support layer structure, which leads to blockage. Table 5.8 gives an overview of the crud formation of different amines in the U-tube setup. The classification is done based on Figure 5.11 where the support layer depicted in Figure 5.11 a is covered with a thick crud layer, whereas Figure 5.11 b exhibits no crud formation.

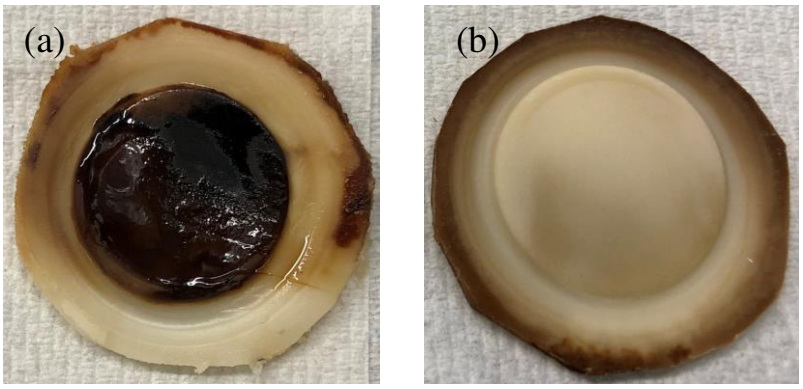

Figure 5.11: Visual evaluation of crud formation for lignosulfonate extraction from spent sulfite liquor using supported liquid membrane permeation (U-tube) and different amines; $c_{LS,0}$ = 80 g·l^{-1}; $pH_{feed,0}$ = 3.60; T = 25 °C; ambient pressure; amine:1-octanol 20:80 wt%; $A_{membrane}$ = 2.27 cm^2; time = 48 hours; support layer: PE 7-12 µm hydrophobic. The extraction with DA:1-octanol (a) shows high, whereas the extraction with TOA:1-octanol (b) shows no crud formation.

As observed for the two-phase experiments (Table 5.7), primary and some secondary amines show high crud formation in the three-phase experiments. In addition, ALIQ exhibits high crud development. This leads to blockage of the support layer and hindrance of the lignosulfonate transport. Tertiary and some secondary amines show no crud formation. With some exceptions, the overall trend is that low crud formation is observed for short chain length of the alkyl chains and high substitution of the nitrogen atom.

In addition to the extraction efficiency and crud formation, the water solubility of the amine is crucial for the application in supported liquid membrane. High water solubility leads to loss of the extractant, especially in continuous operation.

With the findings of the U-tube experiments, TOA and DOA are selected as the two amines working best for reactive extraction of lignosulfonates from spent liquor using supported liquid membrane permeation in the U-tube setup by showing high extraction efficiency, low crud formation and low water solubility.

5.4. Small-scale reactor

To increase the exchange area to feed volume ratio, the experiments were transferred to the small-scale reactor. At first, a hydrophilic PE support layer glued into the membrane module using epoxy resin glue was used. This configuration exhibits the problem that the results were not reproducible which is attributed to the dissolution of the epoxy resin glue into the membrane phase. The dissolved glue interacts with the aqueous phase and interferes with the UV-Vis measurements resulting in strong fluctuations in the lignosulfonate concentration in both aqueous phases. To prove this assumption, 1-octanol, TOA, and TOA:1-octanol (20:80 wt%) were brought into contact with a small piece of epoxy resin glue (Figure 5.12 a) for 120 hours. After mixing the three membrane phases with water (120 hours), UV-Vis spectra of the aqueous phases were recorded. The spectra displayed in Figure 5.12 b clearly show that TOA interacts with the glue and results in an absorption band at about 270 nm in the aqueous phase.

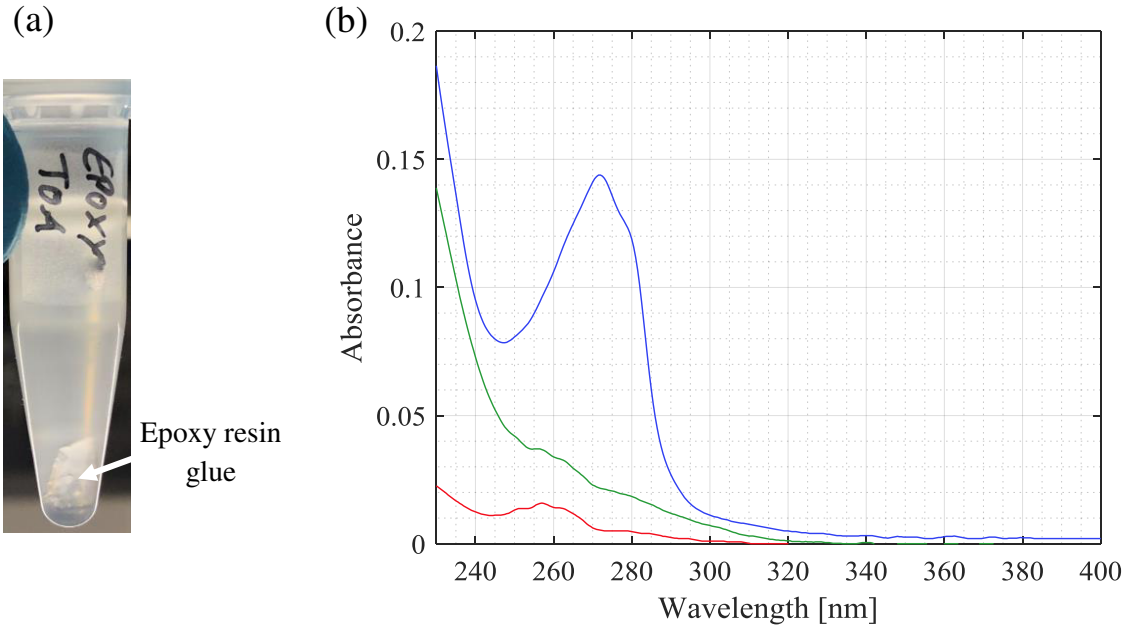

Figure 5.12: (a) A piece of epoxy resin glue in pure TOA. (b) UV-Vis spectrum of water which was in contact with 1-octanol (red), TOA (blue), and TOA:1-octanol 20:80 wt% (green) used for the dissolution experiment of epoxy resin glue; T = 25°C; ambient pressure.

The same behavior is seen for hydrophobic PE support layers but the fluctuations are not as strong as for hydrophilic support layers. The concentrations in the feed and stripping compartment over time can be seen in the appendix in Table 12.11, Table 12.12, Figure 12.1, Figure 12.2, Figure 12.3, and Figure 12.4.

To solve this issue, another module was made with a hydrophobic PE support layer and superglue as adhesive. In this case the results fit well and reproducibility was given. Figure 5.13 shows the concentration in the feed and stripping compartment over 172 hours.

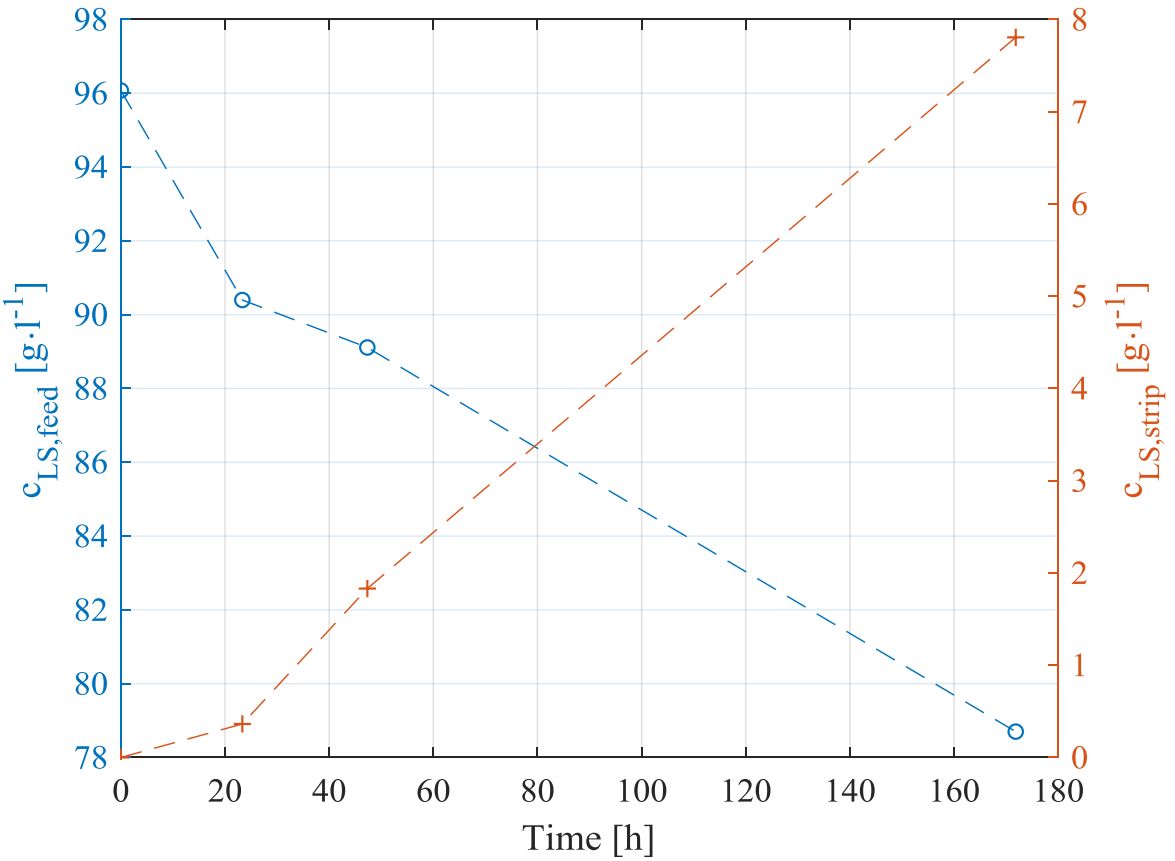

Figure 5.13: Lignosulfonate extraction from spent sulfite liquor using supported liquid membrane permeation (small-scale membrane reactor) and TOA:1-octanol; blue (o) = feed side; orange (+) = stripping side; $c_{LS,0}$ = 96 g·l^{-1}; $pH_{feed,0}$ = 3.60; T = 25 °C; ambient pressure; amine: 1-octanol 20:80 wt%; $A_{membrane}$ = 25 cm^2; time = 172 hours; support layer: PE 7-12 µm hydrophobic; glue = suberglue.

The lignosulfonate concentration in the feed compartment decreases, whereas the concentration in the stripping compartment rises. The uniform trends of the two concentrations indicate that no breakthrough occurred within the considered interval, and lignosulfonate extraction can be successfully performed with this setup. The linear decrease in the feed phase and the linear increase in the stripping phase indicate that the system is not in equilibrium within 172 hours, and a constant lignosulfonate flux across the liquid membrane is maintained.

5.5. Lab-scale reactor

To perform continuous lignosulfonate extraction from spent liquor, the lab-scale membrane reactor was used. Figure 5.14 shows the lignosulfonate concentration in the stripping phase and the pH value of the feed solution over 6 hours. The concentration in the stripping phase shows a higher increase, compared to the small-scale reactor. The reason for that is the higher exchange area to feed volume ratio and the continuous operation which enhances the lignosulfonate transport. This was demonstrated by Chakrabarty et al. for the lignosulfonate extraction using bulk liquid membranes. They stated that the highest extent of extraction is achieved when both aqueous phases are stirred, but stirring of the feed phase has the higher impact on the efficiency. In contrast, stirring of the membrane phase has no effect. These findings indicate that the diffusion of lignosulfonates across the feed-membrane interface controls the rate of extraction in bulk liquid membranes. [25]

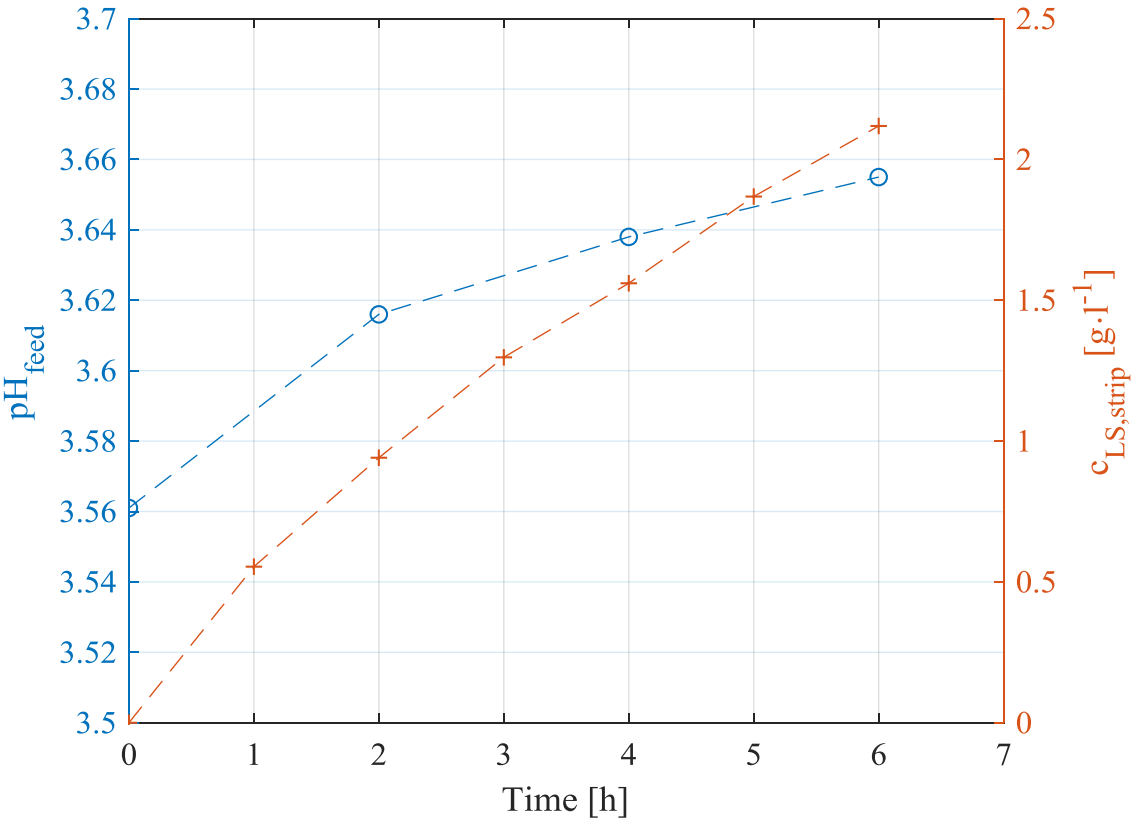

Figure 5.14: Continuous lignosulfonate extraction from spent sulfite liquor using supported liquid membrane permeation (lab-scale membrane reactor) and TOA:1-octanol; blue (o) = pH in the feed solution; orange (+) = concentration in the stripping phase; $c_{LS,0}$ = 96 g·l^{-1}; $pH_{feed,0}$ = 3.60; T = 25 °C; ambient pressure; amine:1-octanol 20:80 wt%; $A_{membrane}$ = 123 cm^2; time = 6 hours; support layer: PE 7-12 µm hydrophobic.

The effective mass transfer area of the lab-scale membrane reactor is 4.9 times higher, compared to the small-scale membrane reactor. The time needed to reach a lignosulfonate concentration of 2 $g \cdot l^{-1}$ in the stripping phase is about 50 hours for the small-scale reactor and approximately 5.5 hours for the lab-scale reactor, which results in a decrease of extraction time by the factor of 9.1. From these results it can be concluded, that the mass transfer of lignosulfonates in SLM can massively be enhanced by turbulence in the aqueous phases and by an increase in mass transfer area.

The increase in the feed pH is related to the decrease of hydrogen ions (H^+) in the feed phase as explained for the two-phase experiments in section 5.2.

The experiment was continued overnight. However, on the next day deposition of dry matter in the stripping compartment blocked the inlets of the stripping phase (Figure 5.15 a). In addition, the feed-side of the support layer was covered with a layer of brown material (Figure 5.15 b). The fact that both compartments were affected is a hint for crud formation caused by the interactions between the membrane phase, the aqueous phases and lignosulfonates. If the solids content in the feed phase was the reason for the deposition layer and not the membrane phase, there would be no deposition in the stripping compartment. To solve this issue, a modification of the membrane phase, e.g. variation of the amine, is necessary. One possible amine is DOA, which showed good results in the two phase experiments.

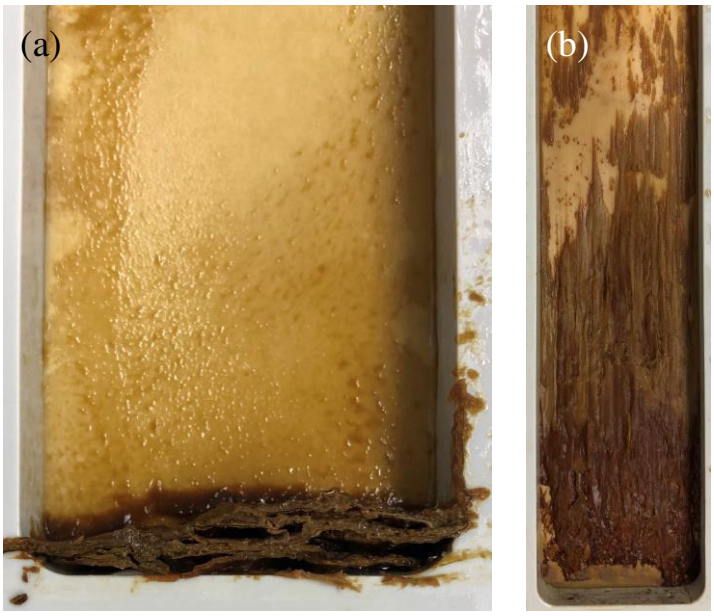

Figure 5.15: Deposition of matter in the stripping (a) and feed compartment (b) in continuous lignosulfonate extraction from spent sulfite liquor using supported liquid membrane permeation (lab-scale membrane reactor) and TOA:1-octanol after 24 hours; $c_{LS,0} = 96\ g \cdot l^{-1}$; $pH_{feed,0} = 3.60$; T = 25 °C; ambient pressure; amine:1-octanol 20:80 wt%; $A_{membrane} = 123\ cm^2$; support layer: PE 7-12 µm hydrophobic.

5.6. Tubular reactor

The second setup investigated for the continuous extraction of lignosulfonates was the tubular membrane reactor. Figure 5.16 a shows the mantle pipe filled with spent liquor with an overpressure of 100 mbar. After half an hour, no solution passed through the PTFE hoses and the membrane phase was introduced. 10 minutes later, the aqueous phase started to pass through the PTFE hoses (Figure 5.16 b and Figure 5.16 c) and accumulated in the storage flask of the membrane phase (Figure 5.16 d). The experiment had to be stopped. Two more attempts were conducted but the same issue was observed again, although no breakthrough was observed with the test system water and TOA:1-octanol.

The conclusion of this experiment is that modifications of the membrane phase, e.g. increase of the hydrophobicity, are necessary in order to enable stable operation. In addition, pulse-free pumps can help to further stabilize the system.

Despite the fact that stable operation was not achieved, this membrane reactor offers huge potential for separation of lignosulfonates from spent liquor because of high mass transfer area and simple cleaning. Further improvements of the setup and the membrane phase have to be conducted in the future.

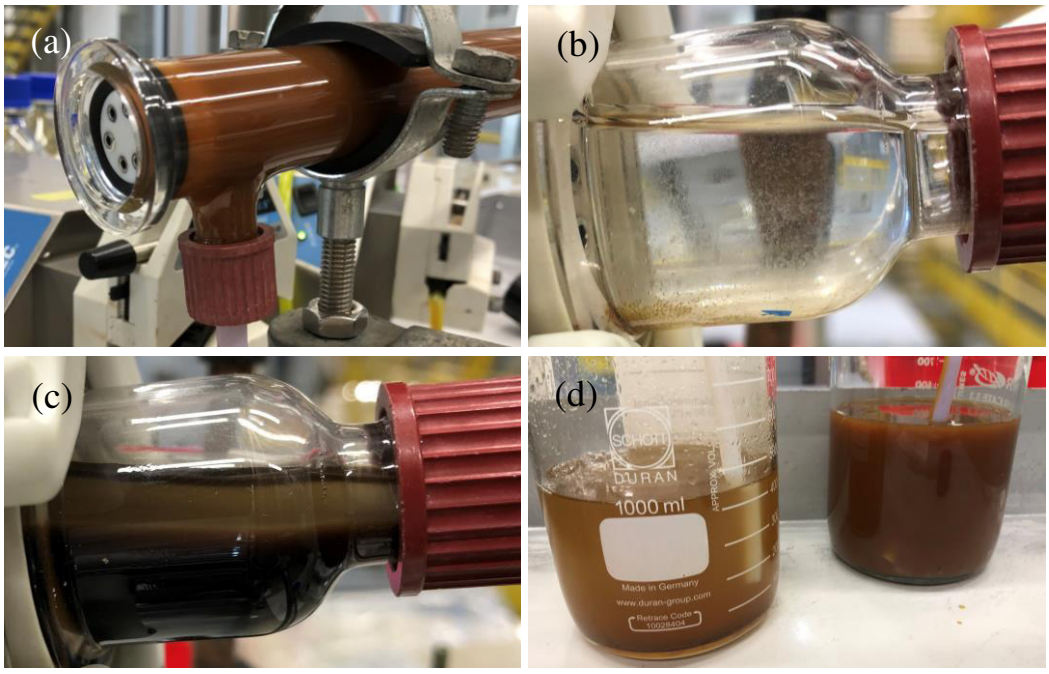

Figure 5.16: Continuous lignosulfonate extraction from spent sulfite liquor using the tubular membrane reactor and TOA:1-octanol; $c_{LS,0}$ = 96 g·l^{-1}; $pH_{feed,0}$ = 3.60; T = 25 °C; amine:1-octanol 20:80 wt%; $A_{membrane}$ = 435 cm^2; support layer: PTFE < 0.1 µm. (a) Filling of the glass tube with spent liquor. (b) Breakthrough of the aqueous phase starts. (c) Aqueous phase is mixed with membrane phase. (d) Mixture of aqueous and membrane phase in the storage flasks.

6. Conclusion and outlook

In the present thesis the reactive extraction of lignosulfonates from both, model solutions and spent sulfite liquor was investigated using different amines dissolved in 1-octanol as extractant phase. The dependence of the extraction efficiency on the substitution of the nitrogen atom and the chain length of the alky chains was examined, and the experiments were carried out in two-phase and three-phase contact.

The first part of this work dealt with the phase equilibria measurement of lignosulfonates in separation funnels at 25 °C and ambient pressure. Based on the results, it can be concluded that lignosulfonates can be extracted most efficiently under acidic conditions, although crud formation is higher under these conditions. No crud formation was observed under alkaline conditions. Further, the overall extraction efficiency was in the same order of magnitude for sodium and calcium lignosulfonate model solutions. The two-phase extraction experiments performed with calcium lignosulfonate model solutions with a concentration of 100 $g \cdot l^{-1}$ and different amines as extractant showed that the extraction efficiency decreases in the order quaternary > primary > secondary > tertiary with values between 80.5 and 18.1 %. The degree of back-extraction was between 94.0 and 99.9 % for primary, secondary and tertiary amines, and 11.0 % for the quaternary amine Aliquat336. While no clear dependence of the chain length of the alkyl chains on the overall extraction efficiency was observed, crud formation increased with increasing substitution of the nitrogen atom. The experiments performed with spent liquor showed the same results but crud formation in the extraction step decreased with increasing substitution of the nitrogen atom. Summing up, dioctylamine in 1-octanol (20:80 wt%) worked best as extractant for lignosulfonates from spent liquor in the two-phase experiments in terms of efficiency and crud formation.

Supported liquid membrane equipment operated in batch mode was used for the lignosulfonate extraction from spent liquor in three-phase contact. The trends for the U-tube setup using different amines were the same as for the two-phase experiments with spent liquor. Beside a high extraction efficiency and low crud formation tendency a low water solubility of the extractant is in general required. Therefore, dioctylamine and trioctylamine were selected as the best amines for lignosulfonate extraction using supported liquid membrane permeation. To increase the mass transfer area, the small-scale membrane reactor was used. A hydrophobic PE support layer glued into the membrane module with superglue and trioctylamine:1-octanol

(20:80 wt%) as extractant phase lead to a lignosulfonate concentration of 8 $g \cdot l^{-1}$ in the stripping phase after 172 hours. Further, no crud formation was observed.

Continuous lignosulfonate extraction was performed using two different setups and trioctylamine:1-octanol (20:80 wt%) as extractant phase. With the flat sheet lab-scale membrane reactor, stable operation was maintained for 6 hours and the lignosulfonate concentration in the stripping phase reached 2 $g \cdot l^{-1}$. The increase in transport was achieved by the higher transfer area and the turbulences in the aqueous phases. The second setup was the tubular membrane reactor (Memo3) which further increased the exchange area. Here, stable operation was not accomplished because of breakthrough and subsequent accumulation of the aqueous phase in the storage flask of the membrane phase. Improvements of the extractant phase are needed to enable stable operation with this apparatus. In addition, pulse-free pumps can help to stabilize the system.

The overall conclusion of the present thesis is that lignosulfonate extraction from model solutions and spent liquor is feasible using supported liquid membrane permeation in batch and continuous mode. In future experiments, the temperature influence should be investigated to increase the efficiency. Additionally, alternatives to 1-octanol should be considered to further increase the stability of the extraction process.

7. Bibliography

1. Aro, T. and Fatehi, P., "Production and Application of Lignosulfonates and Sulfonated Lignin," *ChemSusChem* 10(9):1861–1877, 2017, doi:10.1002/cssc.201700082.
2. Ek, M., Gellerstedt, G., and Henriksson, G., "Pulp and Paper Chemistry and Technology 1 - Wood Chemistry and Wood Biotechnology," ISBN 9783110213409, 2009, doi:http://d-nb.info/997670428.
3. Fatehi, P., Chen, J., Fang, Z., Smith, R.L., and Editors, J., "Production of Biofuels and Chemicals from Lignin," Chapter 2, 2016, doi:10.1007/978-981-10-1965-4.
4. Zhou, H., Yang, D., and Zhu, J.Y., "Molecular Structure of Sodium Lignosulfonate from Different Sources and their Properties as Dispersant of TiO 2 Slurry," *J. Dispers. Sci. Technol.* 37(2):296–303, 2016, doi:10.1080/01932691.2014.989572.
5. Arel, H.Ş., "The effect of lignosulfonates on concretes produced with cements of variable fineness and calcium aluminate content," *Constr. Build. Mater.* 131(November 2016):347–360, 2017, doi:10.1016/j.conbuildmat.2016.11.089.
6. Vanholme, R., Demedts, B., Morreel, K., Ralph, J., and Boerjan, W., "Lignin Biosynthesis and Structure," *Plant Physiol.* 153(3):895–905, 2010, doi:10.1104/pp.110.155119.
7. Saake, B. and Lehnen, R., "Lignin," *Ullmann's Encycl. Ind. Chem.* 21:21–36, 2012, doi:10.1002/14356007.a15.
8. Stewart, J.J., Akiyama, T., Chapple, C., Ralph, J., and Mansfield, S.D., "The Effects on Lignin Structure of Overexpression of Ferulate 5-Hydroxylase in Hybrid Poplar1," *Plant Physiol.* 150(2):621–635, 2009, doi:10.1104/pp.109.137059.
9. Key, R.E. and Bozell, J.J., "Progress toward Lignin Valorization via Selective Catalytic Technologies and the Tailoring of Biosynthetic Pathways," *ACS Sustain. Chem. Eng.* 4(10):5123–5135, 2016, doi:10.1021/acssuschemeng.6b01319.
10. Calvo-Flores, F.G., Dobado, J.A., Isac-GarcÃa, J.Ã., MartÃn-MartÃnez, F.J., and Isac-Garcia, J., "Lignin and Lignans as Renewable Raw Materials - Chemistry, Technology and Applications," Wiley, ISBN 9781118597866, 2015.
11. Klapiszewski, Ł., Zdarta, J., Szatkowski, T., Wysokowski, M., Nowacka, M., Szwarc-Rzepka, K., Bartczak, P., Siwińska-Stefańska, K., Ehrlich, H., and Jesionowski, T., "Silica/lignosulfonate hybrid materials: Preparation and characterization," *Cent. Eur. J. Chem.* 12(6):719–735, 2014, doi:10.2478/s11532-014-0523-5.
12. Mussatto, S.I., "Biomass Fractionation Technologies for a Lignocellulosic Feedstock Based Biorefinery," Elsevier, 2016.
13. Shu, R., Xu, Y., Ma, L., Zhang, Q., Wang, T., Chen, P., and Wu, Q., "Hydrogenolysis process for lignosulfonate depolymerization using synergistic catalysts of noble metal and metal chloride," *RSC Adv.* 6(91):88788–88796, 2016, doi:10.1039/C6RA16725J.
14. Ringena, O., Saake, B., and Lehnen, R., "Isolation and fractionation of lignosulfonates by amine extraction and ultrafiltration: A comparative study," *Holzforschung* 59(4):405–412, 2005, doi:10.1515/HF.2005.066.
15. Xian, C.K., Othman, N., Harruddin, N., Nasruddin, N.A., and Ooi, Z.Y., "Extraction of Lignosulfonate using TOA-Kerosene-PVDF in Supported Liquid Membrane Process," *J. Teknol. (Sciences Eng.* 67(2):59–63, 2014.

16. Riedl, W. and Raiser, T., "Membrane-supported extraction of biomolecules with aqueous two-phase systems," *Desalination* 224:160–167, 2008, doi:10.1016/j.desal.2007.02.088.

17. Kienberger, M., Hackl, M., and Siebenhofer, M., "Emulsion Prevention with Supported Liquid Membrane Permeation," *Chem. Eng. Technol.* 41(3):504–508, 2018, doi:10.1002/ceat.201700484.

18. Fritz, M. and Siebenhofer, M., "New Developments in Liquid Membrane Permeation with Support Layers," *Chem Ing Tech* 82(12):2103–2108, 2010, doi:10.1002/cite.201000080.

19. Kontturi, A. and Sundholm, G., "The Extraction and Fractionation of Lignosulfonates with Long Chain Aliphatic Amines," *Acta Chem. Scand.* 40(40):121–125, 1986.

20. Chakrabarty, K., Saha, P., and Ghoshal, A.K., "Separation of lignosulfonate from its aqueous solution using emulsion liquid membrane," *J. Memb. Sci.* 360(1–2):34–39, 2010, doi:10.1016/j.memsci.2010.04.043.

21. Sixta, H., "Handbook of Pulp," ISBN 9788120341999, 2006, doi:10.1002/9783527619887.

22. Ek, M., Gellerstedt, G., and Henriksson, G., "Pulp and Paper Chemistry and Technology 2 - Pulping Chemistry and Technology," Walter de Gruyter, Berlin, New York, ISBN 9783110213423, 2009, doi:10.1515/9783110213423.

23. Bajpai, P., "Green Chemistry and Sustainability in Pulp and Paper Industry," Springer International Publishing, Cham, ISBN 978-3-319-18743-3, 2015, doi:10.1007/978-3-319-18744-0.

24. Holik, H., "Handbook of Paper and Board Edited by," ISBN 9788120341999, 2013.

25. Chakrabarty, K., Krishna, K.V., Saha, P., and Ghoshal, A.K., "Extraction and recovery of lignosulfonate from its aqueous solution using bulk liquid membrane," *J. Memb. Sci.* 330(1–2):135–144, 2009, doi:10.1016/j.memsci.2008.12.069.

26. Fatehi, P. and Chen, J., "Extraction of Technical Lignins from Pulping Spent Liquors, Challenges and Oppertunities," *Production of Biofuels and Chemicals from Lignin*, ISBN 978-981-10-1964-7: 35–54, 2016, doi:10.1007/978-981-10-1965-4.

27. Kontturi, A.-K., Kontturi, K., Niinikoski, P., and Sundholm, G., "Extraction and fractionation of lignosulfonate by a supported liquid membrane," *Prog. Colloid Polym. Sci.* 88:90–95, 1992.

28. Müller, E., Berger, R., Blass, E., Sluyts, D., and Pfennig, A., "Liquid-Liquid Extraction," *Ullmann's Encycl. Ind. Chem.* 21:249–307, 2012, doi:10.1002/14356007.b03.

29. Robbins, L.A. and Cusack, R.W., "Liquid-Liquid Extraction Operations and Equipment," *Perry's Chemical Engineers' Handbook*, ISBN 0071422943: 15-1-15–47, 2008, doi:10.1036/0071511385.

30. Couper, J.R., Penney, W.R., Fair, J.R., and Walas, S.M., "Extraction and Leaching," *Chemical Process Equipment*, Elsevier, ISBN 978-0-12-396959-0: 487–528, 2012, doi:10.1016/B978-0-12-396959-0.00014-8.

31. Mersmann, A., Kind, M., and Stichlmair, J., "Thermal Separation Technology," Springer Berlin Heidelberg, Berlin, Heidelberg, ISBN 978-3-642-12524-9, 2011, doi:10.1007/978-3-642-12525-6.

32. Aguilar, M. and Cortina, J.L., "Solvent Extraction and Liquid Membranes - Fundamentals and Applications in New Materials," 2008.

33. SUGAI, H., “Crud in Solvent Washing Process for Nuclear Fuel Reprocessing,” *J. Nucl. Sci. Technol.* 29(5):445–453, 1992, doi:10.1080/18811248.1992.9731550.

34. Rydberg, J., Cox, M., Musikas, C., and Choppin, G.R., “Solvent Extraction - Principles and Practice,” ISBN 0-8247-5063-2, 2004.

35. Bart, H.-J., “Reactive Extraction,” ISBN 9783642621505, 2001.

36. Lux, S. and Siebenhofer, M., “Investigation of liquid-liquid phase equilibria for reactive extraction of lactic acid with organophosphorus solvents,” *J. Chem. Technol. Biotechnol.* 88(3):462–467, 2013, doi:10.1002/jctb.3847.

37. Datta, D., Kumar, S., and Uslu, H., “Status of the Reactive Extraction as a Method of Separation,” *J. Chem* 2015(i):1–16, 2015.

38. Willersinn, S. and Bart, H.-J., “Reactive Extraction and Critical Raw Materials: Industrial Recovery of Tungsten,” *Chemie Ing. Tech.* 89(1–2):82–91, 2017, doi:10.1002/cite.201600079.

39. S, M.S., A, H.A., S, K.R., S, S.S., J, N.S., M, H.S., and M, B.N., “Expulsion by Ionic Complexation: Benchmark Therapy for Atherosclerosis A Review,” *Indian J. Pharm. Biol. Res.* 2(01):103–107, 2014, doi:10.30750/ijpbr.2.1.17.

40. Bart, H.-J. and Pilz, S., “Industrial Scale Natural Products Extraction,” ISBN 9783527325047, 2011, doi:10.1002/9783527635122.ch4.

41. Li, F., Gong, A., Qiu, L., Zhang, W., Li, J., Liu, Y., Liu, Y., and Yuan, H., “Simultaneous determination of trace rare-earth elements in simulated water samples using ICP-OES with TODGA extraction/back-extraction,” *PLoS One* 12(9):e0185302, 2017, doi:10.1371/journal.pone.0185302.

42. Moore, R.E., Shaffer, J.H., Baes, C.F., McDuffie, H.F., and Bamberger, C.E.L., “Purification of Beryllium by Acetylacetone-EDTA Solvent Extraction,” *Nucl. Sci. Eng.* 17(2):268–273, 1963, doi:10.13182/NSE63-A28889.

43. Parhi, P.K., “Supported Liquid Membrane Principle and Its Practices: A Short Review,” *J. Chem.* 2013:1–11, 2013, doi:10.1155/2013/618236, 10.1155/2013/618236.

44. Melin, T. and Rautenbach, R., “Membranverfahren - Grundlagen der Modul- und Anlagenauslegung,” ISBN 9788578110796, 2007, doi:10.1017/CBO9781107415324.004.

45. Marr, R., Bart, H.J., and Draxler, J., “Liquid membrane permeation,” *Chem. Eng. Process.* 27(1):59–64, 1990, doi:10.1016/0255-2701(90)85007-Q.

46. Baylan, N., Çehreli, S., and Özparlak, N., “Transport and separation of carboxylic acids through bulk liquid membranes containing tributylamine,” *J. Dispers. Sci. Technol.* 38(6):895–900, 2017, doi:10.1080/01932691.2016.1214841.

47. Kislik, V.S., “Liquid membranes, Principles & Applications in Chemical Separations & Wastewater treatment,” ISBN 9780444532183, 2010, doi:10.1016/B978-0-444-53218-3.00001-5.

48. Rathore, N.S., Sonawane, J. V., Kumar, A., Venugopalan, A.K., Singh, R.K., Bajpai, D.D., and Shukla, J.P., “Hollow fiber supported liquid membrane: A novel technique for separation and recovery of plutonium from aqueous acidic wastes,” *J. Memb. Sci.* 189(1):119–128, 2001, doi:10.1016/S0376-7388(01)00406-9.

49. Riedl, W., Mollet, D., and Grundler, G., “Using Membrane-Supported Liquid–Liquid Extraction for the Measurement of Extraction Kinetics,” *Chim. Int. J. Chem.* 65(5):370–

372, 2011, doi:10.2533/chimia.2011.370.

50. Noll, H., “Füssigmembranpermeation mit gestützten Membranen,” Graz University of Technology, 2012.

51. Schlosser, Š., Sabolová, E., Kertész, R., and Kubišová, L., “Factors influencing transport through liquid membranes and membrane based solvent extraction,” *J. Sep. Sci.* 24(7):509–518, 2001, doi:10.1002/1615-9314(20010801)24:7<509::AID-JSSC509>3.0.CO;2-R.

52. Panja, S., Mohapatra, P.K., Tripathi, S.C., and Manchanda, V.K., “Transport of Thorium(IV) Across a Supported Liquid Membrane Containing N,N,N′,N′-Tetraoctyl-3-oxapentanediamide (TODGA) as the Extractant,” *Sep. Sci. Technol.* 45(8):1112–1120, 2010, doi:10.1080/01496391003697416.

53. Jr, V. and Pathway, R., “Biomass and Green Chemistry,” Springer International Publishing, Cham, ISBN 978-3-319-66735-5, 2018, doi:10.1007/978-3-319-66736-2.

54. Perkampus, H.-H., “UV/Vis Spectroscopy and Its Applications,” ISBN 978-3-540-69751-0, 1992, doi:10.1007/b94239.

55. Chakrabarty, K., Saha, P., and Ghoshal, A.K., “Separation of lignosulfonate fromits aqueous solution using supported liquid membrane,” *J. Memb. Sci.* 340(1–2):84–91, 2009, doi:10.1016/j.memsci.2010.04.043.

56. Frolov, Y.G., Ochkin, A.V., and Sergievskii, V.V., “THEORETICAL ASPECTS OF AMINE EXTRACTION,” *At. Energy Rev.* 7:71–138, 1969.

57. Ochkin, A. V and Sergievskii, V. V, “Thermodynamics of extraction by solutions of amines and salts of substituted ammonium bases,” *Russ. Chem. Rev.* 58(9):835–847, 1989, doi:10.1070/RC1989v058n09ABEH003481.

58. Shanker, R., Venkateswarlu, K.S., and Shankar, J., “Extraction of ruthenium(III) by long-chain amines from sulphuric acid solutions,” *J. Less Common Met.* 15(1):75–88, 1968, doi:10.1016/0022-5088(68)90008-8.

59. Hong, Y.K. and Hong, W.H., “Influence of chain length of tertiary amines on extractability and chemical interactions in reactive extraction of succinic acid,” *Korean J. Chem. Eng.* 21(2):488–493, 2004, doi:10.1007/BF02705439.

60. Hong, Y.K., Hong, W.H., and Han, D.H., “Application of reactive extraction to recovery of carboxylic acids,” *Biotechnol. Bioprocess Eng.* 6(6):386–394, 2001, doi:10.1007/BF02932319.

8. List of abbreviations

A/O/A	aqueous/organic/aqueous
ALIQ	aliquat336
aqu	aqueous phase
back-extr	back-extraction
BLM	bulk liquid membrane
Ca-LS	calcium lignosulfonate
conc	concentration
DA	dodecylamine
DDA	didodecylamine
DEA	decylamine
DHA	dihexylamine
DOA	dioctylamine
EDTA	ethylenediaminetetraacetic acid
ELM	emulsion liquid membrane
eff	effective
equil	phase equilibrium measurement
extr	extraction
feed	feed phase
FKM	fluoroelastomer
G unit	guaiacyl unit
H unit	p-hydroxyphenyl unit
HPLC	high-performance liquid chromatography
lab	lab-scale membrane reactor
LS	lignosulfonates
max	maximum
MIBK	methyl-isobutyl ketone
min	minimum

Na-LS	sodium lignosulfonate
O/A/O	organic/aqueous/organic
OA	octylamine
org	organic solvent/membrane phase
PE	polyethylene
PTFE	polytetrafluoroethylene
PVC	polyvinylchloride
S unit	syringyl unit
SLM	supported liquid membrane
strip	stripping phase
TDA	tridodecylamine
THA	trihexylamine
TOA	trioctylamine
TOAH	trioctylamine-HCl

9. List of symbols

A	targeted component in the feed	
A_{aqu}	species A in the aqueous phase	
$A_{membrane}$	effective membrane area	[cm²]
A_{org}	species A in the organic solvent phase	
An^{m-}	anion	
AX	complex containing A in the aqueous phase	
AY	complex containing A in the organic solvent phase	
AZ	complex containing A in the stripping phase	
B	solvent phase	
C	remaining components in the feed phase	
Cat^{n+}	cation	
$c_{A,aqu}$	concentration of A in the aqueous phase	$[g \cdot l^{-1}]$ / $[mol \cdot l^{-1}]$
$c_{A,org}$	concentration of A in the organic solvent phase	$[g \cdot l^{-1}]$ / $[mol \cdot l^{-1}]$
$c_{AX,t,aqu}$	concentration of the complex containing A in the aqueous phase	$[g \cdot l^{-1}]$ / $[mol \cdot l^{-1}]$
$c_{AY,t,org}$	concentration of the complex containing A in the organic solvent phase	$[g \cdot l^{-1}]$ / $[mol \cdot l^{-1}]$
$c_{AZ,t,strip}$	concentration of the complex containing A in the stripping phase	$[g \cdot l^{-1}]$ / $[mol \cdot l^{-1}]$
c_i	concentration of component i	$[g \cdot l^{-1}]$ / $[mol \cdot l^{-1}]$
$c_{LS,mean}$	lignosulfonate concentration	$[g \cdot l^{-1}]$
$c_{LS,0}$	initial lignosulfonate concentration in the feed phase based on weighted amount of LS	$[g \cdot l^{-1}]$
$c_{LS,F,0}$	initial lignosulfonate concentration in the feed phase, determined by UV-Vis spectroscopy at 280 nm	$[g \cdot l^{-1}]$
$c_{LS,F,1}$	lignosulfonate concentration in the feed phase after the extraction step, determined by UV-Vis spectroscopy at 280 nm	$[g \cdot l^{-1}]$

$c_{LS,O,0}$	initial lignosulfonate concentration in the solvent/membrane phase	$[g \cdot l^{-1}]$
$c_{LS,O,1}$	lignosulfonate concentration in the solvent/membrane phase after the extraction step, determined by balances	$[g \cdot l^{-1}]$
$c_{LS,O,3}$	lignosulfonate concentration in the solvent/membrane phase after the back-extraction step, determined by balances	$[g \cdot l^{-1}]$
$c_{LS,S,0}$	initial lignosulfonate concentration in the stripping phase	$[g \cdot l^{-1}]$
$c_{LS,S,3}$	lignosulfonate concentration in the stripping phase after the back-extraction step, determined by UV-Vis spectroscopy at 280 nm	$[g \cdot l^{-1}]$
d	path length of light in the UV cuvette	[cm]
D_A	distribution ratio according to IUPAC	
$D_{A,extr}$	distribution ratio according to IUPAC for the extraction step	
$D_{A,back\text{-}extr}$	distribution ratio according to IUPAC for the back-extraction step	
d_o	outer diameter	[cm]
d_i	inner diameter	[cm]
d_{pore}	pore size	[µm]
ε	extinction coefficient	$[l \cdot g^{-1} \cdot cm^{-1}]$
$\varepsilon_{Ca\text{-}LS}$	extinction coefficient for calcium lignosulfonates at 280 nm	$[l \cdot g^{-1} \cdot cm^{-1}]$
$\varepsilon_{Na\text{-}LS}$	extinction coefficient for sodium lignosulfonates at 280 nm	$[l \cdot g^{-1} \cdot cm^{-1}]$
$\varepsilon_{LS\ spent\ liquor}$	extinction coefficient for lignosulfonates in spent liquor at 280 nm	$[l \cdot g^{-1} \cdot cm^{-1}]$
E_{extr}	extraction efficiency for the extraction step	[%]
$E_{back\text{-}extr}$	extraction efficiency for the back-extraction step	[%]
E_{tot}	extraction efficiency for the whole process	[%]
$\gamma_{A,aqu}$	activity coefficient of A in the aqueous phase	
γ_i	activity coefficient of component i	

$\gamma_{A,org}$	activity coefficient of A in the organic solvent phase	
H	depth	[m]
I	intensity of monochromatic light leaving the sample	
I_0	intensity of monochromatic light entering the sample	
$K_{D,A}$	distribution constant for species A according to Nernst	
$K^0_{D,A}$	distribution constant for species A according to Nernst for non-ideal systems	
L	length	[m]
M	metal ion	
m_i	mass of component i	[g]
N_{tubes}	number of tubes	
$pH_{feed,0}$	initial pH value of the feed solution	
pH_{feed}	equilibrium pH value of the feed solution after the extraction for two-phase experiments and pH value of the feed solution at a certain time for three-phase experiments	
pH_{strip}	equilibrium pH value of the stripping solution after the back-extraction	
R	gas constant	$[J \cdot mol^{-1} \cdot K^{-1}]$
$RH_{(org)}$	extraction agent for the cation exchange	
S	surface area	[m²]
σ	standard deviation	
T	temperature	[K] or [°C]
V	volume	[l]
W	width	[m]
x_{wall}	wall thickness	[mm]

10. List of figures

11. List of tables

12. Appendix

12.1.Analysis

Table 12.1: Measured data for the UV-Vis calibration curve of Na-LS in 0.3 M NaOH; $m_{Na\text{-}LS}$…mass of Na-LS; V_{water}…volume 0.3 M NaOH; $c_{Na\text{-}LS,0}$…starting LS concentration based on weight; $c_{Na\text{-}LS}$…calculated LS concentration in the diluted samples.

$m_{Na\text{-}LS}$	0.0502 g	V_{water}	0.05 l	$c_{Na\text{-}LS,0}$	1.004 g/l	

Sample	Dilution [ml]		Dilution total	$c_{Na\text{-}LS}$ [$g \cdot l^{-1}$]	Absorbance	ε [$l \cdot g^{-1} \cdot cm^{-1}$]
1	1	2	3	0.335	2.248	6.72
2	0.5	2.5	6	0.167	1.113	6.65
3	0.3	3	11	0.091	0.601	6.58
4	0.1	3	31	0.032	0.209	6.44
5	0.05	3	61	0.016	0.106	6.46
6	0.02	3	151	0.007	0.044	6.57

Table 12.2: Measured data for the UV-Vis calibration curve of Ca-LS in 0.3 M NaOH; $m_{Ca\text{-}LS}$…mass of Ca-LS; V_{water}…volume 0.3 M NaOH; $c_{Ca\text{-}LS,0}$…starting LS concentration based on weight; $c_{Ca\text{-}LS}$…calculated LS concentration in the diluted samples.

$m_{Na\text{-}LS}$	0.2004 g	V_{water}	0.2 l	$c_{Na\text{-}LS,0}$	1.002 g/l	

Sample	Dilution [ml]		Dilution total	$c_{Na\text{-}LS}$ [$g \cdot l^{-1}$]	Absorbance	ε [$l \cdot g^{-1} \cdot cm^{-1}$]
1	1	2	3	0.333	2.584	7.75
2	0.5	2.5	6	0.167	1.266	7.60
3	0.3	3	11	0.091	0.692	7.61
4	0.15	3	21	0.048	0.365	7.67
5	0.1	3	31	0.032	0.245	7.61
6	0.05	3	61	0.016	0.122	7.44
7	0.02	3	151	0.007	0.046	6.90

12.2.Setups used for the isolation of lignosulfonates

Table 12.3: Specifications of the different membrane reactors for calculation of the exchange area to feed volume ratio.

U-TUBES							
volume aqueous phase	V_{aqu}	15	[ml]	area of support layer	$A_{membrane}$	2.54	[cm²]
inner diameter tube	$d_{i,tube}$	1.7	[cm]	total volume aqueous phase	V_{aqu}	15	[cm³]
				exchange area / feed volume	S/V	0.17	[cm²/cm³]
SMALL-SCALE MEMBRANE REACTOR							
volume aqueous phase	V_{aqu}	99.5	[ml]	area of support layer	$A_{membrane}$	25	[cm²]
effective membrane diameter	$d_{membrane,eff}$		[cm]	total volume aqueous phase	V_{aqu}	99.5	[cm³]
				exchange area / feed volume	S/V	0.25	[cm²/cm³]
LAB-SCALE MEMBRANE REACTOR							
length of feed chamber	L	30	[cm]	area of support layer	$A_{membrane}$	123	[cm²]
width of feed chamber	W	4.1	[cm]	total volume aqueous phase	V_{aqu}	123	[cm³]
depth of feed chamber	H	1	[cm]	exchange area / feed volume	S/V	1.00	[cm²/cm³]
TUBULAR MEMBRANE REACTOR							
pore size	d_{pore}	< 0.1	[µm]	outer surface area tube	$S_{tube\ outer}$	7.257E-03	[m²]
porosity		50-70	[%]	total surface area tubes	$S_{total\ tube}$	4.354E-02	[m²]
length module	L_{module}	77	[cm]	total surface area tubes	$S_{total\ tube}$	435	[cm²]
number of tubes	N_{tubes}	6	[-]	"outer" Volume tube	$V_{tube\ outer}$	5.443E-06	[m³]
thickness wall tubes	$x_{wall,tube}$	150	[µm]	total "outer" Volume tubes and steel	$V_{tube\ total}$	3.810E-05	[m³]
outer diameter tubes	$d_{o,tube}$	3	[mm]	total inner volume module	$V_{module\ total}$	4.088E-04	[m³]
inner diameter tubes	$d_{i,tube}$	2.7	[mm]	net inner volume module	$V_{module\ netto}$	3.707E-04	[m³]
thickness wall module	$x_{wall,module}$	2	[mm]	net inner volume module	$V_{module\ netto}$	371	[cm³]
outer diameter module	$d_{o,module}$	3	[cm]	exchange area / feed volume	S/V	1.17	[cm²/cm³]
inner diameter module	$d_{i,module}$	2.6	[cm]				

12.3.Equilibrium measurements

Table 12.4: Equilibrium concentrations (c_{LS}) for Na-LS and Ca-LS solutions with a starting concentration of 100 g·l^{-1} and pH of 3.75 (T = 25 °C; ambient pressure; solvent phase: amine: 1-octanol 20:80 wt%).
Indices: LS,0…initial feed concentration based on the weighted mass of LS. 1…extraction; 3…back-extraction; F…feed phase; O… solvent phase; S…stripping phase.

Amine	LS	$c_{LS,0}$ [g·l^{-1}]	$c_{LS,F,0}$ [g·l^{-1}]	$c_{LS,F,1}$ [g·l^{-1}]	$c_{LS,O,1}$ [g·l^{-1}]	$c_{LS,S,3}$ [g·l^{-1}]	$c_{LS,O,3}$ [g·l^{-1}]
OA	Na-LS	100	89.03	30.39	58.64	46.61	12.04
DOA	Na-LS	100	89.03	40.89	48.14	38.09	10.05
TOA	Na-LS	100	89.03	50.51	38.52	32.16	6.36
OA	Ca-LS	100	97.92	37.28	60.65	58.18	2.47
DOA	Ca-LS	100	97.92	53.35	44.57	43.56	1.01
TOA	Ca-LS	100	97.92	72.96	24.97	24.94	0.03

Table 12.5: Equilibrium concentrations (c_{LS}) for Ca-LS solutions with a starting concentration of 100 g·l^{-1} and pH of 3.75 (T = 25 °C; ambient pressure; solvent phase: amine:1-octanol 20:80 wt%) for the extraction with different amines.
Indices: LS,0…initial feed concentration based on the weighted mass of LS. 1…extraction; 3…back-extraction; F…feed phase; O…solvent phase; S…stripping phase.

Amine	$c_{LS,0}$ [g·l^{-1}]	$c_{LS,F,0}$ [g·l^{-1}]	$c_{LS,F,1}$ [g·l^{-1}]	$c_{LS,O,1}$ [g·l^{-1}]	$c_{LS,S,3}$ [g·l^{-1}]	$c_{LS,O,3}$ [g·l^{-1}]
OA	100	97.92	37.28	60.65	58.18	0.00
DEA	100	97.78	35.62	62.16	54.44	7.71
DA	100	95.95	39.66	56.29	52.96	0.00
DHA	100	99.54	58.47	41.07	38.60	0.00
DOA	100	97.92	53.35	44.57	43.56	0.00
THA	100	97.78	65.64	32.14	32.56	0.00
TOA	100	97.92	72.96	24.97	25.51	0.00
TDA	100	95.95	78.57	17.38	17.84	0.00
ALIQ	100	97.78	19.06	78.72	8.63	70.09

Table 12.6: Equilibrium concentrations (c_{LS}) for spent liquor with a starting concentration of 80 $g \cdot l^{-1}$ and pH of 3.60 (T = 25 °C; ambient pressure; solvent phase: amine:1-octanol 20:80 wt%) for the extraction with different amines.
Indices: LS,0…initial feed concentration based on the weighted mass of LS. 1…extraction; 3…back-extraction; F…feed phase; O…solvent phase; S…stripping phase.

Amine	$c_{LS,0}$ [$g \cdot l^{-1}$]	$c_{LS,F,0}$ [$g \cdot l^{-1}$]	$c_{LS,F,1}$ [$g \cdot l^{-1}$]	$c_{LS,O,1}$ [$g \cdot l^{-1}$]	$c_{LS,S,3}$ [$g \cdot l^{-1}$]	$c_{LS,O,3}$ [$g \cdot l^{-1}$]
OA	100	80.84	17.69	63.14	40.19	22.96
DEA	100	80.84	17.76	63.07	41.89	21.19
DA	100	80.84	9.22	71.61	40.99	30.63
DHA	100	78.18	48.20	29.98	27.86	2.12
DOA	100	78.18	49.12	29.06	26.74	2.32
THA	100	78.18	57.25	20.93	20.72	0.21
TOA	100	80.84	60.26	20.58	18.20	2.38
TDA	100	78.18	61.11	17.07	14.32	2.75
ALIQ	100	78.18	24.17	54.01	4.01	49.99

Table 12.7: Equilibrium concentrations (c_{LS}) for the lignosulfonate extraction with DOA:1-octanol from a Ca-LS solution with an initial concertation of 100 $g \cdot l^{-1}$ and pH of 3.71 (T = 25 °C; ambient pressure) in dependency of the amine concentration (c_{amine}) in the solvent phase.
Indices: LS,0…initial feed concentration based on the weighted mass of LS. 1…extraction; 3…back-extraction; F…feed phase; O…solvent phase; S…stripping phase; E_{tot}…overall extraction efficiency.

c_{DOA} [wt%]	$c_{LS,0}$ [$g \cdot l^{-1}$]	$c_{LS,F,0}$ [$g \cdot l^{-1}$]	$c_{LS,F,1}$ [$g \cdot l^{-1}$]	$c_{LS,O,1}$ [$g \cdot l^{-1}$]	$c_{LS,S,3}$ [$g \cdot l^{-1}$]	$c_{LS,O,3}$ [$g \cdot l^{-1}$]	E_{tot} [%]
1	100	102.60	96.65	5.95	7.82	0.00	7.62
5	100	102.60	78.24	24.36	23.31	1.05	22.72
10	100	102.60	77.78	24.82	25.32	0.00	24.68
15	100	102.60	72.08	30.52	28.93	1.59	28.20
25	100	97.80	72.72	25.07	25.08	0.00	25.65
30	100	102.60	74.26	28.34	27.80	0.55	27.09

Table 12.8: Equilibrium pH, equilibrium concentrations (c_{LS}) and distribution ratio (D_A) for the lignosulfonate extraction with DOA:1-octanol (20:80 wt%) at different pH values and different starting concentrations (T = 25 °C; ambient pressure).
Indices: LS,0…initial feed concentration based on the weighted mass of LS. 1…extraction; 3…back-extraction; F…feed phase; O…solvent phase; S…stripping phase; E_{tot}…overall extraction efficiency.

pH_{eqil}	$c_{LS,0}$ [g·l^{-1}]	$c_{LS,F,0}$ [g·l^{-1}]	$c_{LS,F,1}$ [g·l^{-1}]	$c_{LS,O,1}$ [g·l^{-1}]	$D_{A,extr}$
12.98	10	10.41	10.87	0.00	0.00
12.98	50	51.32	54.23	0.00	0.00
12.98	100	104.61	108.13	0.00	0.00
9.61	10	10.41	9.30	1.11	0.12
9.61	50	51.32	45.51	5.81	0.13
9.61	100	104.61	91.32	13.29	0.15
8.44	10	9.55	7.65	1.90	0.25
8.44	50	50.40	41.13	9.27	0.23
8.44	100	100.65	82.70	17.95	0.22
1.28	10	9.55	0.22	9.33	41.93
1.28	50	50.40	2.30	48.10	20.94
1.28	100	100.65	6.85	93.80	13.69
1.28	300	306.92	53.58	253.33	4.73
7.73	10	9.96	2.24	7.72	3.45
7.73	50	49.20	11.03	38.17	3.46
7.73	100	99.03	25.14	73.90	2.94
6.72	10	10.34	0.37	9.97	26.69
6.72	50	52.28	3.49	48.80	14.00
6.72	100	102.96	9.64	93.32	9.68
6.72	300	302.39	118.97	183.42	1.54

Table 12.9: Visual evaluation of crud formation for the lignosulfonate extraction with DOA:1-octanol (20:80 wt%) at different pH values and different starting concentrations (T = 25 °C; ambient pressure).

c_{LS} [g/l]	pH	crud	pH	crud
10		NO		LOW
50	1.28	LOW	8.44	MEDIUM
100		LOW		MEDIUM
10		NO		NO
50	6.72	LOW	9.61	NO
100		LOW		NO
10		LOW		NO
50	7.73	LOW	12.98	NO
100		LOW		NO

12.4.U-tubes

Table 12.10: Equilibrium pH, equilibrium concentrations (c_{LS}) and distribution ratio (D_A) for the lignosulfonate extraction with DOA:1-octanol (20:80 wt%) at different pH values and different starting concentrations; T = 25 °C; ambient pressure.
Indices: LS,0…initial feed concentration based on the weighted mass of LS. 1…extraction; 3…back-extraction; F…feed phase; O…membrane phase; S…stripping phase; E_{tot}…overall extraction efficiency.

pH_{eqil}	$c_{LS,0}$ [$g \cdot l^{-1}$]	$c_{LS,F,0}$ [$g \cdot l^{-1}$]	$c_{LS,F,1}$ [$g \cdot l^{-1}$]	$c_{LS,O,1}$ [$g \cdot l^{-1}$]	$D_{A,extr}$
12.98	10	10.41	10.87	0.00	0.00
1.28	50	50.40	2.30	48.10	20.94
6.72	10	10.34	0.37	9.97	26.69
6.72	50	52.28	3.49	48.80	14.00
6.72	100	102.96	9.64	93.32	9.68
6.72	300	302.39	118.97	183.42	1.54

12.5.Small-scale membrane reactor

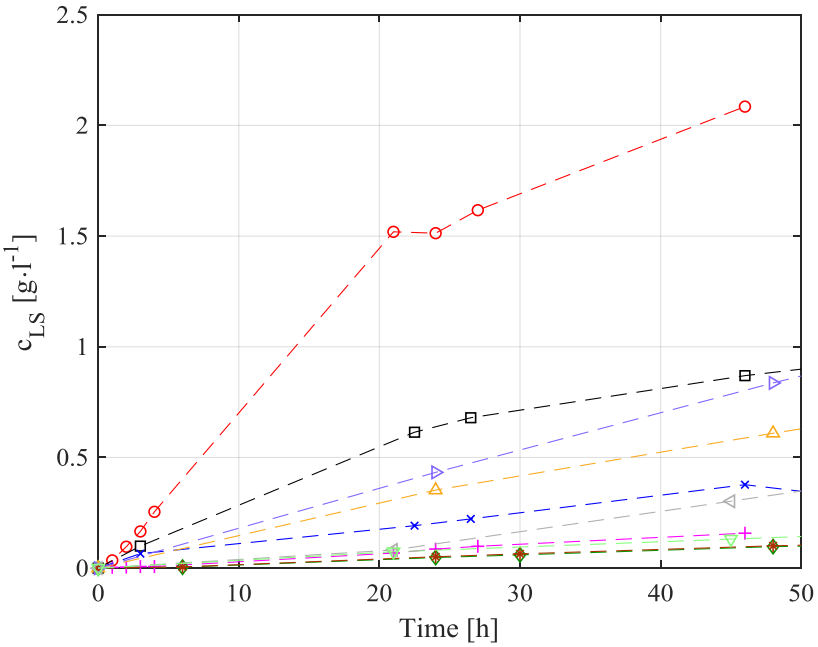

Figure 12.1: Concentration in the stripping compartment for the lignosulfonate extraction from spent sulfite liquor using supported liquid membrane permeation (small-scale membrane reactor) and TOA:1-octanol; $c_{LS,0}$ = 96 g·l^{-1}; $pH_{feed,0}$ = 3.60; T = 25 °C; ambient pressure; amine:1-octanol 20:80 wt%; $A_{membrane}$ = 25 cm^2; time = 50 hours; support layer: PE 7-12 µm hydrophilic; glue: epoxy resin.

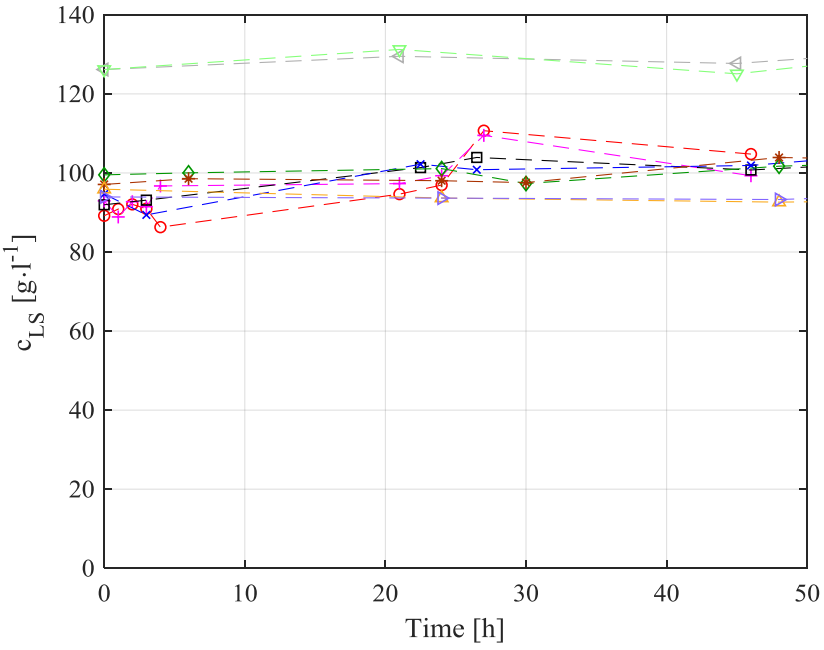

Figure 12.2: Concentration in the feed compartment for the lignosulfonate extraction from spent sulfite liquor using supported liquid membrane permeation (small-scale membrane reactor) and TOA:1-octanol; $c_{LS,0}$ = 96 g·l^{-1}; $pH_{feed,0}$ = 3.60; T = 25 °C; ambient pressure; amine:1-octanol 20:80 wt%; $A_{membrane}$ = 25 cm^2; time = 50 hours; support layer: PE 7-12 µm hydrophilic; glue: epoxy resin.

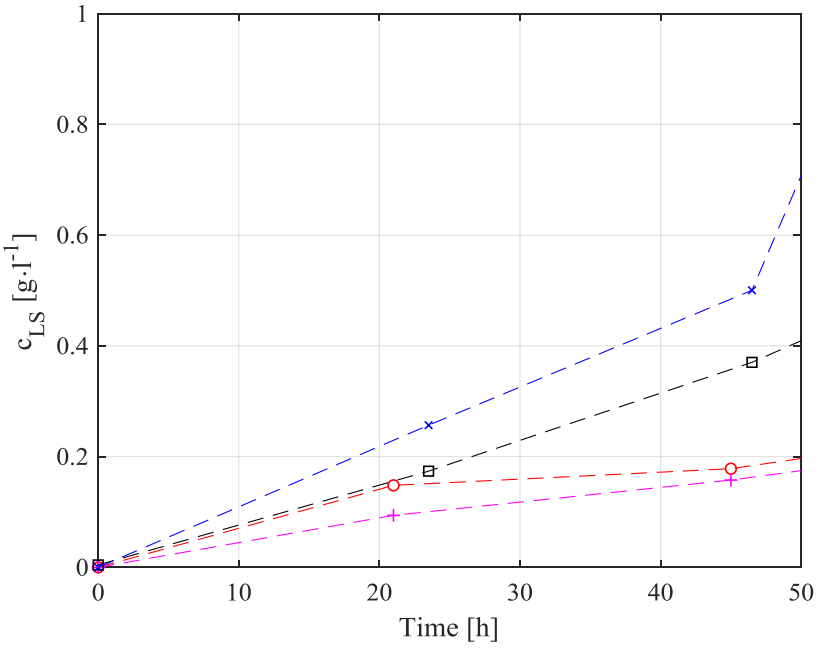

Figure 12.3: Concentration in the stripping compartment for the lignosulfonate extraction from spent sulfite liquor using supported liquid membrane permeation (small-scale membrane reactor) and TOA:1-octanol; $c_{LS,0}$ = 96 g·l^{-1}; $pH_{feed,0}$ = 3.60; T = 25 °C; ambient pressure; amine:1-octanol 20:80 wt%; $A_{membrane}$ = 25 cm^2; time = 50 hours; support layer: PE 7-12 µm hydrophobic; glue: epoxy resin.

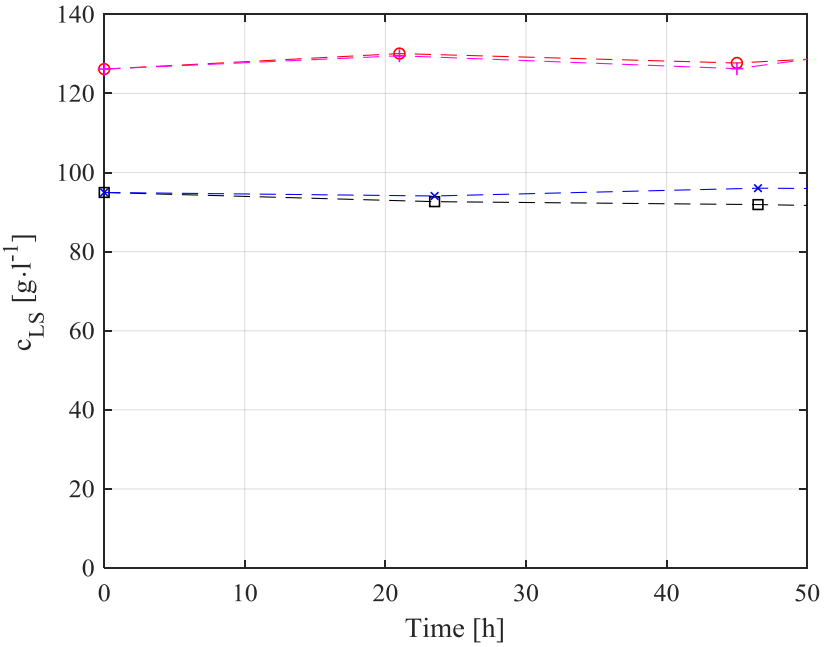

Figure 12.4: Concentration in the feed compartment for the lignosulfonate extraction from spent sulfite liquor using supported liquid membrane permeation (small-scale membrane reactor) and TOA:1-octanol; $c_{LS,0}$ = 96 g·l^{-1}; $pH_{feed,0}$ = 3.60; T = 25 °C; ambient pressure; amine:1-octanol 20:80 wt%; $A_{membrane}$ = 25 cm^2; time = 50 hours; support layer: PE 7-12 µm hydrophobic; glue: epoxy resin.

Table 12.11: Concentration in the feed and stripping compartment for the lignosulfonate extraction from spent sulfite liquor using supported liquid membrane permeation (small-scale membrane reactor) and TOA:1-octanol; $c_{LS,0}$ = 96 g·l^{-1}; $pH_{feed,0}$ = 3.60; T = 25 °C; ambient pressure; amine:1-octanol 20:80 wt%; $A_{membrane}$ = 25 cm^2; support layer: PE 7-12 µm hydrophilic; glue: epoxy resin.

Time [h]	$c_{LS,feed}$ [g·l^{-1}]	$c_{LS,strip}$ [g·l^{-1}]	Time [h]	$c_{LS,feed}$ [g·l^{-1}]	$c_{LS,strip}$ [g·l^{-1}]	Time [h]	$c_{LS,feed}$ [g·l^{-1}]	$c_{LS,strip}$ [g·l^{-1}]	Time [h]	$c_{LS,feed}$ [g·l^{-1}]	$c_{LS,strip}$ [g·l^{-1}]
0	89.17	0.00	0	92.94	0.00	0	91.95	0.00	0	94.67	0.00
1	90.87	0.03	1	88.88	0.00	3	93.12	0.10	3	89.39	0.07
2	92.05	0.10	2	92.72	0.00	23	101.36	0.61	23	102.21	0.19
3	90.95	0.17	3	91.46	0.01	27	103.92	0.68	27	100.81	0.22
4	86.29	0.25	4	96.71	0.01	46	100.75	0.87	46	101.90	0.38
21	94.64	1.52	21	97.30	0.07	51	101.69	0.91	51	103.35	0.34
24	96.93	1.51	24	99.30	0.09	72	105.03	1.06	72	106.80	0.41
27	110.69	1.62	27	109.50	0.10						
46	104.77	2.08	46	99.30	0.16						

Time [h]	$c_{LS,feed}$ [g·l^{-1}]	$c_{LS,strip}$ [g·l^{-1}]	Time [h]	$c_{LS,feed}$ [g·l^{-1}]	$c_{LS,strip}$ [g·l^{-1}]	Time [h]	$c_{LS,feed}$ [g·l^{-1}]	$c_{LS,strip}$ [g·l^{-1}]	Time [h]	$c_{LS,feed}$ [g·l^{-1}]	$c_{LS,strip}$ [g·l^{-1}]
0	94.67	0.00	0	99.51	0.00	0	97.09	0.00	0	95.89	0.00
3	89.39	0.07	6	100.02	0.00	6	98.55	0.01	24	93.66	0.35
23	102.21	0.19	24	101.10	0.05	24	98.04	0.05	48	92.62	0.61
27	100.81	0.22	30	97.33	0.06	30	97.55	0.06	72	93.54	0.85
46	101.90	0.38	48	101.71	0.10	48	103.91	0.10	144	96.42	1.43
51	103.35	0.34	120	109.35	0.16	120	99.60	0.20	168	96.33	1.61
72	106.80	0.41	144	107.04	0.18	144	107.92	0.25	192	97.03	1.75
			168	110.77	0.19	168	109.24	0.38	216	97.42	1.92
			192	111.87	0.21	192	108.07	0.67	240	98.18	2.08
			287	117.55	0.27	287	113.71	1.48			

Time [h]	$c_{LS,feed}$ [g·l^{-1}]	$c_{LS,strip}$ [g·l^{-1}]	Time [h]	$c_{LS,feed}$ [g·l^{-1}]	$c_{LS,strip}$ [g·l^{-1}]	Time [h]	$c_{LS,feed}$ [g·l^{-1}]	$c_{LS,strip}$ [g·l^{-1}]	Time [h]	$c_{LS,feed}$ [g·l^{-1}]	$c_{LS,strip}$ [g·l^{-1}]
0	93.93	0.00	0	126.16	0.00	0	126.16	0.00			
24	93.64	0.43	21	129.51	0.08	21	131.24	0.07			
48	93.28	0.84	45	127.69	0.30	45	125.08	0.13			
72	96.03	1.21	71	134.28	0.54	71	135.12	0.19			
144	95.80	2.14	145	132.26	2.05	145	140.14	0.44			
168	95.64	2.43	168	131.30	3.18	168	135.49	0.64			
192	97.67	2.89	192	132.78	5.11	191	135.92	0.74			
216	97.90	3.35	214	131.80	5.74	214	133.72	0.82			

Table 12.12: Concentration in the feed and stripping compartment for the lignosulfonate extraction from spent sulfite liquor using supported liquid membrane permeation (small-scale membrane reactor) and TOA:1-octanol; $c_{LS,0}$ = 96 g·l^{-1}; $pH_{feed,0}$ = 3.60; T = 25 °C; ambient pressure; amine:1-octanol 20:80 wt%; $A_{membrane}$ = 25 cm^2; support layer: PE 7-12 µm hydrophobic; glue: epoxy resin.

Time [h]	$c_{LS,feed}$ [g·l^{-1}]	$c_{LS,strip}$ [g·l^{-1}]	Time [h]	$c_{LS,feed}$ [g·l^{-1}]	$c_{LS,strip}$ [g·l^{-1}]	Time [h]	$c_{LS,feed}$ [g·l^{-1}]	$c_{LS,strip}$ [g·l^{-1}]	Time [h]	$c_{LS,feed}$ [g·l^{-1}]	$c_{LS,strip}$ [g·l^{-1}]
0	126.16	0.00	0	126.16	0.00	0	94.96	0.00	0	94.96	0.00
21	130.09	0.15	21	129.53	0.09	24	92.64	0.17	24	94.08	0.26
45	127.70	0.18	45	126.27	0.16	47	91.90	0.37	47	96.05	0.50
71	132.66	0.27	71	138.55	0.25	70	90.47	0.63	70	95.58	1.89
145	129.77	0.49	145	130.86	0.48	190	93.61	4.75	190	96.28	11.71
168	134.40	0.57	168	135.84	0.55						
191	137.97	0.65	191	135.16	0.59						
214	133.44	0.73	214	136.00	0.64						

Table 12.13: Concentration in the feed and stripping compartment for the lignosulfonate extraction from spent sulfite liquor using supported liquid membrane permeation (small-scale membrane reactor) and TOA:1-octanol; $c_{LS,0}$ = 96 g·l^{-1}; $pH_{feed,0}$ = 3.60; T = 25 °C; ambient pressure; amine: 1-octanol 20:80 wt%; $A_{membrane}$ = 25 cm^2; support layer: PE 7-12 µm hydrophobic; glue: superglue.

Time [h]	$c_{LS,feed}$ [g·l^{-1}]	$c_{LS,strip}$ [g·l^{-1}]	Time [h]	$c_{LS,feed}$ [g·l^{-1}]	$c_{LS,strip}$ [g·l^{-1}]
0	96.08	0.00	0	91.68	0.00
23	90.40	0.36	24	89.40	0.31
47	89.11	1.83	48	87.24	1.23
172	78.70	7.81			
243	99.74	31.08			

Table 12.14: Concentration in the stripping phase and pH in the feed phase for the lignosulfonate extraction from spent sulfite liquor using supported liquid membrane permeation (lab-scale membrane reactor) and TOA:1-octanol; $c_{LS,0}$ = 96 g·l^{-1}; $pH_{feed,0}$ = 3.60; T = 25 °C; ambient pressure; amine: 1-octanol 20:80 wt%; $A_{membrane}$ = 123 cm^2; support layer: PE 7-12 µm hydrophobic.

Time [h]	$c_{LS,strip}$ [g·l^{-1}]	pH_{feed} [g·l^{-1}]
0	0.00	3.561
1	0.55	-
2	0.94	3.616
3	1.30	-
4	1.56	3.638
5	1.87	-
6	2.12	3.655